Synthesis, modification and characterisation of magnetic micro-matrices for covalent immobilisation of biomolecules. Model investigations with penicillin amidase from *E.coli*

Dissertation zur Erlangung des Doktorgrades der Naturwissenschaften der
Naturwissenschaftlichen Fakultät IV – Chemie und Pharmazie
der Universität Regensburg

vorgelegt von

Daniela Petrova Bozhinova

aus Plovdiv, Bulgarien

2004

Promotionsgesuch eingereicht am:

Die Arbeit wurde angeleitet von: Prof. Dr. habil. Rainer Köster
Universität Regensburg, Forschungszentrum Karlsruhe

Begutachtung:

1. Gutachter:	Prof. Dr. habil Rainer Köster
2. Gutachter:	Prof. fil. dr. Volker Kasche

Prüfungsausschuss:

Vorsitz:	Prof. Dr. habil. Hans-Helmut Kohler *Universität Regensburg*
Prüfer:	Prof. Dr. habil Rainer Köster *Universität Regensburg, Forschungszentrum Karlsruhe*
Prüfer:	Prof. fil. dr. Volker Kasche *Technische Universität Hamburg-Harburg*
Prüfer:	Prof. Dr. habil. Claudia Steinem *Universität Regensburg*

To my grandmother Dimitria
На баба ми Димитрия

ZUSAMMENFASSUNG

Aus überwiegend ökonomischen Gründen ist die Immobilisierung und der wiederholte Einsatz von Enzymen in industriellen biotechnologischen Anwendungen erforderlich.

In den letzten Jahren wurden magnetische Trägermaterialien, die in vielen Trennverfahren effizient verwendet werden können, in der Biotechnologie, Molekularbiologie und Medizin etabliert.

Das Ziel dieser Arbeit war die Entwicklung und Charakterisierung von magnetischen Mikroträgern für die kovalente Immobilisierung von Biokatalysatoren. Als Modellenzym wurde Penicillin Amidase aus *E. coli*, das durch seine Verwendung bei der semi-synthetischen β-Lactam-Antibiotika-Herstellung große industrielle Bedeutung erlangt hat, herangezogen.

Zu diesem Zweck wurden Magnetpartikel mit einer Größe von 2 bis 20 µm aus Polyvinylacetat (PVAc) und Polymethylacrylat (PMA) durch die „Öl-in-Wasser-Suspensions-Polymerisationsmethode“ synthetisiert. Quervernetzte Polymethylmethacrylat (PMMA) Träger mit einem Durchmesser von 6 µm wurden durch die Einlagerung von Magnetitnanokristallen aus einem magnetischem Fluid mit Toluen als Lösungsmittel im „swell-deswell“-Verfahren mit magnetischen Eigenschaften ausgestattet und mit einer Tensiddoppelschicht versehen. Aminosilanisierte magnetische Partikel mit einem Durchmesser von 1–2 µm wurden durch die Fällung von Eisen(II)- und Eisen(III)salzen in stark alkalischen Milieu dargestellt und mit jeweils einer Schicht aus Aminosilan und Polyglutaraldehyd umgeben.

Polyvinylalkoholträger, bekannt unter dem Handelsnamen M-PVA und mit einem Partikeldurchmesser von 1–3 µm, wurden von der chemagen Biopolymer Technologie AG zur Verfügung gestellt und eingehend untersucht.

Alle untersuchten Magnetträger hatten eine Größe von einigen Mikrometern (1–20 µm) und zeigten superparamagnetisches Verhalten, so dass sie keine Remanenzmagnetisierung aufwiesen. Die magnetische Sättigung der verwendeten Träger betrug 11 bis 40 $A \cdot m^2 \cdot kg^{-1}$. Environmental Scanning Electron Microscopy (ESEM) – Aufnahmen zeigten bei den Polyvinylacetat-, Polymethylacrylat- und Polymethylmethacrylat- Partikeln keinerlei Poren, die groß genug wären, dass in ihnen Enzymmoleküle immobilisiert werden könnten.

Die spezifischen Oberflächen der Träger wurden mittels BET-Messungen bestimmt. Die gemessenen Oberflächen der PVAc-, PMA- und PMMA- Partikel im Bereich von 3 bis 15 $m^2 \cdot g^{-1}$ korrelieren sehr gut mit den theoretisch Berechneten, die auf der Annnahme

einer glatten Oberfläche beruhen. Für Polyvinylalkohol- und aminosilanisierte Magnetpartikel lagen die gemessenen spezifischen Oberflächen deutlich höher, als theoretisch erwartet. Es wurde ein vereinfachtes „self-scaling“ Modell, dass die Unebenheiten der Oberfläche beschreibt, erarbeitet, dass diese Diskriminanz bei den M-PVA-Trägern erklärt.

Ausgehend von diesem Modell konnte der Durchmesser der Oberflächeneinbuchtungen zu ungefähr 1 Å errechnet werden. Diese sind somit eine Größenordnung kleiner als das untersuchte Enzym (70*50*55 Å) (Duggleby et al. 1995). Das hat zur Folge, dass die Oberflächen, die zur Immobilisierung zur Verfügung standen, geringer waren als die mittels BET bestimmten.

Die hohen spezifischen Oberflächen der aminosilanisierten Partikel sind wahrscheinlich auf das Erhitzen auf 60 °C vor der BET-Messung zurückzuführen, da dabei der Polyglutaraldehyd- bzw. der Aminosilanüberzug durchbrochen wird, was zu einer Erhöhung der Oberfläche führt.

Das Zetapotential der Trägeroberflächen in wässriger Lösung wurde für den pH-Bereich von 7.0 bis 7.5 bestimmt. Es ist für die Immobilisierung von Enzymen auf der Oberfläche von entscheidender Bedeutung, insbesondere bei der Verwendung kurzer Spacer zwischen Enzym und Träger.

Die Oberflächen der Magnetträger wurden hauptsächlich mit Epoxy- oder Amino- und Aldehyd- Spacern modifiziert, um geeignete funktionelle Gruppen zur kovalenten Immobilisierung zu erhalten.

M-PVA- (modifiziert mit Epichlorhydrin), Poly(methylmethacrylat)- (modifiziert mit Glycidol) und PVAc- (modifiziert mit Epichlorhydrin) Träger wiesen hohe Konzentrationen an Epoxygruppen auf (400 bis 700 $\mu mol \cdot g^{-1}$ getrockneter Träger). Die Konzentration der freien Aminogruppen war für die kommerziell erhältlichen M-PVA N12-Träger (650 $\mu mol \cdot g^{-1}$ getrockneter Träger) und die PMA-Träger (modifiziert mit Ethylendiamin) (640 $\mu mol \cdot g^{-1}$ getrockneter Träger) am höchsten.

Penicillin Amidase aus *E.coli* wurde mittels diverser Spacer und Kopplungsreaktionen kovalent an die untersuchten Magnetträger gebunden.

Für die kommerziell erhältlichen M-PVA-Träger konnte gezeigt werden, dass die Menge an gebundenem Enzym mit zunehmender Spacerlänge bis zu einem Maximalwert von 22 mg Enzym pro Gramm getrockneten Träger bei 20.8 Å zunimmt. Unter vergleichbaren Immobilisierungsbedingungen (I = 0.2 M) konnte auf demselben Trägertyp mit einem Spacer von 6.0 Å Länge nur 4 mg Enzym pro Gramm getrockneten Träger gebunden werden.

Analoge Ergebnisse wurden für amino-silanisierte Magnetpartikel mit einer unterschiedlichen Anzahl an Hexamethylendiamin / Glutardialdehyd – Spacereinheiten unter denselben Reaktionsbedingungen beobachtet.

Für diese Träger wurde ein Immobilisierungsmaximum von 74 mg pro Gramm getrockneten Träger bei einer Spacerlänge bestehend aus 4 Spacereinheiten, was einer Länge von 64.9 Å entspricht, erreicht. Dieses Enzymimmobilisierungsmaximum war auch die größte Beladung, welche im Rahmen dieser Arbeit mit dem gewählten Enzym und bei diesen Immobilisierungsbedingungen erzielt wurde.

Für Polyvinylacetatträger nahm die Menge an immobilisiertem Enzym von 3 auf 24 mg bei einer Verlängerung des Spacers von 6.0 Å (epoxy spacer) auf 21.0 Å (Hexamethylendiamin / Glutardialdehyd Spacer) zu.

Des weiteren wurde für M-PVA-Träger ein stärkerer Einfluss der Ionenstärke der Pufferlösung, in der die Immobilisierung erfolgte, bei der Verwendung kürzer Epoxy- und Imidazolyl-carbamat- Spacer, als bei längeren festgestellt. Für beide Spacertypen wurde eine signifikante Zunahme bis zur dreifachen Menge an immobilisiertem Enzym erreicht, als die Ionenstärke auf bis zu I = 1 M erhöht wurde.

Dies konnte auf die Minimalisierung von unerwünschten Ladungswechselwirkungen zwischen der Trägeroberfläche (negatives Zeta-potential bei pH = 7.5) und den Enzymmolekülen (negativ geladen bei pH = 7.5) während der Immobilisierung zurückgeführt werden.

Logischer Weise ist dieser Effekt der Ionenstärke bei kürzeren Spacern signifikanter als bei längeren, da die Stärke der elektrostatischen Wechselwirkungen mit zunehmendem Abstand des Enzyms vom Träger abnimmt.

Vergleichbare Ergebnisse wurden für Polyvinylacetatpartikel erhalten.

Polymethylacrylatträger, aminomodifiziert und weiter funktionalisiert mit Glutardialdehyd, zeigten vergleichbare Enzymbeladungen wie die kommerziell erhältlichen M-PVA-Träger bei denselben Immobilisierungsbedingungen.

Mit der Verlängerung der Reaktionszeit der Immobilisierung von 24 h auf 72 h erhöhte sich die Menge an immobilisierter Penicillin Amidase von 35 auf 54 mg pro Gramm getrockneten Träger.

Die scheinbaren kinetischen Konstanten K_m und k_{cat} der immobilisierten Penicillin Amidase aus *E.coli* wurden anhand der Hydrolyse von Penicillin G untersucht. Die ermittelten scheinbaren K_m – Konstanten waren um ein vielfaches höher, als die des freien Enzyms, aber

um ein bis zwei Größenordnungen kleiner als die für an große poröse Partikel (>100 μm) gebundene Penicillin Amidase.

Die Selektivität des auf M-PVA-Trägern immobilisierten Enzyms wurde anhand der kinetisch kontrollierten Synthese von Cephalexin aus R-Phenylglycinamid und 7-Aminodeacetoxycephalosporansäure bei 5 °C mit einem Nucleophilüberschuß untersucht. Die Selektivität des gebundenen Enzyms betrug $\nu_{syn} / \nu_{hyd} = 8$ und ist vergleichbar mit der des freien Enzyms ($\nu_{syn} / \nu_{hyd} = 13$).

Die Enantioselektivität der immobilisierten Penicillin Amidase aus *E.coli* wurde mittels der gleichgewichtskontrollierten Hydrolyse racemischer Mischungen von Phenylacetylphenylalanin und der kinetischkontrollierten Kondensation von R-Phenylglycinamid mit racemischem oder enatiomerenreinem Phenylalanin bestimmt.

Die immobilisierten Enzyme zeigten unabhängig vom Trägertyp und der Art der Immobilisierung eine Enantioselektivität $E_{hyd\ rac} > 100$ für die untersuchte Hydrolysereaktion.

Für die Kondensationsreaktion mit enantiomerenreinem Phenylalanin zeigte die auf M-PVA E02 immobilisierte Penicillin Amidase die höchste Enantioselektivität ($E_{syn} = 460$).

Die oben genannte Kondensationsreaktion wurde für auf PVAc und M-PVA E02 immobilisierte Penicillin Amidase ebenfalls mit racemischem Phenylalanin durchgeführt.

An PVAc gebundene Penicillin Amidase aus *E.coli* hatte eine Enantioselektivität $E_{syn,\ rac} = 500$, welche um über das 10fache größer ist als für das enantiomerenreine Substrat ($E_{syn} = 40$), während die Enantioselektivität der auf M-PVA E02 immobilisierten Penicillin Amidase in derselben Größenordnung für racemische Substrate ($E_{syn,\ rac} = 500$) und enantiomerenreinem Substrat $E_{syn} = 460$ lag.

Offensichtlich beeinflußt die elektrische Doppelschicht des Trägers die Enantioselektivität des darauf immobilisierten Biokatalysators, was noch weitere detaillierte Studien der Wechselwirkungen zwischen Träger und Enzym und des Einflusses des Trägers auf die Enzymeigenschaften auf dem nanometrischen Level erfordert.

Acknowledgements

I would like to express my deep gratitude to Prof. Dr. Rainer Köster for the interesting subject of my PhD thesis, fruitful discussions and his helpful criticism throughout my work, as well as for giving me an opportunity to realise own ideas. I would like to thank him also for the very good laboratory equipment and his help by the numberless organizational and administrative obstacles during this work.

I am very grateful to PD Dr. Matthias Franzreb for his great attention to my work, the countless discussions, forwarding suggestions throughout its duration and generous financial support of my scientific stay in TU-Hamburg-Harburg (Abt. Biotechnologie II).

I would like to acknowledge Prof.fil.dr. Volker Kasche (Abt. Biotechnologie II, TU Hamburg-Harburg) for providing me the opportunity to collaborate with his working group and for the interesting discussions in the area of enzyme (enantio)selective catalysis.

I am grateful to Dr. Boris Galunsky (Abt. Biotechnologie II, TU Hamburg-Harburg) for the guidance in the area of enzyme kinetics, stereoselective biocatalysis and HPLC analysis.

Furthermore, I would like to acknowledge Prof. Dr. Rolf Nüesch for providing me the chance to complete my work in the Institute for Technical Chemistry, Water and Geotechnology Division (ITC-WGT, Forschungszentrum Karlsruhe) and to thank the colleagues in ITC-WGT for the friendly working atmosphere.

I am grateful to acknowledge: Dr. G. Yueping (Institute of Process Engineering, Chinese Academy of Sciences) for his help and good cooperation in the area of polymerisation processes; Dr. L. Black and Dr. G. Beuchle (ITC-WGT, FZK) for their guidance in the field of Environmental Scanning Electron Miccroscopy; Dr. P. Weidler for the BET analysis and fruitful discussion concerning the theoretical self-scaling model of the carriers surface relief.

My very special thank goes to my diploma student Bertolt Kranz for his help in accomplishment of several immobilisation experiments, as well as for his friendship and support in the end of this work.

I am grateful to Prof. Dr. A. Assenov (UCTM, Sofia, Bulgaria) and to Dr. M. Kostova (UCTM, Sofia, Bulgaria) for providing me the opportunity to contact Prof. Dr. R. Köster and their encouragement throughout my work.

I would like to thank also all staff in Abteilung Biotechnologie II (TU Hamburg-Harburg) for the very good collaboration and friendly atmosphere in the department.

I would like to express my deep gratitude to my family:

Мила Цеци, благодаря ти за обичта и искрената подкрепа, както и за многобройните съвети, които ми помагаха винаги през тези три години.

Мила Мамо, благодаря ти за майчината топла любов, както и за грижите за мен в трудните моменти през този период.

Благодаря и на теб Татко за обичта и подкрепата.

I am grateful to Nikolay Milanov for his sincere friendship and encouragement throughout these years and hopefully in the future.

I would like to thank my friend Ralf for his love, support and great patience.

TABLE OF CONTENTS I - IV

INTRODUCTION 1

AIM OF THE THESIS 4

Part A: Matrices for enzyme immobilisation 6

1. Knowledge basis 6
1.1. Natural matrices 7
1.2. Synthetic matrices 10
1.3 Magnetic matrices 14

2. Materials and methods 19
2.1. Synthesis of the magnetic matrices 19
2.1.1. Materials 19
2.1.2. Synthesis of surfactant coated magnetic gel 19
2.1.3. Transformation of poly(methyl methacrylate) (PMMA) beads into magnetic modifications by "swell-deswell" manufacturing method 21
2.1.4 Synthesis of poly(methylacrylate) (PMA) magnetic beads by suspension polymerisation method 22
2.1.5. Synthesis of poly(vinylacetate) (PVAc) magnetic beads by suspension polymerisation method 24
2.1.6. Synthesis, aminosilane- and poly(glutaraldehyde)- coating of iron oxide crystals (Amino-Silanised-Magnetic-Particles ASMP) 26
2.2. Surface modification of the magnetic matrices 30
2.2.1 Epoxy-modification of the polymer magnetic beads 30
2.2.2. Amino-modification of the magnetic matrices 31
2.2.3. Glutardialdehyde modification of the amino-charged magnetic matrices 33
2.2.4. N,N'-carbonyl diimidazole (CDI)-modification of M-PVA magnetic matrices 34
2.3. Analytical methods and apparatuses 35
2.3.1. Determination of the epoxy group concentration of the magnetic matrices 35
2.3.2. Determination of the amino group concentration of the magnetic matrices 36
2.3.3. Separation of the matrices 37
2.3.4. Method for determination the dry-weight of the magnetic particles 37
2.3.5. Spectrophotometric measurements 37
2.3.6. Measurements of the magnetic saturation of the matrices 37
2.3.7. Size determination of the magnetic particles 37
2.3.8. Measurements of the Zeta potential 38
2.3.9. Measurements of the specific surface area 38

3. Results and discussion 39
3.1. Size determination of the magnetic matrices. BET specific surface area evaluation 39
3.2. Magnetic properties of the matrices 43
3.3. Zeta-potential (ξ) measurements 45
3.4. Chemical modification of the magnetic matrices surface with different functional sites 46

4. Summary and conclusions 49

5. Symbols and abbreviations 50

6. References 52

Part B: Immobilisation of penicillin amidase from *E.coli* onto magnetic matrices 56

1. Knowledge basis 56
1.1. Immobilisation of enzymes – an introduction. Immobilisation methods 56
1.2. Penicillin amidase 62
1.3. Immobilisation of penicillin amidase 64

2. Materials and methods 68
2.1. Materials 68
2.2. Immobilisation of penicillin amidase from E.coli onto epoxy-modified magnetic polymer matrices 68
2.3. Immobilisation of penicillin amidase from E.coli onto glutardialdehyde-modified (previously amino-charged) magnetic matrices 70
2.4. Immobilisation of penicillin amidase from E.coli onto N,N'-carbonyl diimidazole (CDI)-modified magnetic matrices 71
2.5. Analytical methods 72
2.5.1. Penicillin amidase activity assay 72
2.5.2. Penicillin amidase active site titration 73
2.5.3. Protein assay 73
2.5.4. Spectrophotometric measurements 74
2.5.5. Separation of the magnetic matrices 74
2.5.6. Method for determination of the dry-weight of the magnetic particles 74

3. Results and discussion 75
3.1. Immobilisation of penicillin amidase from E.coli onto M-PVA magnetic matrices 75
3.2. Immobilisation of penicillin amidase (E.coli) onto PVAc and PMMA magnetic matrices 78
3.3. Immobilisation of penicillin amidase (E.coli) onto amino / glutardialdehyde modified PMAb and PMAs magnetic beads 80
3.4. Immobilisation of penicillin amidase from E.coli onto amino-activated / glutardialdehyde modified ASMP (poly(glutaraldehyde) coated matrices 81

4. Summary and conclusions 84

5. Symbols and abbreviations 87

6. References 89

Part C: Evaluation of the selectivity and stereoselectivity of penicillin amidase from *E.coli* immobilised onto magnetic micro-matrices 93

1. Knowledge basis 93
1.1. Enzyme catalysis and kinetics 93
1.2. Chirality. Chiral molecules. Racemic resolutions 99
1.3. Kinetically and equilibrium controlled processes catalysed by hydrolases. Enantioselectivity of the penicillin amidase 101
1.4. Penicillin amidase in the synthesis of semi-synthetic β-lactam antibiotics 106

2. Materials and methods 109
2.1. Materials 109
2.2. Penicillin amidase catalysed equilibrium and kinetically controlled model processes 109
2.3. HPLC methods, used for the identification and analysis of the substrates and the products in the penicillin amidase catalysed model reactions 112
2.4. Other analytical methods 114

3. Results and discussion 116
3.1. Apparent kinetic parameters of the immobilised penicillin amidase (E.coli) for benzylpenicillin hydrolysis 116
3.2. Penicillin amidase catalysed equilibrium and kinetically controlled processes 117
3.2.1. Study of the penicillin amidase S'_1 enantioselectivity in equilibrium controlled hydrolysis of racemic phenylacetylphenylalanine and kinetically controlled condensation of R-phenylglycine amide with R-, S-, or R,S- phenylalanine 117
3.2.2. Penicillin amidase selectivity in the kinetically controlled synthesis of cephalexin 120

4. Summary and conclusions 123

5. Symbols and abbreviations 125

6. References 127

Part D: Summary. Outlook and future work 131

SUMMARY 131

OUTLOOK AND FUTURE WORK 135

Error discussion 137
1. Particle size measurements 137
2. BET specific surface area (SSA) measurements 137
3. Determination of the concentration of the dry magnetic particles in suspension 138
4. Penicillin amidase activity assay 138
5. HPLC analysis 138

APPENDIX I: 140

APPENDIX II: 143

APPENDIX III: 144

APPENDIX IV: 145

APPENDIX V: 146

Eidesstattliche Erklärung 148

INTRODUCTION

The term enzyme ("in yeast") was used for the first time by Kuhne in 1876. By the beginning of the 20th century the structure of enzymes started to be evaluated. Urease was the first enzyme to be crystallised, and was recognised to be a simple protein. Enzymes (called also biocatalysts) are important compounds in living cells, where they catalyse and regulate the reactions of all biochemical pathways. According to the International Enzyme Commission they are classified (on the basis of the reaction they catalyse) into six main classes: oxidoreductases, transferases, hydrolases, lyases, isomerases, ligases. Every enzyme is assigned by a code (E.C. number) that consists of four numbers, based on the catalysed reaction type. The first number denotes to which of the six classes the enzyme belongs. The second number indicates the sub-class (defines the chemical structures changed in the reaction), the third the sub-subclass (defines the properties of the enzyme) and the fourth is the running number of the enzyme. Penicillin amidase used here as a model enzyme has EC number 3.5.1.11. Enzymes with the same function (the same E.C. number), but from diverse sources may have different intrinsic properties due to differences in the primary structure.

Similarly to chemical catalysts, enzymes can accelerate the attainment of reaction equilibrium. Compared to the non-catalysed reaction, an enzyme can increase the rate of the catalysed process by a factor of up to 10^{10}. The end-point of the enzyme catalysed transformations must be selected with respect to give the highest possible yield. Enzyme catalysed synthesis of condensation products can be performed either as an equilibrium controlled or a kinetically controlled process. In equilibrium controlled condensation reactions catalysed by hydrolyses the yield depends on physical parameters such as: ionic strength, pH, temperature and solvent composition. Non-equilibrium concentrations can be obtained in kinetically controlled reactions (Figures 8 and 9, Part C), where the enzyme acts as a transferase between the activated substrate and the nucleophile, and the yield of condensation product can be influenced additionally by the properties of the biocatalyst. Moreover, in kinetically controlled processes with the same enzyme amount, the maximum yield is also reached much more rapidly than in the equilibrium controlled process (Figure 7, Part C) (Kasche 1986).

The world market for industrial enzymes was ~ $ 500 million in 1990 (Sheldon 1993) and ~ $ 2000 million in 2003 (data from www.novozymes.com, report 2003), 75 % of which separated between the three major applications: detergents, dairy products and starch processing. Considering that biocatalysts exhibit principally a high activity only a small amount of enzyme is utilised in the bioconversions. Having this in mind, an important parameter for the characterisation of the enzyme, called the productivity number was introduced (Sheldon 1993):

*Productivity Number = amount of product (kg) / dry wt of catalyst (kg) * time (h)*

The application of free enzymes as catalysts in many industrial processes is restricted mainly by economical reasons (high price of the biocatalyst) therefore necessitating their separation and re-use after completion of the reaction. In this context immobilised enzyme technology offers many advantages, such as: increased in general enzyme stability; precise control of the desired reaction; possibility for the separation and re-use of the immobilised enzyme. It can be distinguished between carrier-bound and carrier-free (e.g. cross-linked enzyme aggregates; cross-linked enzyme crystals etc.) immobilised enzymes (Cao et al. 2003). The choice of a matrix to which the biocatalysts can be attached directly or *via* a spacer* is determined by making compromises between several requirements according its properties (morphological, chemical, mechanical), its economical evaluation (reliable source at a reasonable price) and not least the separation opportunities. The majority of the immobilisation matrices (supports; carriers) widely used in the biotechnology are large porous particles (100-200 μm) with high specific surface areas, which allow high enzyme loadings. Although one of the main disadvantages of such matrices is the appearance of diffusional limitations for the substrates and/or the products during the course of the enzyme catalysed process. Moreover another negative effect can be fouling of the matrix-pores with substrate/product by reactions with low or poor soluble compounds (reactions in suspension). All these negative effects can be minimised or in some cases completely avoided, by using smaller (1 μm or less), non-porous matrix-particles.

*low molecular weight compound covalently bound on the matrix, which increases the distance between it and the biocatalyst

However the range of the separation options for such supports is very narrow.

In this contexts ***magnetic carrier technology*** offers a new convenient manner for the separation of small (1µm or less) particles. The application of magnetic matrices for the purposes of biotechnology and molecular biology is ever greater (Dunlop et al. 1984, Setchell 1985, Haukanes and Kvam 1993).

The development and application of smaller, non-porous and relatively easily separable magnetic matrices can be favourable for several biotechnological processes.

AIM OF THE THESIS

The immobilised enzymes offer several advantages compared to the free ones, such as the possibility for easier separation and re-use of the biocatalyst as well as finer control of the reaction course. However there is no matrix or immobilisation manner, which can be evaluated as «the best». In this context a precise optimisation of the matrix properties (chemical, morphological, mechanical) and immobilisation process for certain biotechnological application becomes necessary.
The aim of this thesis was:

- To produce and characterise different magnetic micro-sized matrices suitable for covalent immobilisation of enzymes. These manufacturing procedures as well as diverse modifying methods in order to obtain spacers with different functional sites on the matrices surface for covalent binding of the biocatalyst are discussed in **Part A**.

- To study the properties of the synthesised magnetic particles as matrices for the covalent immobilisation of a chosen model enzyme system: penicillin amidase from *E.coli.* The optimisation the immobilisation conditions (type of spacer; length of spacer; ionic strength of immobilisation buffer, in which the reaction is performed) in order to obtain high enzyme loadings of the magnetic matrices is presented in **Part B**.

- To study the kinetic parameters of penicillin amidase (EC 3.5.1.11) from *E.coli* immobilised onto different magnetic matrices, for benzylpenicillin hydrolysis. To investigate the catalytic properties of immobilised enzyme in model processes (**Part C**).

  To evaluate the enantioselectivity of the immobilised biocatalysts in equilibrium controlled hydrolysis of racemic phenylacetylphenylalanine and kinetically controlled condensation of R-phenylglycine amide with R-,S-,or R,S- phenylalanine and their selectivity in kinetically controlled synthesis of cephalexin (**Part C)**. In all cases the properties of the penicillin amidase from

E.coli immobilised onto different magnetic matrices were evaluated comparatively to these of the free enzyme.

Part A: Matrices for enzyme immobilisation

1. Knowledge basis

In principle a matrix for enzyme immobilisation could be any material to which the enzyme may be attached directly or by means of a spacer. Usually, but not always the insoluble matrix is solid (Hermanson et al. 1992).
Hundreds of substances have been described and employed as matrices, from ground shrimp shells (chitin) to grass pollen, sea sand, volcanic pumice and, of course, to processed seaweed extract (agarose) and a wealth of synthetic matrices. However, in spite of this apparently large range of choices, an applicable matrix must satisfy several requests, which strongly reduces the amount of useful resources (Buchholz 1979, Buchholz and Kasche 1997, Hermanson et al. 1992, Bickerstaff 1997). Some desired characteristics converting certain material into a matrix suitable for enzyme immobilisation are listed below:

- *chemical*: hydrophilicity in order to avoid non-specific binding interactions or hydrophobicity in the case of non-covalent adsorptive binding; in the case of covalent binding is desired presence of an optimal amount of functional groups and reaction-options for subsequent activation and attachment of the enzyme; chemical stability (solubility), resistance to microbial attack, low toxicity
- *morphological*: large specific surface area (through high porosity or small size) and subsequently high achievable loading capacities for the target biomolecule
- *mechanical*: stability with regard to avoid degradation by heat, withstand for example the shear forces in a fluidized bed reactor, cleaning or sanitation protocols, flow resistance
- *economical*: reliable source at a reasonable price, feasibility for scale-up, reusability of the matrix, effective working life, technical skill required.

One property of high importance is the carrier porosity. The matrices can be separated generally into: non-porous and porous.

Several advantages as well as disadvantages of these two carrier types are described by Gemeiner (1992) and references therein. The porous supports offer high surface areas and high enzyme loading capacities, but also high diffusional limitations, high costs (controlled pore size) and high pressure drops in the case of gels. It must be stressed also that a lot of difficulties could appear in the case where insoluble or low-soluble substrates or products participate in the reaction, by fouling the matrices pores (Halling and Dunnill 1980). In contrast, the non-porous matrices provide low diffusional limitations, but low specific surface areas and enzyme loadings. Only in the case of very small particle diameters of a few μm or less the specific surface areas of non-porous matrices approaches these areas of large, but porous matrices. However difficulties to remove the above-described small particles from the reaction solution and to run continuous process occur. Methods for evaluation the carrier characteristics are described by Buchholz (1979). Looking at the different support types described in the literature, between three groups can be distinguished:

- natural matrices - organic or inorganic
- synthetic matrices - mainly organic
- *magnetic matrices* - special group of the synthetic matrices, studied extensively in the recent years, enhanced attention on which will be paid in this work.

1.1. Natural matrices

Polysaccharides as agarose, cellulose, alginates, carrageenans, chitin are greatly used for the immobilisation of biomolecules, because of the large spectrum in their functional properties and commercially available products (Braun et al. 1989, Alvaro et al. 1990, Fernández-Lafuente et al. 1992, Bickerstaff 1997, Amorim et al. 2003, Çetinus and Öztop 2003).

Silica, alumina and glass can be also included into the group of the natural matrices, because of their natural abundance (Robinson et al. 1971, Hermanson et al. 1992, Fonseca et al. 1993). Usually these matrices require substantial chemical modification and engineering in order to be applied as immobilisation carriers.

Agarose is a linear polysaccharide, which consists of alternating residues of β-D-galactose and 3,6-anhydro-α-L-galactose (Fig. 1A). The secondary and tertiary

structure of agarose can be described as a single fiber spun into a yarn of fibers, that is in turn "implemented" into a remarkable network with pentagonal pores (Fig. 1B). These pores are large enough to be entered by proteins with molecular weights of several millions Da and in the same time strong enough to be shaped into definite spherical beads with good flow characteristics (Gemeiner 1992). The stability of the pores depends on hydrogen bond formation in the triple helix of agarose chains. These bonds can be disrupted by heating or in the presence of strong denaturants, which will cause dissolving of the agarose particles. If the agarose is crosslinked by epichlorohydrine or divinyl sulfone, in order to enhance its structural and chemical resistance, it will not undergo the liquification under the above-mentioned conditions (Hermanson et al. 1992).

Hydrophilicity of agarose, low non-specific adsorption features, wealth of the primary and secondary alcohols - suitable for variety of chemical modifications, convert it into one of the most largely used enzyme immobilisation matrices. Industrial agarose contains highly ionic sulphate groups. Some of the most widely employed commercially available beaded agarose supports are tabulated by Hermanson et al. (1992).

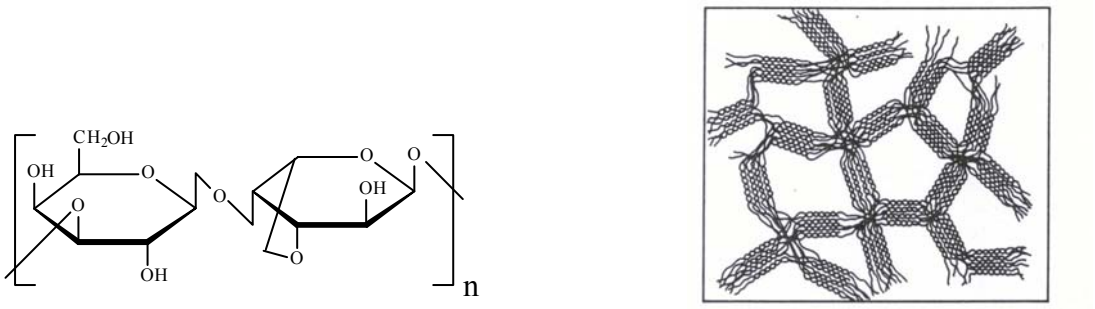

A **B**

Figure 1: Chemical structure of agarose: **A** - repeat unit of agarose polymer (Buchholz and Kasche 1997); **B** - schematic representation of agarose gel network (Gemeiner and references therein 1992).

Cellulose is a linear plant polymer, which consists of 1,4 β-D-glucose building-blocks (Fig. 2). The size of natural cellulose is defined by its degree of polymerisation or chain length, which in some cases may exceed a value of 10 000. These long cellulose molecules aggregate through inter- and intra- molecular hydrogen bridges between

three hydroxyl groups to form ribbon-like strands called microfibrils. The finest agglomeration within a microfibril is called an elementary fibril (3.5 nm in width). The cellulose does not posses the high effective porosity of agarose, but consists of polycrystalline assembles separated by amorphous areas. Industrially available low-porous celluloses are designed mainly as microgranular, microcrystalline, fibrous and powders. The problem with the unsuitable physical structure (low effective surface area), large microcrystalline regions inside the carrier and irregular particle shape of the low-porosity celluloses, can be undergo, by developing of high porous celluloses. Their preparation includes: liquefaction of the natural celluloses, subsequent dispersion in a non-miscible medium, solidification and shaping of the beads. Produced in this manner beads or irregular particles posses some advantages as: large internal specific surface area (~190 m^2/g) (Gemeiner 1992), chemical purity (contains substantially lower amount of lipids than the natural one) and therefore hydrophilicity, which contributes avoiding of undesired non-specific adsorption interactions. Activation methods that form cross-links, for example *N,N'*-carbonyldiimidazole appear to alter the porosity of the beaded cellulose (Hermanson et al. 1992).

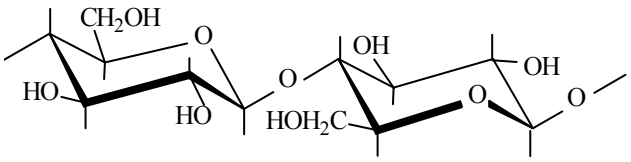

Figure 2: Repeating structure unit of a cellulose polymer based on 1,4-linked β-D-glucose residues (Gemeiner 1992).

Chitin is a natural by-product of the fishing (shrimp and crab) industry. This polysaccharide consists of fibrous (1→4)-linked 2-acetamido-2-deoxy-β-D-glucose which is acetylated incompletely to a different extend. The term chitosan is used generally for artificially deacetylated chitins ((1→4)-linked 2-amino-2-deoxy-β-D-glucose) with nitrogen content higher than 7% w/w (Gemeiner 1992). The properties of chitin and chitosan and various manufacturing approaches of fibers from the two natural polymers are reviewed (Agbah and Qin 1997). Chitin and chitosan are inexpensive matrices containing amino groups, which are used for enzyme immobilisation by adsorption and consequent cross-linking with glutardialdehyde.

Covalent attachment onto a carbonyl derivative, obtained by pre-treatment with glutardialdehyde, is another immobilisation manner.

Dextrans are linear water-soluble polysaccharides based on (1→6)-linked α-D-glucopyranosyl monomer blocks, which may be branched. Because of their low toxicity they are used widely for drug delivery as well as for the enzyme immobilisation. Cross-linked dextrans are known under the trade name Sephadex®. Primary developed as supports for exclusion chromatography (because of their molecular sieving features) later they are applied also as enzyme immobilisation matrices either by covalent binding *via* appropriate spacers or by ionic interactions to special Sephadex® derivatives. Due to its hydrophilic properties immobilisation of enzymes onto dextran shows almost no loss of catalytic activity. The low mechanical stability and complicated activation methods (using compounds of high toxicity) are the main factors explaining utilising of this matrix mainly for laboratory research purposes (Buchholz and Kasche 1997).

Inorganic matrices

Among the inorganic matrices as alumina, silica, zeolites, *porous glass* is the most used one (Robinson et al. 1971). The controlled porous glass is synthesised by special methods at high temperatures (800°C), which separate the glass into two phases (silicate- and borate- rich).

This material shows high resistance against pressure and microbial attacks, as well as to most of the organic solvents and extremely high temperatures (~300 °C), but is very labile at pH > 8 (Hermanson et al. 1992).

1.2. Synthetic matrices

The synthetic matrices are produced by polymerisation of functional monomers to give materials suitable for enzyme immobilisation. The polymerisation reactions could be separated principally into *chain-* and *stepwise-* reactions, which differ in mechanism and kinetics (Braun et al. 2001). *Chain reactions* start by generating in the most cases by an initiator or a catalyst of active centers – macro-radicals or macro-ions, which cause very rapid propagation process. The following chain termination

produces inactive macromolecules. Most types of polymerisation processes could be included in this group. In contrary the *stepwise reactions* proceed very often without catalyst and any true termination *via* following (sequential) addition of reactive monomer, oligomer or polymer molecules. Typical stepwise processes are the polycondensation and polyaddition reactions. Plenty of procedures for the synthesis of different polymer species is summarised by Sorensen and Campbell (1962).

The methods for manufacturing macromolecular materials could be divided into three different categories described by Braun et al. (2001) (Table 1). *Polyreactions in bulk* proceed without solvent and therefore very pure polymers of high molecular weight could be obtained with high reaction rates. By addition of a solvent (*polyreactions in solution*) the viscosity of the reaction mixture decreases, which speeds up the heat and mass transfer processes. By the *dispersion processes*, used also here, a liquid monomer is dispersed by stirring in a liquid, in which it is insoluble or only partly soluble. The polymerisation process occurs in the formed small droplets. Some dissimilarities between the emulsion and suspension polymerisation concerning the initiator; the solubility of the monomer in the liquid phase; the "dispersion regions" in which the initiation and propagation occur; and the sizes of the produced particles are discussed by Braun et al. (2001). Through precise control of parameters such as: reaction temperature, concentration of the dispersant (surfactant), volume ratio monomer/water, geometry of the reactor and intensity of stirring, beads with a defined particle size distribution can be manufactured.

Table 1: Processes for manufacturing macromolecular compounds (Braun et al. 2001).

Processes in bulk	• liquid state • solid state • gas phase
Processes in solution	• aqueous solutions • organic solutions
Processes in dispersion	• suspension • emulsion

Polymer supports typically have superior physical and chemical stability and can withstand the rigors of long time applications better than natural soft gels. The physical strength of the synthetic supports often allows increased linear flow rates and

thus greater throughput (Hermanson et al. 1992). These advantages are the primary reasons for the current growing popularity of polymeric carriers in the biotechnology industry. Suitable chemical modification (covalent attachment of a low molecular weight chemical compound to the polymer macromolecule (Braun et al. 2001)) of these matrices will provide functional sites for enzyme immobilisation.

Widely applied in the biotechnology matrices are: acrylamide derivatives; methacrylate derivatives; polystyrene and its derivatives; and recently poly(vinylalcohol) (Fig. 3).

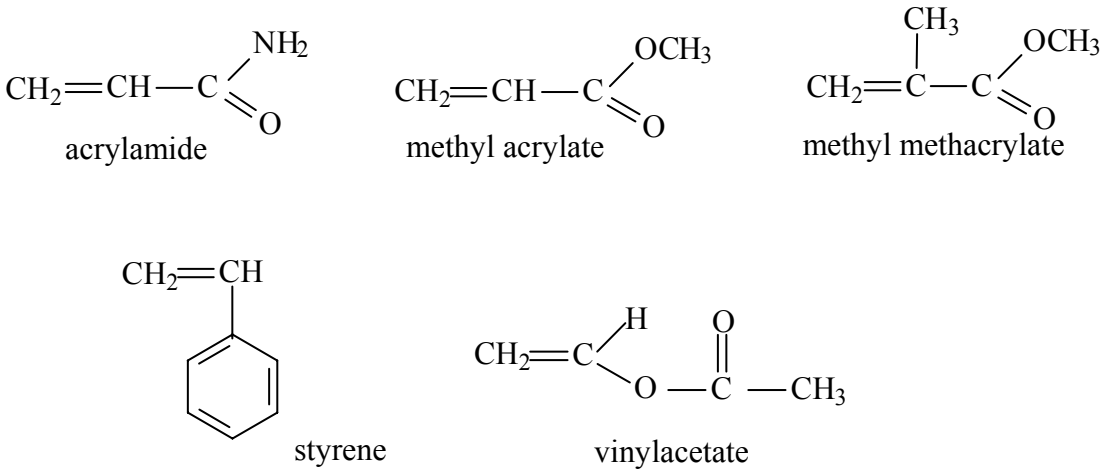

Figure 3: Chemical structure of different monomers used as basic blocks in the synthesis of polymer matrices.

Porous *polyacrylamide beads* were probably the first synthetic polymer chromatography matrix to be described in the literature (Hermanson et al. 1992). The material consists of polyacrylamide chains cross-linked by *N,N´*-methylene-bis(acrylamide). Principle suppliers of acrylamide-relevant matrices are BioRad Laboratories (USA) - different modifications of polyacrylamide under the trade name "Bio-Gel P" and IBF Biotechnics - beaded polyacrylamide derivative known as "Trisacryl". Several advantages of these supports are: good pH stability, chemical and microbial resistance, low non-specific binding ability. Due to the poor mechanical features of "Bio-Gel P" (resistance against increasing pressure) and tendency to swell in various buffer compositions, this matrix never became in high favour for the affinity separations. In contrary "Trisacryl" provides much higher mechanical resistance.

Widely applied in biotechnology *methacrylate derivative*, which contains epoxy groups, is known under the trade name Eupergit® (Rohm Pharma, Germany); (Katchalski-Katzir and Kraemer 2000, Mateo et al. 2000a, Mateo et al. 2000b, Janssen et al. 2002). The base-matrix is available in four particle size-distribution forms: 30 μm, 150 μm, 250 μm and a non-porous type of 1 μm. The first three groups of beads possess sophisticated porous structure consisting of relatively large cavities and channels (0.1-2.5 μm), constructed from a network of small micro-beads (Hermanson et al. 1992). The above-mentioned structure is a precondition for high effective internal surface area, as well as good mechanical and physical stability. Even high concentrations of buffer salts, organic solvents and detergents can not affect the spatial structure of Eupergit®. Biomolecules can be coupled to this matrix either directly (reaction of its epoxy-groups with -SH, -OH, $-NH_2$ groups of the bioligand) or by further modification of the epoxy-sites in order to increase the distance matrix-bioligand. Different fabrication methods, properties and/or possible biotechnological applications of other methacrylate derivatives were described by (Koilpillai et al. 1990, Li and Stöver 1999, Cipran et al. 2003).

A plenty of procedures for preparation of different types (size distribution, chemical structure, mechanical and morphological properties) of *methyl methacrylate derivatives* were represented in the literature in the recent years (Chen and Lee 1999, Li and Salovey 2000, Avella et al. 2001). The application of these beaded polymer species in the biotechnology and biomedicine rises (Langer et al. 1997, Arica et al. 2000).

Polystyrene is one of the polymers extensively used as a matrix in ion-exchange techniques (Buchholz and Kasche, and references therein 1997). Porous supports made-up of polystyrene (PerSeptive Biosystems, USA) represent a new development in chromatographic media (Hermanson et al. 1992). The large network of pores in the matrix allows higher diffusion flow-rates inside the particle; the cross-linked polysryrene beads are resistant to pH and pressure changes, and can withstand the cleaning and sanitation procedures without suffering the structure changes. Manufacturing of a large selection of polystyrene beads was developed in the recent years (Hatate et al. 1994, Pişkin et al. 1996, Okubo et al. 1998, Watanabe et al. 2000). Due to its extreme hydrophobicity the polystyrene is employed for non-covalent

attachment of bioligands, through a passive adsorption. The unmodified polymer does not contain appropriate active functional sites for covalent attachment of bioligands. About 80% of the polymer matrices established on the market consist of hydrophobic materials, which are often not biocompatible, which results in a limited usefulness. *Polyvinylalcohol* due to its hydrogel-like properties overcomes this problem and it is easy to be manufactured and modified. Polyvinylalcohol-based matrices can be functionalised with many different groups (-SH, -COOH, $-NH_2$, $-NH(NH_2)$ etc.) and modified with individually tuneable loadings. The application of this matrix (also in the form of magnetic polymer beads) for biotechnological and biomedical purposes rises (Manecke and Vogt 1980, Manecke and Polakowski 1981, Bergemann et al. 1999, Akgöl et al. 2001).

1.3. Magnetic matrices

Magnetic carrier technology originates from studies on waste water-treatment, where the objective was to adsorb organic matter onto small particles of magnetite (Fe_3O_4) and to separate the loaded magnetite from the bulk process liquor. The separation stage was affected first by means of an external magnetic field, allowing then these larger coagula to sediment under gravity; a technique sometimes referred as magneto-flocculation (Pieters et al. and references therein 1992). In particular magnetic carrier technology offers also a novel and convenient way to selectively separate the magnetic matrix with immobilised enzyme from the mixture of substrates and products. Besides the general criteria (mentioned above) defining the choice of an enzyme matrix, the magnetic carries must possess also suitable magnetic properties. The basis of the magnetism aspects is described in Appendix I.

Types of magnetic matrices

Magnetic support materials can be produced mainly in three different manners (Thomas and Franzreb will be published) (Fig. 4):

- *coating of a magnetic core* with different natural or synthetic polymers or inorganic materials.
- *encapsulation* of magnetic solids within natural gels or synthetic polymers.

- *infiltration* of porous matrices with fine magnetic sub-micron particles, or aqueous mixtures of Fe^{2+} and other metal ions (e.g. Fe^{3+}, Ni^{2+}, Mn^{2+}, Zn^{2+}, Cu^{2+}) capable of forming magnetic ferrites.

Detailed classification of the magnetic matrices, according the manner of their synthesis and areas of application, can be found also in Pieters et al. (1992).

Among the materials, which could be utilised as *magnetic cores* ferrites are available in large amounts and have the common chemical structure $MO{\cdot}Fe_2O_3$, where M is Fe, Ni, Mn. The magnetic iron oxide magnetite ($FeO{\cdot}Fe_2O_3$ or Fe_3O_4) is the most widely employed for these purposes and can be synthesised from $1Fe^{2+}/2Fe^{3+}$ salts aqueous solution - heated up to 70°C and precipitated by increasing the pH, or isolated from magneto-lactic algae or bacteria. The sizes and the form of the magnetic core as well as the coating material can be varied in order to produce a magnetic matrix with defined properties (with respect to the separation technique and/or bioligand-immobilisation).

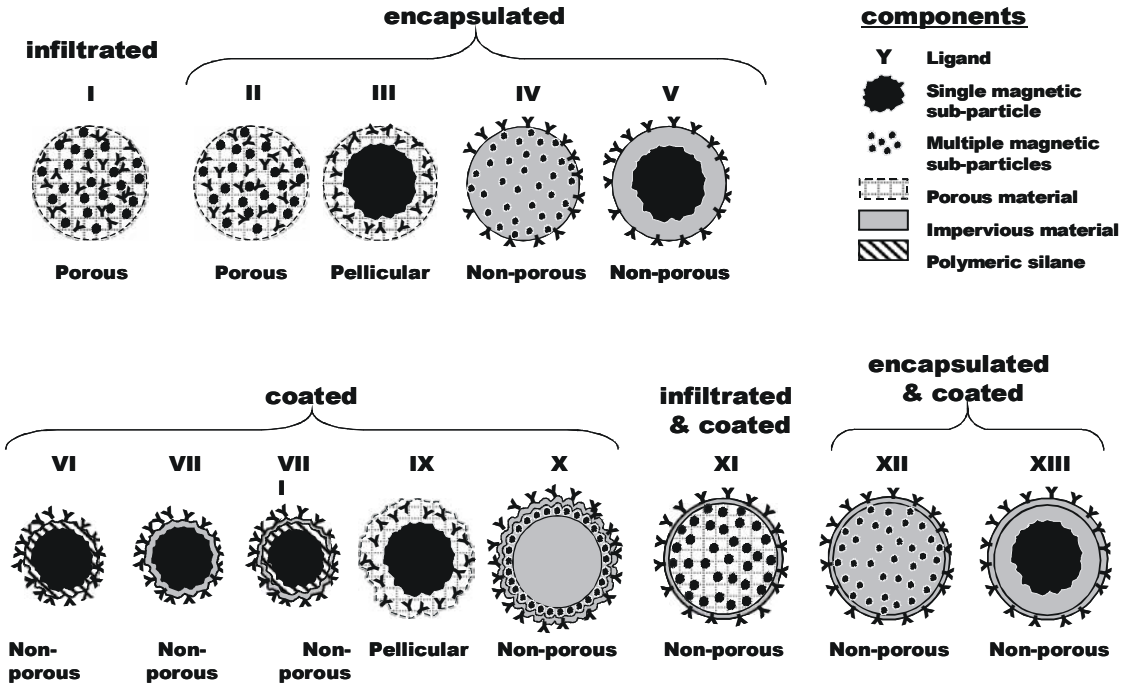

Figure 4: Different types of magnetic matrices (Thomas and Franzreb will be published).

The four most largely employed coating methods are: polymer adsorption, silanisation, graft polymerisation and co-precipitation. In the first case different

natural or synthetic polymers can be electro-statically adsorbed onto the surface of magnetic particles, which are charged, providing coatings for further chemical modification (Fig. 4-VII). Silane coupling chemicals are utilised to introduce reactive organo-functional moieties (most often primary amino- or epoxy- groups) to the magnetic crystals or particles (Whitehead et al. 1987, Shinkai et al. 1991, Hubbuch 2001). The best known micro-sized silane-coated magnetic carrier is BioMag (Polysciences, Inc., UK) (Fig. 4-VI). Introducing a polymer graft, which can "grow" at the surface of the magnetic particle is another way to produce coated non-porous magnetic supports. In these methods usually a suitable monomer is polymerised, forming a thin layer onto the surface of silanised magnetic particles (Halling and Dunnill 1980, Hubbuch 2001, Thomas and Franzreb, and references therein will be published) (Fig. 4–VIII). Figures 4-XII and 4-XIII represent the appearance of the materials obtained by polymer grafting to the surfaces of encapsulated non-porous magnetic supports of types IV and V in the same figure. Co-precipitation of $2Fe^{3+}$ and $1Fe^{2+}$ salts in aqueous solutions (producing in alkali conditions (pH 9-10) magnetic iron oxide crystals) in the presence of a suitable polymer (dextran, chitosan etc.) provides an elegant method for the synthesis of magnetic core matrices (Yen 1981, Thomas and Franzreb, and references therein will be published) (Fig. 4-VII). *Encapsulation* of the magnetic sub-particles in different natural (Guesdon et al. 1979, Šafaříková et al., in press 2003) and synthetic polymers, or inorganic materials (e.g. magnetic porous glass- Fig. 4-II) is another manner of magnetic carrier manufacturing. Among the different polymerisation processes of magnetic (micron and sub-micron-sized) carrier fabrication "water-in-oil" and "oil-in-water" techniques are some of the most widely used. Magnetic matrices of this type are produced by high speed stirring a solution in an aqueous or a hydrophobic media of monomer (and co-monomer), initiators, surfactants and iron oxides (in a form of a fine powder or ferrofluids - suitably tenside-stabilised) in a hydrophobic or aqueous phase. In the first case the process is called "water-in-oil" and in the second "oil-in-water" method (Dixon et al. 1980, Clemence et al. 1984, Setschell 1985 and references therein, Akgöl et al. 2001, Muller-Schulte 2001). Due to the stirring the beaded droplets are formed in the dispersed reaction mixture. Their size depends on the stirring rate, reactor shape, as well as on type and percent of the surfactants in the reactor. Solid beads are then formed by polymerisation in the above-mentioned droplets. Most types of the particles produced in this manner have the characteristics of non-porous

supports (Fig. 4-IV and 4-V). The schematic structure of porous macro-beads synthesised in a similar way is represented in the figures 4-II and 4-III. Commercial polyvinyl alcohol magnetic beads (used in this work) fabrication is described by Muller-Schulte (2001). The process itself is "water-in-oil" polymerisation, where the water phase consists of aqueous polyvinyl alcohol solution in which suitable surfactants as well as magnetic ferrofluids are dissolved / dispersed. The oil-phase is a common vegetable oil. Homogenised (ultrasound treatment) water phase is suspended by stirring (speeds up to 2000 rpm) into the oil phase, followed by addition of a cross-linker in order to create (within minutes) a polymer network for entrapment of the sub-micron sized magnetic material. Spherically shaped magnetic particles of high hydrophilicity and 1-10 μm sizes are obtained. *Infiltration* includes penetration (permeation) of magnetic crystals within macro-porous matrices (Fig. 4-I). Mosbach and Anderson (1977) as well Torchilin et al. (1985), infiltrated and trapped magnetic materials into commercially available Sepharose (in the first case) or Sephadex (in the second case) supports. A novel infiltration/precipitation/coating route is employed to produce one of the most largely applied polymer magnetic matrices - Dynabeads (Dynal A/S, Norway), which are offered on the market in extremely discrete sizes of 2.8, 4.5 or 5.0 μm. Synthesised in the first step polymer particles of uniform size are then suspended in an aqueous Fe^{2+} salt solutions, which permeates into the particle pores. There a part of Fe^{2+} is oxidized to oxy / hydroxide intermediates, which under following heating is transformed into small crystals of magnetite and maghemite. The synthesised magnetic polymer beads are then treated with synthetic polymers in order to fill their pores and coat their surface. After completion of all three processes non-porous magnetic polymer matrices of very discrete size-distributions are obtained (Ugelstad et al. 1987) (Fig. 4-XI). Some disadvantages of this method are the high hydrophobicity of the basic polymer (polystyrene) as well as the long reaction times. Most of the suppliers of magnetic micro-matrices can be found under http://www.magneticmicrosphere.com.

Magnetic matrices for biotechnological applications – criteria of choice

In order to be applied in the immobilisation technology, magnetic particles must fulfill not only the general criteria defining the choice of appropriate matrix for a desired biotechnological process, but also certain characteristics with respect to their

magnetic properties. Aggregation tendency of the carrier due to remanent magnetism can be avoided by utilising superparamagnetic materials. Such “species” will become magnetised and aggregate when an external magnetic field is applied, but once the field is removed they will easy re-disperse, because of the absence of a “magnetic memory”. Magnetic susceptibility of the carrier is also an important criteria for the separation techniques. Higher susceptibility will augment the effectiveness of the magnetic separation in generally. However, higher amounts of a magnetic material within the matrix (higher magnetic susceptibility) will increase also the overall density of the particles and therefore the gravitational sedimentation will become more rapid (Pieters et al. 1992). Non-magnetically aggregation can be controlled to some extend, by adapting the particle size, the surface chemistry or by choosing proper suspending electrolytes. The choice of a suitable magnetic matrix is a compromise between all these criteria. The utilising of magnetic beads in different bioassays has been reviewed by Haukanes and Kvam, (1993); several clinical applications are described by Häfeli et al. (1997). Superparamagnetic supports magnetic with sizes of 0.5-1 µm and magnetic susceptibility > 35 $A \cdot m^2 \cdot kg^{-1}$ (ρ= 2-4 $g \cdot cm^{-3}$; magnetic core contents of 50 % or higher) settle only very slowly, but are rapidly separable by moderate magnetic fields (Thomas and Franzreb will be published).

2. Materials and methods

2.1. Synthesis of the magnetic matrices

2.1.1. Materials

Poly(vinyl alcohol) magnetic beads: M-PVA 012 (non-modified); M-PVA E02 (epoxy-modified); M-PVA N12 (amino-modified) were kindly donated by chemagen Biopolymer Technologie AG (Baesweiler, Germany). Poly(methyl methacrylate) beads Calibre CA 6-6 were from Microbeads (Norway). Oleic acid - extra pure, methylacrylate, divinylbenzene (55 % tech. mixture of isomers), glutardialdehyde (25 % and 50 % v/v), were obtained from Merck (Germany). Vinyl acetate (99 %; GC), methylene blue (0.05 % w/v), 3-aminopropyltriethoxysilane, 2,4,6-trinitrobenzenesulfonic acid (5 % w/v) were from Sigma-Aldrich Chemie GmbH (Germany). Poly(vinylalcohol) (MW 22 000, 88 % HD) and glycidol were from Acros Organics (Fischer Scientific GmbH, Germany). Polyethersulfone filters 0.45 μm were from PAL Gelman Lab. (PAL Corporation, USA). Polycarbonate filters 0.22 μm were from Osmonics GmbH (Germany). All other chemicals were analytical grade.

2.1.2. Synthesis of surfactant coated magnetic gel

Superparamagnetic Fe_3O_4 nano-particles with a mean diameter of 8-10 nm (Fig. 5) were prepared by chemical co-precipitation of Fe(II) and Fe(III) salts ($2Fe^{3+}$:$1Fe^{2+}$) in an aqueous solution at high pH (reached in the case of this work by use of ammonium hydroxide) and under nitrogen atmosphere.

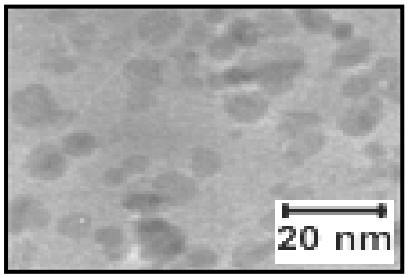

Figure 5: Transmission electron micrograph of the synthesised magnetite nano-particles.

Due to the very fast co-precipitation the produced magnetite (Fe_3O_4) is poorly crystalline and partly oxidized to maghemite Fe_2O_3 (Cornell and Schwertmann and references therein 2000). Therefore it does not have the magnetisation saturation of pure magnetite. By addition of non-ionised oleic acid to the suspension during the precipitation, the formed nano-particles of magnetite were coated with a double surfactant layer (Fig. 6). Similar procedures were described by other authors (Reimers and Khalafalla 1976, Shen et al. 1999). Although some research has been focused on the synthesis of magnetic particles stabilised by surfactant double-layer, the concept of this stabilisation has not yet progressed beyond being a reasonable hypothesis (Shen et al. 1999). The fabrication of the gel was done as follows: in 1 L conical flask equipped with electric heater, paddle stirrer and inlet systems for nitrogen and reactants, a mixture of 8.6 g $FeCl_2 \cdot 4H_2O$ and 23.5 g $FeCl_3 \cdot 6H_2O$ was dissolved into distilled water (500 ml) at 85°C by stirring (700 rpm) and kept under an atmosphere of nitrogen. In the second step aqueous ammonia (28 ml, 25% w/v $NH_3 \cdot H_2O$) was added rapidly to the aqueous solution at 85°C, which was stirred further efficiently with a mechanical paddle. The sum-equation of the chemical reaction proceeded is shown below:

$$Fe^{2+} + 2Fe^{3+} + 8OH^- = Fe_3O_4 + 4H_2O \qquad (1.1)$$

The formed in the process magnetite is black coloured iron oxide, which consists of Fe(II) and Fe(III). It is not thermodynamically stable at atmospheric O_2 pressure and oxidises to maghemite (γ-Fe_2O_3). This oxidation can be traced by colour change from black to red-brown. Both iron oxides are ferrimagnetic, but have different Curie-Temperatures (T_C= 850 K for magnetite and T_C= 820 to 986 K for maghemite). Under a certain particle size (~ 10 nm) and for $T < T_C$ these oxides show superparamagnetic behaviour (Cornell and Schwertmann 1996). Immediately after the addition of the aqueous ammonia, 16 ml oleic acid were added slowly *via* a burette to the magnetite suspension. The process lasted 15-20 min. until there was a clear supernatant. After cooling to ambient temperature, the supernatant was decanted and the black magnetite gel, containing 10g of magnetite was washed with copious amounts of distilled water and in the end collected magnetically.

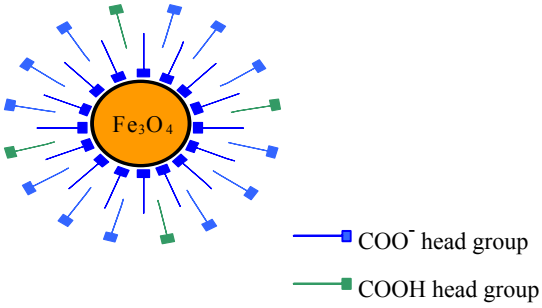

Figure 6: Schematic representation of the structure of the surfactant bi-layer stabilised magnetic particles - modified diagram (Shen et al. 1999).

2.1.3. Transformation of poly(methyl methacrylate) (PMMA) beads into magnetic modifications by "swell-deswell" manufacturing method

Magnetic PMMA beads were produced as described by Franzreb et al. (2002). Magnetic polymer particles (monodisperse or of a narrow size distribution) are fabricated by a two-steps procedure. In the first step hydrophobic polymer particles (PMMA in the case of this work) were swollen with magnetic colloids (stable homogeneous colloidal dispersion of magnetic materials) in a non-polar organic solvent, capable to expand the polymer matrix volume. Then the solvent is removed (extracted) from the swollen magnetic polymer beads, while nano-sized magnetic material is trapped into the polymer structure (Fig. 7).

The PMMA magnetic beads here were produced by swell-deswell manufacture-method as follows:

- 25 ml toluene-based magnetic colloid were produced by dispersing 4.5-5 g magnetite (in the form of a magnetic gel described above) in toluene. The colloid was homogenised ultrasonically for 15-20 min. (ultrasound-bath Sonorex RK 100H).
- 5 g PMMA beads - Calibre CA 6-6, were swollen by immersing into the above-described magnetic colloid and intensively stirred (with magnetic rod) for 4-6 h at 45 °C.
- The swollen polymer magnetic beads were separated from the magnetic colloid by centrifugation.

- The swollen particles were then washed for several times with approx. 200 ml aqueous solution of 0.5 % w/v NaOH and 1 % w/v SDS in order to remove the magnetite excess from the particle surface.
- The washed particles were deswollen by extraction of the toluene in ethanol or acetone for 12 h at room temperature (stirring with a magnetic rod).
- The compact magnetic polymer particles were recovered from the organic solvent by centrifugation.

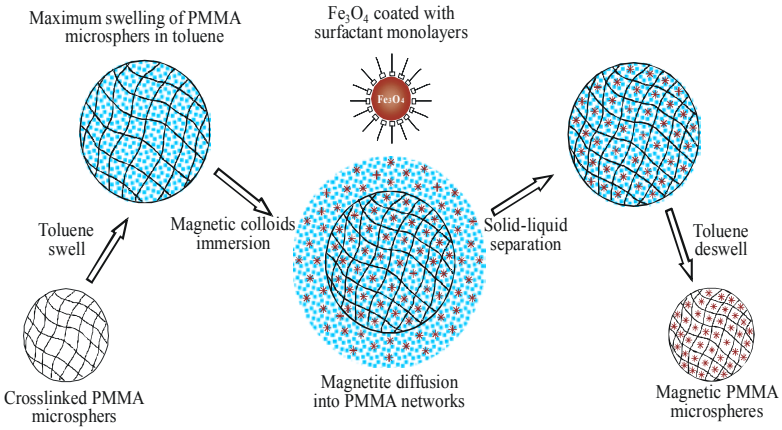

Figure 7: Swell-deswell method for the fabrication of hydrophobic polymer magnetic beads - schematic representation (Franzreb et al. 2002).

2.1.4. Synthesis of poly(methylacrylate) (PMA) magnetic beads by suspension polymerisation method

Superparamagnetic PMA beads of type IV shown in the Fig. 4. were manufactured by "oil-in-water" method described above. By mixing the oil phase (containing the monomer, homogeneously dispersed magnetic gel and a cross-linker) and the water phase (consisting of an aqueous solution of surfactant and stabiliser) at a suitable stirring speed, micro-sized oil droplets are formed into the water media. Therein the monomer polymerises, being in the same time cross-linked. During the polymerisation the magnetic gel (consisting of magnetite / maghemite nano-particles) was entrapped into the cross-linked particles, converting them into magnetic ones. Oil- and water- phases preparation, as well as the suspension polymerisation process for manufacturing of approximately 90-95 g beads are represented below.

Oil phase preparation

25 g magnetic gel were dispersed into a mixture of monomer - 100 ml methylacrylate and cross-linker (10 ml, 55% divinylbenzene - DVB) by intensive stirring (magnetic rod) at room temperature for 30 minutes. For better homogenisation, the mixture was treated for 15-20 minutes ultrasonically in Sonorex RK 100H. Thus a stable hydrophobic monomer-based magnetic fluid was formed. 1-2 g benzoyl peroxide (BPO) were added as a initiator for the polymerisation into the above-described magnetic fluid just before mixing the oil- and the water- phases.

Water phase preparation

25 g poly(vinyl alcohol) (PVA; MW 22 000, 88 % HD) were dissolved by intensive magnetic rod stirring in 500 ml distilled water at 60-70 °C (in a conical flask equipped with a thermometer). Separately 50 g NaCl were dissolved in another 500 ml distilled water by intensive magnetic rod stirring.

Mixing oil and water phases. Performance of the polymerisation process

The above-prepared two components of the water phase, were transferred into a 2.5 L cylindrical four-neck glass reactor equipped with electric heater, paddle stirrer, thermometer and inlet systems for nitrogen and reactants. The water phase was heated up to 50 °C or 60 °C (in order to obtain two types beads – smaller-ones (PMAs) at 50 °C and bigger-ones (PMAb) by starting at 60 °C) under intensive nitrogen flow and stirring with 700 rpm, and 1 ml of water soluble inhibitor methylene blue (MB, 0.05 % w/v solution in water) was added. Once the inhibitor was added and the desired temperature was reached, the oil phase was suspended into the water phase and the process lasted for one hour at 50 °C (respectively 60 °C). In one hour the temperature was increased further up to 70 °C and the process was conducted at these conditions for another three hours. Then the reaction mixture was heated to up to 85 - 90 °C and the reaction was conducted for further one hour. The stepwise increasing of the temperature allows better control of the particle size-distribution. Schematically the suspension polymerisation procedure is shown in the Fig. 8. The

most probable, idealised structure of the DVB-cross-linked polymer is represented in the Fig. 9.

Washing procedure

After the polymerisation was completed, the reaction mixture was cooled down to 60 °C. The synthesised superparamagnetic polymer micro-particles were recovered by magnetic separation. Several washing steps with hot water (approx. 3-4 L) were performed by intensive stirring with a magnetic rod. In the end the polymer superparamagnetic beads were collected magnetically and stored for further use in distilled water at 4 °C.

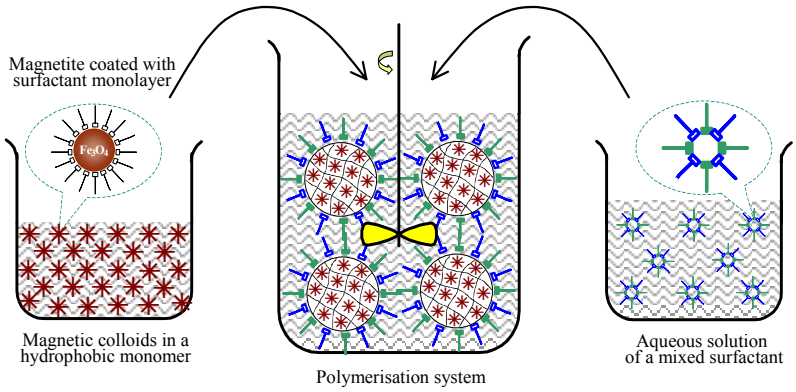

Figure 8: Suspension polymerisation method - schematic representation.

2.1.5. Synthesis of poly(vinylacetate) (PVAc) magnetic beads by suspension polymerisation method

Superparamagnetic poly(vinyl acetate) beads were manufactured in a similar manner as the described above for the poly(methyl acrylate) ones. The suspension polymerisation procedure with regard obtaining approximately 120 g beads was modified as presented below.

Oil phase preparation

35 g magnetic gel were dispersed in mixture of 140 ml vinyl acetate and 15 ml DVB. After appropriate homogenisation of the gel into the hydrophobic monomer 5 g BPO were added.

Water phase preparation

45 g PVA (MW 22 000, 88 % HD) were dissolved in 500 ml distilled water in a way as already described above. Another 500 ml distilled water were added to the solution and it was transfered into the polymerisation reactor.

Mixing oil- and water- phases. Performance of the polymerisation process

- 2 ml methylene blue were added to the stirred in the above-mentioned reactor water phase.
- The initial temperature, at which the oil phase was added in the reactor, was 45 °C and the process was performed at this temperature for 20 min (under nitrogen atmosphere).
- After further increase of the temperature up to 55 °C, the process was conducted for further one hour.
- The reaction mixture was heated up to: 60 °C (process lasted 1 h); 70 °C (for 2 h); 80 °C (for 1 h).

Washing procedure

The washing of the produced superparamagnetic PVAc beads was performed in the same manner as already described for PMA matrix.

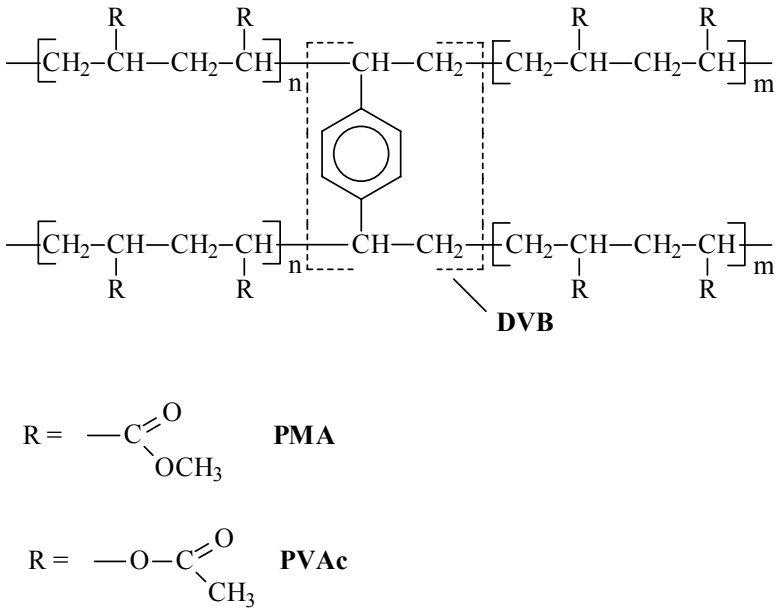

Figure 9: Idealised schematic chemical structure of the DVB-cross-linked PMA and PVAc polymer.

2.1.6. Synthesis, aminosilane- and poly(glutaraldehyde)- coating of iron oxide crystals (Amino-Silanised-Magnetic-Particles ASMP)

Iron oxide nano-crystals preparation

Iron oxide crystals were prepared in a similar way of $1Fe^{2+}$: $2Fe^{3+}$ salts co-precipitation in highly alkaline aqueous media, as already described in this work procedure for magnetic gel fabrication – equation (1.1). The detailed procedure is presented below:

- 200 ml aqueous solution (S1) containing 0.25 M $FeCl_2 \cdot 4H_2O$ and 0.5 M $FeCl_3 \cdot 6H_2O$ were prepared and the insoluble solids were removed by filtration (0.45 μm cellulose nitrate filter).
- 200 ml 5 M NaOH – (S2) solution were prepared.
- 100 ml of distilled water were poured into a 1 L glass beaker and stirred intensively (1000 rpm) with mechanical paddle.
- S1 and S2 solutions were poured simultaneously into the glass beaker and the stirring was continued for further 5 min.

- The pH of the above reaction mixture was reduced to 7 – 8. Several washing procedures (3 times with approx. 600 ml 0.2 M NaCl, followed by 3 times with approx. 600 ml distilled water) were performed. In the end pH was settled to 7 – 8 carefully with 1 M HCl. During the washing procedures the liquid portion was separated by pumping-out after the iron oxides were settled magnetically.
- The end volume of the free supernatant in the magnetic suspension was reduced down to 200 ml.
- 800 ml analytical grade methanol were added to the magnetic suspension (iron oxide crystals in distilled water). After re-suspension, the iron oxides were magnetically settled and the liquid part was again pumped-out.
- Finely two more methanol-washing steps were performed (approx. 400 ml methanol for each step) in order to reduce the water content in the slurry down to ~ 1 % v/v, the final volume of the free supernatant in the magnetic suspension was reduced to 250 ml.

Homogenisation and aminosilane derivatisation

The aminosilane derivatisation as well as the following poly(glutaraldehyde) coating were conducted as described by Hubbuch and references therein (2001).
Detailed procedure of the aminosilane derivatisation follows below (Fig. 10):

- The above-produced iron oxide crystals suspension (in approx. 250 ml methanol) was homogenised for 5 min at 2000 rpm in a 1.5 L cylindrical reactor of Rotor-Stator-System “Polytron PT 6100” (Kinematica AG, Switzerland).
- 5 ml gracial acetic acid and immediately after it 10 ml 3-aminopropyltriethoxysilane (APTES) were added and the homogenisation was continued for further 10 min at 13000 rpm. In the end the reaction mixture was homogenised for next 120 min at 6000 rpm.
- The slurry was poured into a 500 ml beaker containing 200 ml glycerol, while introducing nitrogen flow, and heated at 110 °C for 1.5 – 2 h.

- The silanisation reaction was continued then at 110 °C for 14 h and finally at 160 °C for 30 min. (evaporation of the silane excess). During the whole process the reaction mixture was stirred with a mechanical paddle (600 rpm).
- After cooling down to ambient temperature, the silanised iron oxide crystals were then washed: three times with approx. 200 ml 0.2 M NaCl and then three times with approx. 200 ml distilled water, and stored at 4 °C in distilled water.

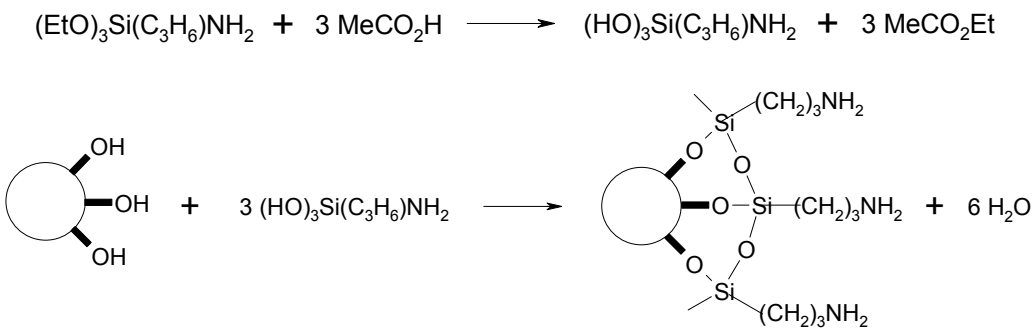

Figure 10: Aminosilane coating of iron oxide crystals - schematic representation.

Poly(glutaraldehyde) coating

The poly(glutaraldehyde) (PGA) coupling procedure to the aminosilanised iron oxide crystals is shown in the Fig. 11.

- 10 g aminosilane coated magnetic particles were transferred into a glass beaker and re-suspended by stirring with a mechanical paddle (550 rpm) in 1200 ml distilled water.
- 70 ml 50 % v/v glutardialdehyde were added and pH was adjusted immediately to 11 with 1 M NaOH.
- The reaction was conducted for 1 h in a fume cupboard at pH 11 (1 M NaOH was used for adjusting the pH).
- After the reaction was completed the supernatant was decanted and the magnetic particles were washed as follows: three times with approx. 500 ml 0.2 M NaCl and in the and three times with approx. 500 ml distilled water, and stored at 4 °C.

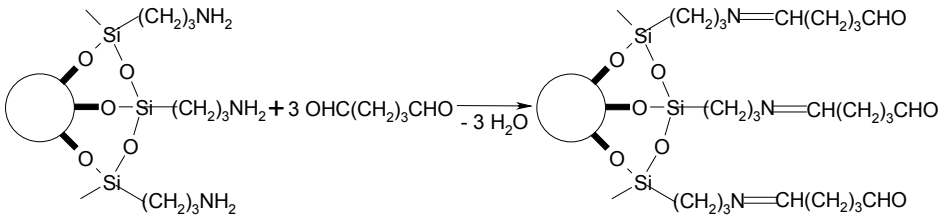

Figure 11: Poly(glutaraldehyde) coating of ASMP - schematic representation.

2.2. Surface modification of the magnetic matrices

2.2.1. Epoxy-modification of the polymer magnetic beads

Epoxy-modification of M-PVA beads

50 mg M-PVA 012 non-functionalised beads were treated with 1 ml epichlorohydrine (ECH) and 0.5 ml 3.5 M NaOH in 0.5 ml dimethylformamide for 22 h at 40°C under intensive mixing in an Eppendorf-Thermomixer (1200 rpm) (Fig. 12). After the reaction was completed, the activated beads were washed intensively with distilled water and in the end washed and stored in acetone at 4 °C.

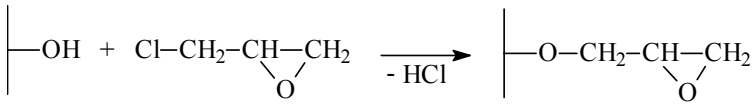

Figure 12: Epichlorohydrine epoxy-modification of non-functionalised M-PVA 012 superparamagnetic beads - schematic representation.

Epoxy-modification of PMMA magnetic beads

1 g superparamagnetic PMMA beads were suspended in 50 ml glycidol containing approx. 0.5 g sodium methylate as a catalyst. The ester-exchange process was conducted under vacuum at 100°C for 6 h under intensive stirring (magnetic rod) (Fig. 13). Similar ester-exchange procedure is described by Kurokawa et al. (1996). Once the process was completed, the beads were washed as described above for PVA matrix ECH-activation.

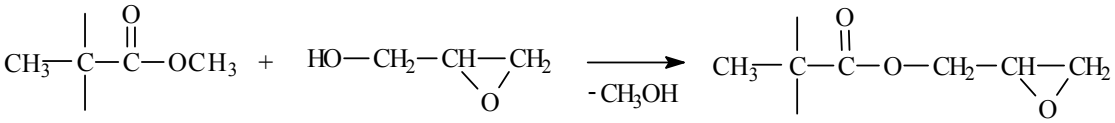

Figure 13: Glycidol epoxy-activation of superparamagnetic PMMA beads - schematic representation.

Epoxy-modification of PVAc magnetic beads

The procedure of epoxy-modification PVAc beads proceeded in two steps (i) alcoholysis with methanol (Fig. 14) and (ii) ECH activation of "poly(vinylalcohol) layer-coated" PVAc beads (Fig. 12).

The alcoholysis reaction was conducted as follows: 20 g magnetic PVAc beads were re-suspended in 200 ml of reaction mixture containing 194 ml analytical grade methanol, 6 ml distilled water and 9 % w/v NaOH and the process was performed at 45 °C for 6 h by intensive magnetic-rod stirring. PVAc magnetic beads covered by a thin outer layer of poly(vinylalcohol) were produced. The beads were washed as already described in PVA matrix ECH-activation

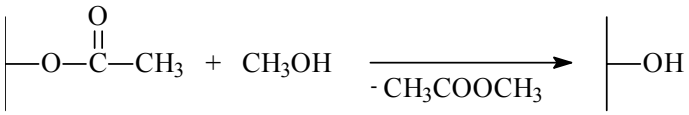

Figure 14: Modification of PVAc magnetic beads in order to obtain an outer layer of poly(vinylalcohol) - schematic representation.

For the epoxy-modification – 5 g PVAc hydroxyl-terminated magnetic beads were added to a mixture containing 50 ml ECH, 1 g NaOH and 50 ml dimethylformamide or acetone. The reaction was conducted for 24 h at 35 °C by intensive magnetic-rod stirring. Once the reaction was completed, the beads were washed and stored as described above for ECH-activation of PVA matrix.

2.2.2. Amino-modification of the magnetic matrices

Amino-modification of epoxy- M-PVA magnetic beads

Amino-functionalisation of M-PVA E02-epoxy particles was performed as described by Muller-Schulte (2001) (Fig. 15). The procedure was modified as follows: 300 mg M-PVA E02 epoxy-activated particles were reacted with 20 ml 10 % w/v 1,6-diaminohexane (hexamethylene diamine, HMDA), in which 0.02 g NaOH were dissolved, for 6 hours at 65 °C under intensive stirring with a magnetic rod. The

modifying agent (HMDA) was taken in 120 fold excess compared to the amount of epoxy-sites of the matrix. After completion of the reaction and several washing steps with distilled water, the amino-charged beads were stored in it at 4 °C.

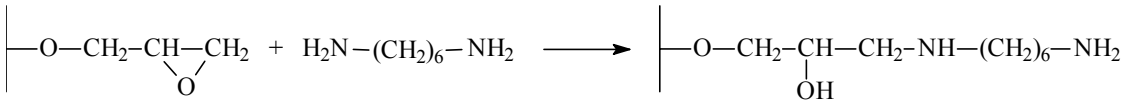

Figure 15: Hexamethylene diamine modification of epoxy-M-PVA and epoxy-PVAc magnetic beads - schematic representation.

Amino-modification of epoxy- PVAc magnetic beads

HMDA-modification of epoxy-charged PVAc magnetic beads was performed by the procedure already presented above for PVA carrier (Fig. 14). The modifying agent was taken in 70 fold excess over the amount of epoxy-sites of the matrix.

Amino-modification of PMA magnetic beads

5 g magnetic PMA beads were added to 100 ml ethylene diamine (EDA) and the ammonolysis reaction was performed at 100 °C for 8 h, by intensive stirring (magnetic rod) (Fig. 16). The modifying agent was taken in 700 fold excess over the amount of methoxy-sites of the matrix. The amino-charged beads were washed and stored in distilled water at 4 °C.

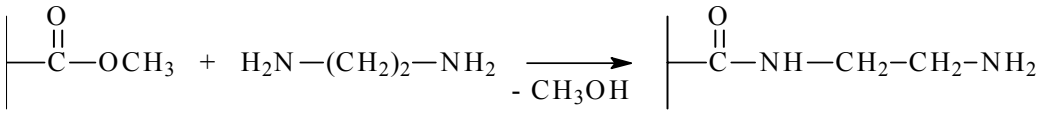

Figure 16: Ethylene diamine modification of PMA magnetic beads - schematic representation.

Amino-modification of poly(glutaraldehyde) coated ASMP particles

Defined amount of ASMP (poly(glutarladehyde) coated) particles was transferred into an Erlenmeyer flask and 0.072 ml water solution of HMDA (10 % w/v, containing

also 2 % w/v NaOH) per mg dry beads were added. The reaction was conducted for 24 h at ambient temperature with intensive stirring (magnetic rod) (Fig. 17). Once the process was completed the particles were washed thoroughly with distilled water.

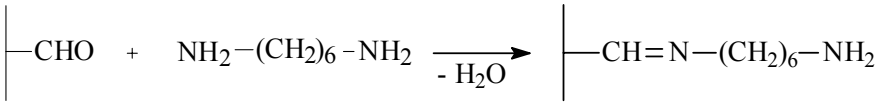

Figure 17: Hexamethylene diamine modification of ASMP/PGA coated magnetic particles - schematic representation.

EDA activation of the particles was done in the same manner but with 0.034 ml water solution of EDA (containing 2 % w/v NaOH) per mg dry beads (Fig. 18).

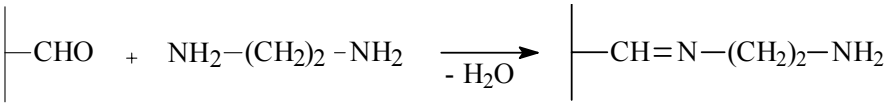

Figure 18: Ethylene diamine modification of ASMP/PGA-coated particles - schematic representation.

In both reactions the modifying agents were taken in 130 fold excess compared to the amount of aldehyde-sites of the matrix.

Due to the use of bi-functional reagents (HMDA; EDA), side "cross-linking" reactions of two neighbouring epoxy-groups of the magnetic matrix can occur.

2.2.3. Glutardialdehyde modification of the amino-charged magnetic matrices

Glutardialdehyde modification of the polymer magnetic matrices

The enzyme was coupled to the amino-charged polymer magnetic beads through glutardialdehyde (GA) linkage (it will be discussed later: Part B). The activation of the magnetic matrices with GA (Fig. 19) was performed just before the enzyme immobilisation. Whereby a slightly modified procedure of those described by Müller-Schulte (2001) was performed.

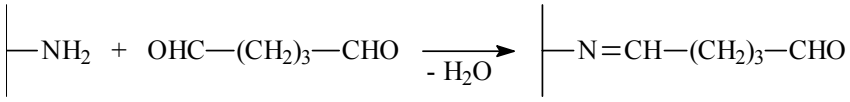

Figure 19: Glutardialdehyde modification of amino-charged magnetic matrices - schematic representation.

300 mg amino-charged polymer magnetic beads were washed twice with approx. 10 ml phosphate buffer (I = 0.2 M, pH 7.5). 20 ml glutardialdehyde (12.5 % v/v in the same phosphate buffer) were poured to the "wet beads" and the process was conducted at 30 °C for 2 h by intensive stirring with a magnetic rod. The modifying agent was taken in 140 to up to 800 fold excess (for different particles types) compared to the amount of amino groups of the matrix. Once the reaction was completed the activated magnetic beads were washed intensively with distilled water.

Glutardialdehyde modification of "amino-charged" ASMP

Defined amount of particles was reacted with 12.5 % v/v water solution of glutardialdehyde (0.06 ml per mg dry particles) (Fig 19). The reaction was performed for 24 h at ambient temperature and intensive stirring (magnetic rod). Once the modification process was completed the particles were washed intensively with distilled water. The modifying agent was taken in 200 fold excess compared to the amount of amino groups of the matrix.

2.2.4. N,N'-carbonyl diimidazole (CDI)-modification of M-PVA matrices

500 mg M-PVA 012 non-functionalised beads were washed in a following manner: once with approximately 20 ml distilled water : acetone (70:30, v/v); once with the same amount distilled water: acetone (30:70, v/v), and in the end extensively with acetone with respect to remove the water (Hermanson et al. 1992). The activation process was a slightly modified variant of those described by Akgöl et al. (2001). 10 ml analytical grade acetone (in which 50 $mg \cdot ml^{-1}$ CDI were dissolved) were added to the previously washed beads and the reaction was conducted at ambient temperature for 6 h by intensive magnetic-rod stirring (Fig. 20). Once the reaction

was completed the magnetic beads were washed thoroughly with acetone in order to remove the formed imidazole. The CDI-activated beads were stored in acetone at 4 °C.

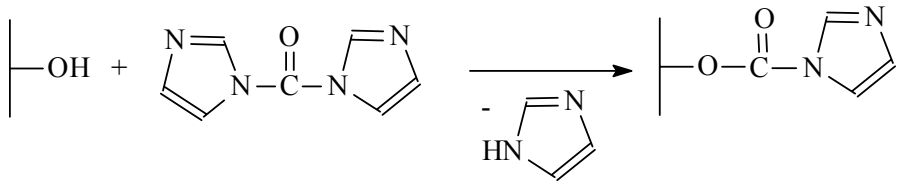

Figure 20: *N,N'*-carbonyl diimidazole modification of non-functionalised M-PVA 012 matrices - schematic representation.

2.3. Analytical methods and apparatuses

2.3.1. Determination of the epoxy group concentration of the magnetic matrices

The approximate concentration of the epoxy groups was determined by a method recommended from the manufacturer of M-PVA particles used here, as follows:

- 25 mg particles were incubated with an excess of 6-aminohexanoic acid for 24 h at 50 °C, pH 12 (adjusted with 1 M NaOH) under intensive stirring (Fig. 21). Once the reaction was completed the matrix was washed thoroughly with distilled water, then with 0.01 M HCl (in order to protonate the COO^-) and than again with distilled water.
- The washed particles were incubated with an excess of 0.01 M NaOH for 3 h at ambient temperature (in order to titrate the COOH groups).
- Once the particles were separated magnetically, the supernatant (containing the un-reacted part of NaOH) was back-titrated with 0.05 M HCl (automatic titration stand - Mettler DL21 Titrator) in order to determine the amount of the NaOH in it.
- The amount of the epoxy groups per gram dry carrier was calculated as a difference between the amount (mmol) NaOH before and after the "carrier" titration.

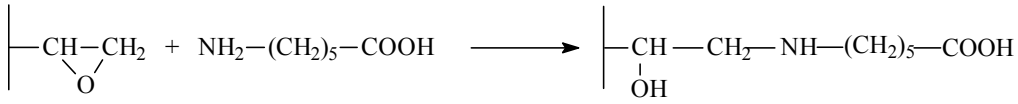

Figure 21: Reaction of 6-aminohexanoic acid with epoxy groups of the magnetic matrix - schematic representation.

2.3.2. Determination of the amino group concentration of the magnetic matrices

The concentration of the amino groups of the activated magnetic matrices was evaluated by TNBS (2,4,6-trinitrobenzenesulfonic acid) method described by Bubnis and Ofner (1992). The method was modified as follows (Fig. 22). A defined amount of magnetic particles was incubated with 1 ml 0.1 % w/v water solution of TNBS (containing also 3% w/v $Na_2B_4O_7$ as a non-nucleophilic base) for 5 min. at 70 °C by intensive mixing. Then the magnetic matrix was washed thoroughly with distilled water and incubated for next 10 min with 1.5 ml 1 M NaOH at 70 °C (by intensive mixing). Once the process was completed the magnetic particles were separated and the OD (optical density) of the supernatant (2,4,6-trinitrophenol) at 410 nm was measured against a blank sample (1 M NaOH). The calibration curve was obtained after incubation of different solutions TNBS (0-500 nmol) with 1.5 ml NaOH (1 M) at 70 °C for 10 min and determination of the OD at 410 nm.

The determined amount of amino groups was re-calculated in µmol -NH_2 per g dry matrix.

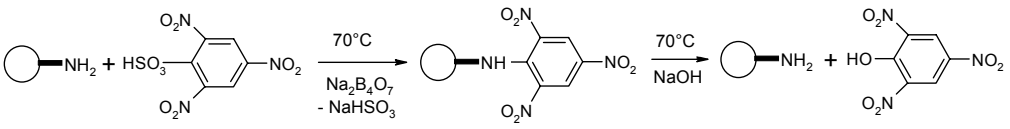

Figure 22: TNBS method - for evaluation the amount of amino groups onto the magnetic matrix.

2.3.3. Separation of the matrices

During different procedures the matrices were separated from the liquid phase using Nd-Fe-B block magnets (48×28×15 mm, 850 mT) from Steinert Elektromagnetbau GmbH (Germany). For centrifugation a 5415 D-Eppendorf Centrifuge (Eppendorf AG, Germany) was utilised.

2.3.4. Method for determination the dry-weight of the magnetic particles

The dry weight of the magnetic matrices was determined as they were filtered on 0.45 μm polyethersulfone filters, washed with copious amounts of distilled water, dried for 8 min. in a microwave oven at 350 W, then cooled for 24 h in a desiccator. The masses of the filters were evaluated on an analytical balance Sartorius BP 221S (Sartorius AG, Germany), and the dry-weight content calculated from the difference in mass before and after sample application.

2.3.5. Spectrophotometric measurements

The spectrophotometric measurements were performed with a Spectrophotometer "Shimadzu UV 1202" (Schimadzu, Japan).

2.3.6. Measurements of the magnetic saturation of the matrices

Magnetic saturation of the carriers was evaluated by measurements with a Magnetometer AGM Type "Micromag 2900" (Princeton Measurement Corporation, USA).

2.3.7. Size determination of the magnetic particles

The size distribution of the synthesised magnetic carriers was estimated by applying three methods: (1) optical microscopy - Dialux 20 microscope (Leitz, Germany) equipped with Sanyo Color CCD, (2) Particle Sizer Cis 100 (Galai, USA),

(3) Environmental Scanning Electron Microscopy (ESEM) - ESEM XL 30 FEG (Philips, The Netherlands).
Samples for ESEM observation were prepared by drying of a water-suspension of magnetic particles onto polycarbonate filters.

2.3.8. Measurements of the Zeta potential

The electrophoretic mobility of the synthesised magnetic particles in aqueous solution was measured and Zeta Potential values calculated, with a ZetaSizer 5000 (Malvern Instruments Ltd., UK) equipped with a 5 mW He-Ne laser operating at 633 nm and using a ZET 5104 capillary cell with Pd microelectrodes at 25 ±1 °C. The dependence of the zeta potential values on pH was measured with an automatic titration stand Mettler DL21 Titrator (Mettler Toledo, Switzerland) connected through a peristaltic pump with the capillary cell of the ZetaSizer. The dispersion was titrated with 0.05 M NaOH from a starting pH ≥ 4 adjusted with 0.05 M HNO_3 to a final pH=8.

2.3.9. Measurements of the specific surface area

N_2 gas adsorption data were measured with an Autosorb-1 device from Quantachrome GmbH (Odelzhausen, Germany). Specific surface area (SSA) was calculated with 7-adsorption data-points according to BET method. Prior to the measurements samples were out-gassed by heating at 60 °C in vacuum for 12 hours.

3. Results and discussion

3.1. Size determination of the magnetic matrices. BET specific surface area evaluation

The size-distributions of the magnetic beads used here were determined either by visual investigation of images from light microscopy or ESEM, or by particle size analysis with a Cis 100 Particle Sizer. Figures 23 and 24 show several ESEM images of different magnetic particle types.

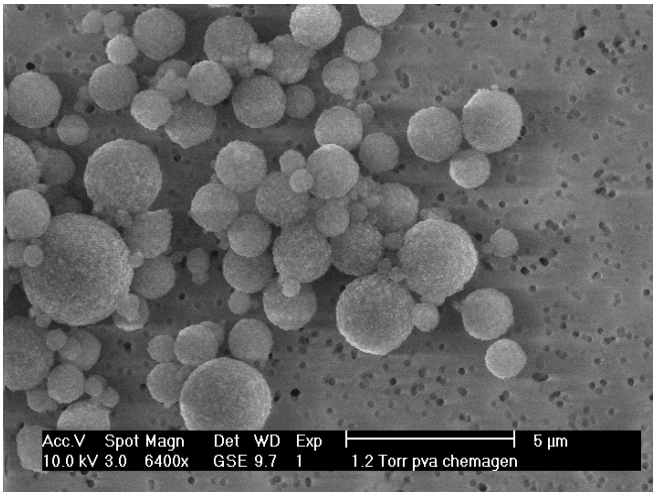

I

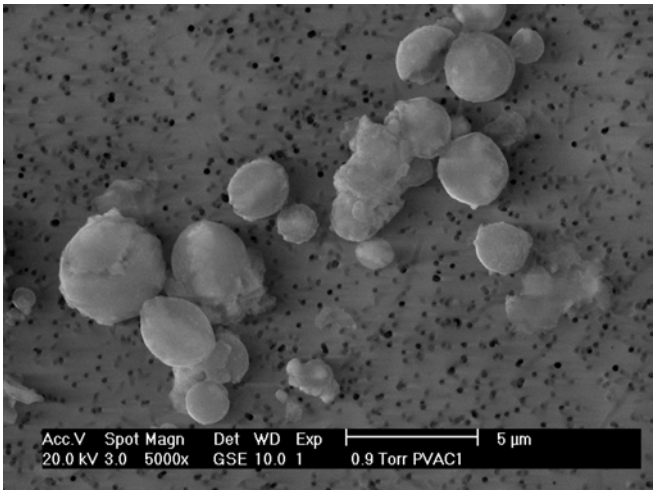

II

Figure 23: ESEM images: I M-PVA 012 beads; II- PVAc beads.

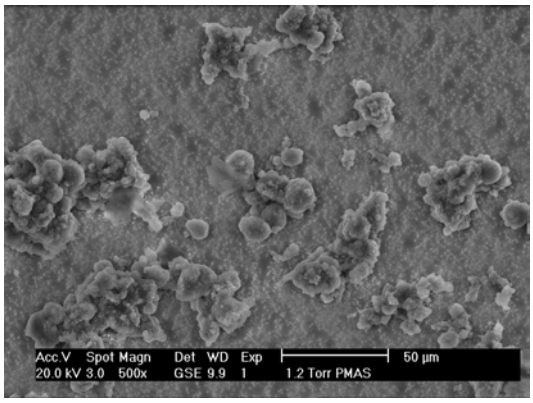

I

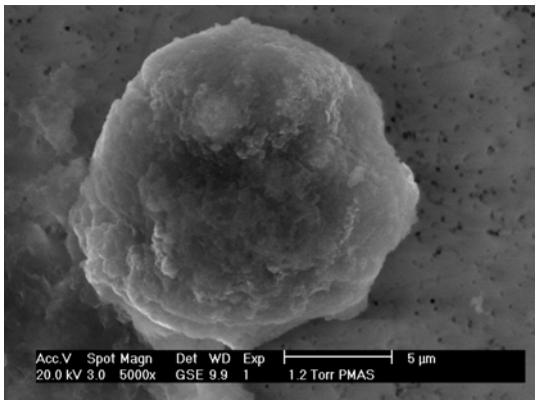

II

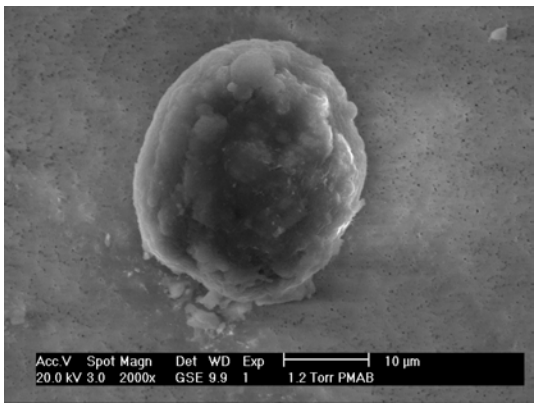

III

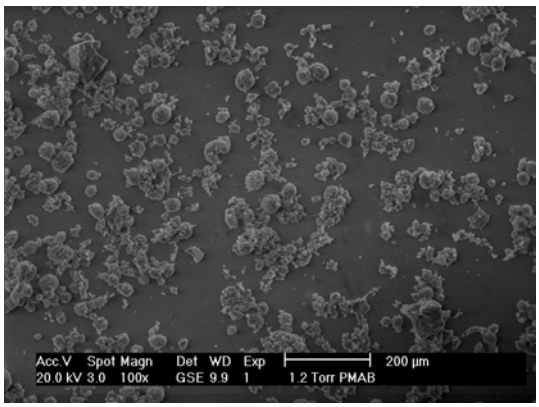

IV

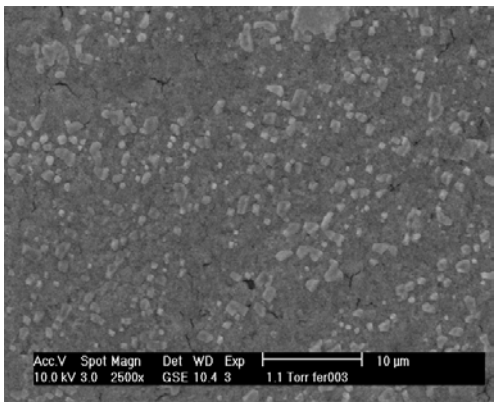

V

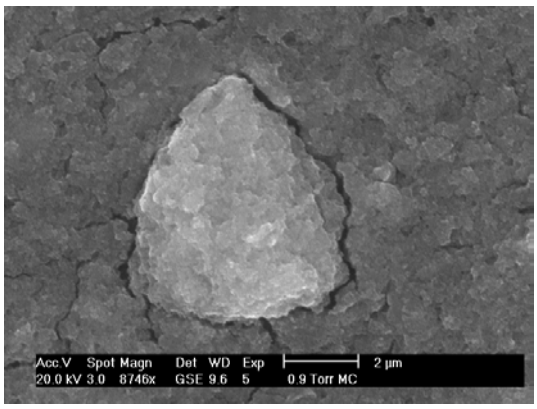

VI

Figure 24: ESEM images: I and II- PMAs (small) beads; III and IV- PMAb (big) beads; V and VI- ASMP beads.

Figure 25 shows light microscopy images of relatively large PMMA particles.

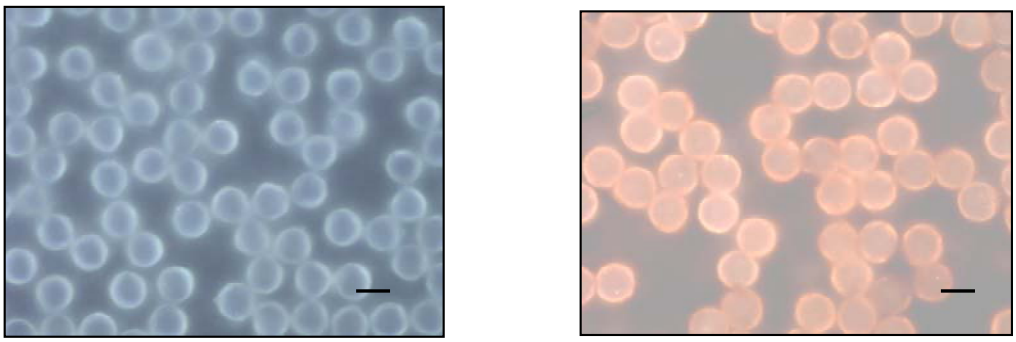

I II

Figure 25: Light microscopy images of PMMA matrix: I- before and II- after the magnetic conversion. * Length of the showed black marker 6 μm.

Fig. 26 shows a principle outlook of the number distribution of the particle size obtained with the Cis-100 for PVAc beads. Comparable number distribution-graphs were obtained for PMAs and PMAb magnetic matrices.

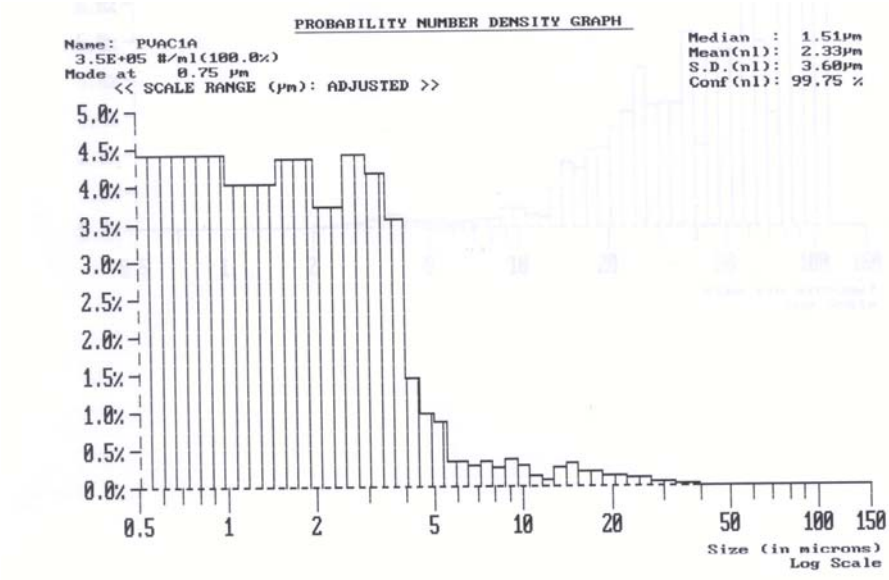

Figure 26: Cis 100 number size-density graph for PVAc beads.

ESEM and light microscopy images as well as size-measurements confirmed that all magnetic matrices, which were object of the study have sizes in a range of several micrometers (up to 20 μm) (Table 2).

Table 2: Size-ranges and BET specific surface areas of the magnetic matrices.

Type of the magnetic matrix	***Size distribution - mean diameter range (μm)***	***BET specific surface area ($m^2 \cdot g^{-1}$)***
M-PVA 012	1 – 3 [a, b]	64
M-PVA E02	1 – 3 [a, b]	84
M-PVA N12	1 – 3 [a]	n.d.
PMMA	6 [a, b]	3
PMAs	5 – 10 [b ,c]	7
PMAb	10 – 20 [b, c]	4
PVAc	2 – 5 [b, c]	15
ASMP/PGA coated	1 – 3 [b]	110

[a] data from the manufacturer, [b] data from ESEM or light microscopy images, [c] data from Cis 100 Particle Sizer

The mean diameter of the magnetic beads (treated as spherical particles) can be calculated also from BET specific surface areas found:

$$d_{BET} = \frac{6}{SSA \cdot \rho} \tag{1.2}$$

where,

d_{BET} - diameter of the beads, calculated from the evaluated specific surface area *SSA*, [m]; *SSA* - specific surface area evaluated with BET method [$m^2 \cdot kg^{-1}$]; ρ - density of the beads [$kg \cdot m^{-3}$].

This is an estimation towards the smallest dimensions (spherical form) of the particles. Every deviation from the spherical form results in a larger specific surface area.

In the case of intensively investigated M-PVA beads was found that $d_{BET,\ M\text{-}PVA\ 012} \approx 0.052$ μm; $d_{BET,\ M\text{-}PVA\ E02} \approx 0.039$ μm (ρ = 1800 $kg \cdot m^{-3}$, data from manufacturer). This means that,

$$d_{BET} \ll d_{ESEM\ image}$$

and subsequently some porosity or roughness of the carrier can exist. Deduced from BET isotherms self-scaling properties of the surface roughness were observed.

A simplified three-dimensional self-scaling model of the "idealised particle surface relief" is represented in the Fig. 27.

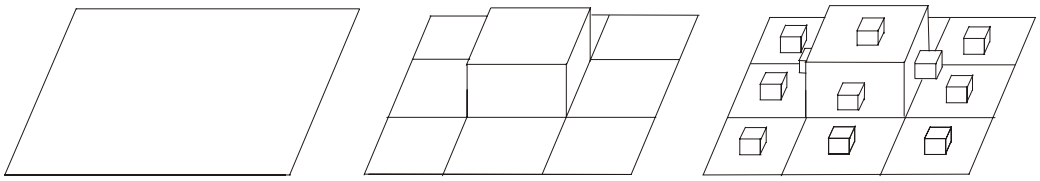

I. II. III.

Figure 27: Idealised three-dimensional model of particle surface relief with convexities, where at every next iteration (here only the first two ones II. and III. are shown) the characteristic length of the convexities decreases with a factor of (1/3). The state "I." represents a smooth surface.

In every next iteration the characteristic length will decrease with a factor of 1/3 and subsequently the corresponding surface area will increase with a factor of 13/9. Therefore the surface area after n-iterations will be $(13/9)^{n-1}$ (Peitgen et al. 1992).
In the case of M-PVA beads large convexities (> 200 nm) were not observed on the obtained ESEM images. Subsequently, if taking the theoretical $SSA_{theoretical} \approx 2$ $m^2 \cdot g^{-1}$ (for 2 μm particle) after several iterations starting with a characteristic length 200 nm (2000 Å) in the Fig. 27-I. it can be calculated, that a theoretical $SSA_{BET} \approx 27$ $m^2 \cdot g^{-1}$ hypothesise convexity minimum roughness height of approximately 1 Å. Penicillin amidase from *E.coli*, used here as a model enzyme system to be immobilised onto the magnetic matrices, is a heterodimer with dimensions of 70*50*55 Å (Duggleby et al. 1995). Therefore the large biomolecule encounters different (smaller) surface area than the much smaller nitrogen molecules.

3.2. Magnetic properties of the matrices

The magnetic measurements were performed as described above in this part. The magnetic saturation of the pure magnetite is in the range of 92-94 $A \cdot m^2 \cdot kg^{-1}$ (Cornell and Schwertmann, 1996). Measured magnetic saturation of the ASMP-PGA coated beads, the cores of which consist of nano-crystals of magnetite was 26 $A \cdot m^2 \cdot kg^{-1}$. This lower value in comparison to the pure magnetite, is due to its particular oxidation to

maghemite (magnetic saturation 60-80 $A \cdot m^2 \cdot kg^{-1}$) and the very small size of the primary crystals. ASMP carriers as well as all other matrices used here show superparamagnetic behaviour - they "are magnetised" when introduced in an external magnetic field, but practically show no "magnetic memory" (no measurable remanent magnetisation) if the field is switched off (Fig. 28). This means that the primary iron oxide crystals (magnetite / maghemite) included into their structure have sizes of less than 10-20 nm. The magnetic saturation values for the magnetic matrices here are represented in Table 3.

Table 3: Measured magnetic saturation (MS) of the carriers.

Type of the magnetic matrix	***MS*** $A \cdot m^2 \cdot kg^{-1}$
M-PVA 012	40
M-PVA E02	34
M-PVA N12	29
PMMA	n.d.
PMAs	11
PMAb	12
PVAc	26
ASMP/PGA coated	26

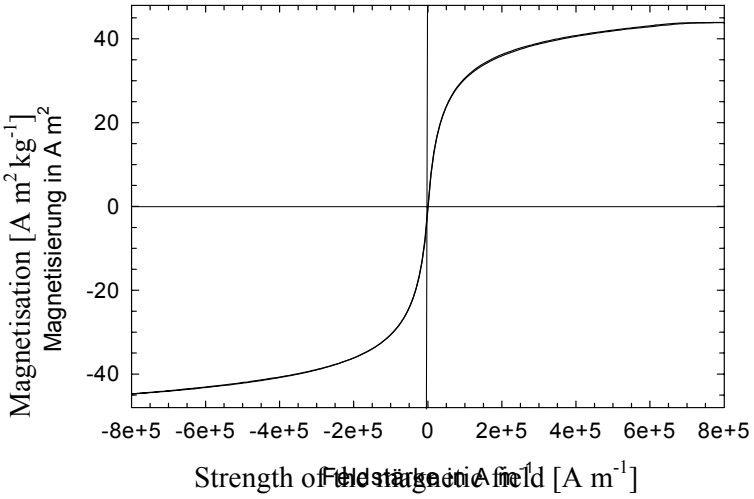

Figure 28: Magnetisation curve for M-PVA 012 beads (comparable curves were obtained for the other magnetic matrices).

3.3. Zeta-potential (ξ) measurements

A significant role for the kinetic stability of the small colloidal particles in aqueous solution plays the existence of an electrical double layer around them. A commonly accepted model explaining the arrangement of "ion-layers" formed on the particle surface (when the particle is situated in an electrolyte) was introduced by Nernst, further developed by Stern (Müller 1996). Apart from the fairly immobile layers that stick tightly to the particle surface, there is an diffusion layer of ions around it. The radius of the first "rigid" layer is called shear radius and its electric potential relative to the value in the distant bulk medium is called Zeta-potential (ZP).

The electrophoretic mobility of the particles was measured and the ZP values were calculated (see also Helmholtz-Smoluchowksi formula: equation (1.3)) as already described above, with regard to be able to predict possible unfavourable charge-charge interactions between the matrix-surface and the biomolecule during the immobilisation.

$$ZP = v / \eta \cdot \varepsilon \cdot E \qquad (1.3)$$

where:

v - velocity of the particle in an electric field [$\mu m \cdot s^{-1}$]; η - viscosity of the media [Pa·s]; ε - dielectricity constant ($=\varepsilon_r \cdot \varepsilon_0$) [$F \cdot m^{-1}$]; E - electric field strength [$V \cdot cm^{-1}$].

In the SI system by multiplication with a factor of 12.85 the ZP could be transformed in mV (Müller 1996).

The ZP values in the pH range of interest (pH at which the immobilisation of the enzyme was conducted) are represented in Table 4. As it will be shown later in this work, the sign and the relative value of this potential and the possibilities to minimize if necessary, e.g. by changing the ionic strength, its effect during the immobilisation procedure play significant role during the covalent attachment of the chosen enzyme system onto the magnetic matrices.

Table 4: Measured ZP-values of the magnetic matrices in aqueous solution, in the pH range 7-7.5.

Type of the magnetic matrix	***ZP mV***
M-PVA 012	-60
M-PVA E02 - ECH epoxy modified	-55
M-PVA N12	+40
PMMA - epoxy modified	-30
PMAs - amino modified	+5
PMAb	n.d.
PVAc - epoxy modified	-5
ASMP/PGA coated	+15

3.4. Chemical modification of the magnetic matrix surface with different functional sites

The magnetic matrices used here were functionalised in order to obtain groups suitable for covalent immobilisation of enzymes. The two most often applied procedures were: epoxy- or amino- modification. In all cases the amino-charged supports were brought to further reaction with glutardialdehyde in order to obtain aldehyde functional sites, suitable for covalent attachment of enzymes *via* nucleophilic groups on the protein molecule surface. Table 5 represents the obtained experimental data for the concentration of the functional groups as well as the spacer length for different types of magnetic matrices. In general the specific concentration (μmol m^{-2}) of the functional sites in the case of M-PVA, PMA, PVAc and ASMP carriers was found to decrease with each next reaction step. The two most probable reasons are: on one hand a decreasing of the yield in every next reaction and on the other hand a loss due to the side-reactions, which cause cross-linking*.

* these reactions are performed with bi-functional agents e.g. hexamethylene diamine, ethylene diamine, glutardialdehyde

Table 5: Specific concentration of the functional groups and approximate spacer length of the modified magnetic matrices. *In the case of amino-matrices modified further with glutaradialdehyde the concentration of the amino groups was determined.

Type of the magnetic matrix / *Type of the modifying method	***Specific concentration of the functional groups µmol/g dry beads***	***Concentration of the functional groups per surface area µmol/m²***	***Approximate spacer length Å***
M-PVA 012-ECH / epoxy groups	400	6.3	5.9
M-PVA E02-HMDA/GA method / amino groups	100	1.2	20.8
M-PVA N12-toluene-2,4-isocyanat/GA method / amino groups[a]	650[a]	n.d.	13.7
PMMA-glycidol method / epoxy groups	500	166	7.2
PMAs-EDA/GA method /amino groups	440	62	12.4
PMAb-EDA /GA method /amino groups	640	160	12.4
PVAc-ECH / epoxy groups	700	46	6.0
PVAc-ECH/HMDA/GA method / amino groups	135	9	20.9
ASMP-PGA coated-HMDA/GA [b](x_i) method / amino groups	(1) 425;(2) 315; (3) 313;(4) 380; (5) 370;(6) 350	(1) 3.8; (2) 2.8; (3) 2.8; (4) 3.5; (5) 3.4; (6) 3.2	(1) 16.2; (2) 32.5; (3) 48.7; (4) 64.9; (5) 81.1; (6) 97.4
ASMP-PGA coated-EDA/GA [b](x_i) / amino groups	(3) 75; (6) 23	(3) 0.7; (6) 0.2	(3) 33.9; (6) 67.9

[a] data from manufacturer, [b] (x_i) (i=1 to 6) denotes the number of the HMDA/GA respectively EDA/GA "units" covalently bound to the matrix. EDA - ethylene diamine, HMDA - hexamethylene diamine, GA -glutardialdehyde.

Glutardialdehyde which was used in many modification processes, is able to polymerise in water solutions it was stored in (Fig. 29). Therefore it is possible to obtain molecules with more than two functional aldehyde groups. Due to this fact the number of the aldehyde sites on the carrier surface after completion of the reaction can be higher than the one available at the beginning. This was observed here for hexamethylene diamine/glutardialdehyde modification of ASMP particles.

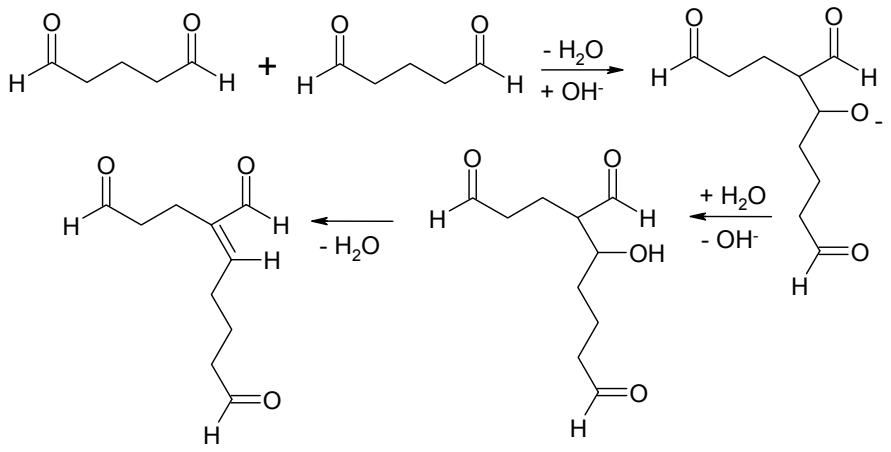

Figure 29: Polymerisation of glutardialdehyde in aqueous solution.

Theoretically the specific concentration of the amino sites is expected to decrease in every next reaction step. Although as was observed here in the case of functionalised with four hexamethylene diamine/glutardialdehyde spacer units matrix the number of the amino groups found was higher than the one determined for the previous reaction step e.g. three spacer units (Table 5). This is only possible if the effect of the glutardialdehyde polymerisation was dominating over the cross-linking process and decreasing of the yield in every next reaction step.

The specific concentrations of the amino groups for modified with ethylene diamine ASMP matrix were lower in comparison to these obtained through hexamethylene diamine functionalisation of the same carrier. This can be due to the negative inductive effect between the two amino groups, which decreases their nucleophilic character. Such inductive effect can not occur in the case of hexamethylene diamine, which posses six methylene residues between the amino groups.

4. Summary and conclusions

Magnetic micro-particles investigated here were manufactured by different methods or donated by chemagen Biopolymer Technologie AG. The supports were characterised with respect to their magnetic and surface properties, as well as their size-distribution. All magnetic matrices showed:

- Superparamagnetic behaviour and magnetic saturation high enough (Table 3) to be separated relatively easily by moderate magnetic field.
- The size distributions of the particle diameters were in the range of 1-20 μm. Some of the matrices (poly(vinylalcohol) – M-PVA; amino-silanised magnetic particles - ASMP) showed rough surface relief (ESEM images) and therefore higher specific surface areas (BET data) in comparison to poly(vinylacetate) - PVAc, poly(methyl methacrylate) - PMMA and poly(methylacrylate) - PMA beads, the surfaces of which were microscopically smooth and the obtained values for the specific surface areas subsequently lower. The simplified model (section 3.1) used for an approximate theoretical calculation of the surface roughness of M-PVA particles found convexities in a range of 1 Å.

  Therefore it can be concluded that the magnetic particles investigated here posses the advantages of "practically non- porous" for the relatively large biomolecules immobilisation matrices.
- Modification of the magnetic matrices with variety of procedures/conditions allows to obtain suitable concentrations of "functional sites" on the particle surface for covalent immobilisation of enzymes and to achieve optimal enzyme loadings.

5. Symbols and abbreviations

Symbols

B	flux density [Tesla]
B_r	remanence [Tesla]
E	electric field strength [$V \cdot cm^{-1}$]
F	force [N]
H	magnetic field strength [$A \cdot m^{-1}$]
I	current [A]
l	wire length [m]
M	magnetisation [$A \cdot m^{-1}$]
MS	magnetic saturatuion [$A \cdot m^2 \cdot kg^{-1}$]
SSA	specific surface area evaluated with BET method [$m^2 \cdot g^{-1}$]
T	Tesla [$Wb \cdot m^{-2}$]

Greek symbols

ξ	zeta-potential [mV]
χ	magnetic susceptibility [-]
ε	dielectricity constant [$F \cdot m^{-1}$]
η	viscosity [Pa·s]
μ_r	permeability [-]
μ_0	permeability of a free space [$4 \cdot \pi\ 10^{-7} \cdot V \cdot s \cdot A^{-1} \cdot m^{-1}$]
ν	velocity of the particle in an electric field [$\mu m \cdot s^{-1}$]
ρ	density [$kg \cdot m^{-3}$]

Abbreviations

ASMP	amino-silanized-magnetic-particles
BPO	benzoyl peroxide

CDI	N,N'-carbonyl diimidazole
DVB	divinyl benzene
ECH	epichlorohydrine
EDA	ethylene diamine
GA	glutardialdehyde
GC	gas chromatography
HD	hydrolysation degree
HMDA	hexamethylene diamine
MB	methylene blue
M-PVA 012	magnetic poly(vinyl alcohol) beads (non-functionalised)
M-PVA E02	magnetic poly(vinyl alcohol) beads (epoxy-functionalised)
M-PVA N12	magnetic poly(vinyl alcohol) beads (amino-functionalised)
PGA	poly(glutaraldehyde)
PVA	poly(vinylalcohol)
PVAc	magnetic poly(vinylacetate) beads
PMAs	magnetic poly(methylacrylate) small beads
PMAb	magnetic poly(methylacrylate) big beads
PMMA	magnetic poly(methyl methacrylate)
ZP	zeta-potential

6. References

Alvaro, G., Fernandez-Lafuente, R., Blanco, R.M., Guisán, J.M. (1990) *Appl. Biochem. Biotechnol*., 181-195

Agbah, O.C., Qin, Y. (1997) *Polymers for Advanced Technologies,* **8**, 355-365

Arica, M.Y., Yavuz, H., Patir, S., Denizli, A. (2000) *J. Mol. Catal. B: Enzymatic*, **11**, 127-138

Akgöl, S., Kaçar, Y., Denizli, A., Arica, M.Y. (2001) *Food Chemistry*, **74**, 281-288

Avella, M., Errico, M.E., Martelli, S., Martuscelli, E. (2001) *Applied Organometallic Chemistry*, **15**, 435-439

Amorim, R.V.S., Melo, E.S., Carneiro-da-Cunha, M.G., Ledingham, W.M., Campos-Takaki, G.M. (2003) *Bioresource Tecnology*, **89**, 35-39

Buchholz, K. (1979) *Characterization of Immobilized Biocatalysts, Dechema Monographs*, **84**, Verlag Chemie Weinheim

Braun, J., Le Chanu, P., Le Goffic, F. (1989) *Biotechnology and Bioengineering*, **33**, 242-246

Bubnis, W.A., Ofner, C.M. (1992) *Analytical Biochemistry*, **207**, 129-133

Bickerstaff, G.F. (1997) *Immobilization of Enzymes and Cells*, Humana Press Inc. New Jersey

Buchholz, K., Kasche, V. (1997) *Biokatalysatoren und Enzymtechnologie*, VCH Verlagsgesellschaft mbH Weinheim

Bergemann, C., Müller-Schulte, D., Oster, J., à Brassard, L., Lübbe, A.S. (1999) *Journal of Magnetism and Magnetic Materials*, **194**, 45-52

Braun, D., Cherdron, H., Ritter, H. (2001) *Polymer Synthesis: Theory and Practice*, Spriger-Verlag

Clemence, L.J., Eldridge, R.J., Lydiate, J. (1984) *Reactive Polymers* **2**, 197-207

Cornell, R.M., Schwertmann, U. (1996) *The Iron Oxides: Structure, Properties, reactions, Occurrence and Uses*, VCH Verlagsgesellschaft mbH, Weinheim

Chen, C-H., Lee, W-C. (1999) *J. Polym. Science: Part A: Polymer Chemisty*, **37**, 1457-1463

Cornell, R.M., Schwertmann, U. (2000) *Iron Oxides in the Laboratory Preparation and Characterisation*, Wiley-VCH Weinheim

Çetinus, Ş.A., Öztop, H.N. (2003) *Enzyme and Microbial Technology*, **32**, 889-894

Cipran, A., Alkan, S., Toppare, L., Hepuzer, Y., Yagci, Y. (2003) *Bioelectrochemistry*, **59**, 29-33

Cao, L., van Langen, L., Sheldon, R.A. (2003) *Current Opinion in Biotechnology*, **14**, 1-8, *article in press*

Dixon, D.R., Lydiate, J. (1980) *J.Macromol. Sci.-Chem.,* A **14 (2)**, 153-159

Dunlop, E.H., Feiler, W.A., Mattione, M.J. (1984) *Biotechnol. Adv.*, **2**(1), 63-74

Duggleby, H.J., Toley, S.P., Hill, C.P., Dodson, E.J., Dodson, G., Moody, C.E. (1995) *Nature*, **373**, 264-268

Fernández-Lafuente, R., Rosell, C.M., Alvaro, G., Guisán, J.M. (1992) *Enzyme Microb. Technol*, **14**, 489-495

Fonseca, L.P., Cardoso, J.P., Cabral, J.M.S. (1993) *J. Chem. Tech. Biotechol*., **58**, 27-37

Franzreb, M., Yueping, G., Bozhinova, D. (2002) *DE Patent Application* 10237742.1

Guesdon, J.-L., Antoine, J.-C., Ternynck, T., Avrameas, S. (1979) *Affinity Chromatography*, **86**, 137-146

Gemeiner, P. (1992) *Enzyme Engineering: Immobilized Biosystems*, Ellis Horwood Ltd. and Alfa Publishers

Halling, P.J., Dunnill, P. (1980) *Enzyme Microb. Technol*, **2**, 2-10

Hermanson, G.T., Mallia A.K., Smith, P.K. (1992) *Immobilized Affinity Ligand Techniques*, Academic Press, Inc.

Haukanes, B.-I., Kvam, C. (1993) *Bio/technology*, **11**, 60-63

Hatate, Y., Kasamatu, K., Uemura, Y., Ijichi, K., Kawano, Y., Yoshizawa, H. (1994) *J. Chem. Eng. of Japan*, **27 (4)**, 479-484

Häfeli, U., Schütt, W., Teller, J., Zborowski, M. (1997) *Scientific and Clinical Applications of Magnetic Carriers*, Plenum Press New York and London

Hubbuch, J.J. (2001) *PhD Thesis*, Technical University of Denmark, Lyngby, Denmark

Janssen, M.H.A., van Langen, L.M., Pereira, S.R.M., van Rantwijk, F., Sheldon, R.A. (2002) *Biotechnology and Bioengineering*, **78** (4), 425-432

Kasche, V. (1986) *Enzyme Microb. Technol*., **8**, 4-16

Koilpillai, L., Gadre, R.A., Bhatnagar, S., Raman, R.C., Ponrathnam, S., Kumar, K.K., Ambekar, G.R., Shewale, J.G. (1990) *J. Chem. Tech. Biotechnol*., **49**, 173-182

Kurokawa, M., Honma, A., Isozaki, T. (1996) *US Patent* 5,527,927

Katzir-Katschlaski, E., Kraemer, D.M. (2000) *J. Mol. Catal. B: Enzymatic*, **10**, 157-176

Langer, K., Stieneker, F., Lambrecht, G., Mutschler, E., Kreuter, J. (1997) *International Journal of Pharmaceutics*, **158**, 211-217

Li, W.-H., Stöver, H.D.H. (1999) J. *Polymer Science: Part A: Polymer Chemistry*, **37**, 2899-2907

Li, J.Q., Salovey, R. (2000) *J. Polymer Science: Part A. Polymer Chemistry*, **38**, 3181-3187

Mosbach, K., Anderson, L. (1977) *Nature*, **270**, 259-261

Manecke, G., Vogt, H.-G. (1980) *J. Membrane Science*, **6**, 61-67

Manecke, G., Polakowski, D. (1981) *J. Chromatography*, **215**, 13-24

Müller, R.H., (with contributions from Nitzsche, R., Paulke B.R. (1996) *Zetapotential und Partikelladung in der Laborpraxis: Einführung in die Theorie, praktische Messdurchführung, Dateninterpretation*, Wissenschaftliche Verlagsgesellschaft mbH Stuttgart

Mateo, C., Abian, O., Fernández-Lafuente, R., Guisán, J.M. (2000)a *Enzyme and Microbial Technology*, **26**, 509-515

Mateo, C., Fernández-Lorente, G., Abian, O., Fernández-Lafuente, R., Guisán, J.M. (2000)b *Biomacromolecules*, **1**, 739-745

Muller-Schulte, D. (2001) *US Patent* 6,204,033

Okubo, M., Ise, E., Yamashita, T. (1998) *J. Polymer Science: Part A: Polymer Chemistry*, **36**, 2513-2519

Peitgen, H.-O., Jürgens, H., Saupe, D. (1992) *Bausteine des Chaos Fraktale*, Springer-Verlag, Klett-Gotta

Pieters, B.R., Williams, R.A., Webb, C. (1992) *Colloid and Surface Engineering: Application in the Process Industries* Chapter 8*: Magnetic Carrier Technology*, Oxford

Pişkin, E., Kesenci, K., Şatiroğlu, N., Genç Ö. (1996) *J. Appl. Polymer Sci*., **59**, 109-117

Robinson, P.J., Dunnill, P., Lilly, M.D. (1971) *Biochim. Biophys. Acta*, **242**, 659-661

Reimers, G.W., Khalafalla, S.E. (1976) *US Patent* 1 439 031

Sorenson, W.R., Campbell, T.W. (1962) *Präparative Methoden der Polymeren-Chemie*, Verlag Chemie GmbH Weinheim

Setchell, C.H. (1985) *J. Chem. Tech. Biotechnol*., **35B**, 175-182

Shinkai, M., Honda, H., Kobayashi, T. (1991) *Biocatalysis,* 61-69

Sheldon, R.A. (1993) C*hirotechnology*, Marcel Dekker, Inc.

Shen, L., Laibinis, P.E., Hatton, T.A. (1999) *Langmuir*, **15**, 447-453

Šafaříková, M., Roy, I., Gupta, M.N., Šafařík, I. (2003) *Journal of Biotechnology*, article in press

Torcilin, V.P., Papisov, M.I., Smirnov, V.N. (1985) *Journal of Biomedical Materials Research*, **19**, 461-466

Thomas, O.R.T., Franzreb, M. *Bioseparation Processes* ***Chapter 8***, will be published

Ugelstad, J., Ellingsen, T., Berge, A., Helgee, O.B. (1987) *US Patent* 4,654,267

Whitehead, R.A., Chagnon, M.S., Groman, E.V., Josephson, L. (1987) *US Patent* 4,695,393

Watanabe, S., Ueno, K., Kudoh, K., Murata, M., Masuda, Y. (2000) *Macromol. Rapid Commun*., **21**, 1323-1326

Yen, S.-P.S., Rembaum, A., Landel, R.F. (1981) *US Patent* 4,285,819

Part B: Immobilisation of penicillin amidase from *E.coli* onto magnetic matrices

1. Knowledge basis

1.1. Immobilisation of enzymes – an introduction. Immobilisation methods

Application of immobilised enzymes in the biotechnological processes offers many advantages such as: reusability of the biocatalyst and thus greater productivity; easy separation of the enzyme from the mixture of products and substrates; improved control of the reaction course; enhanced stability; capability of automation and continuous operation. It is accepted to use the term "immobilised" instead of "insolubilised" enzyme (Mosbach 1976). The immobilised biocatalysts are in a state, which allows their reuse - insoluble enzymes are e.g. used in a fixed bed reactor or soluble enzymes are e.g. used in a semi-permeable membrane reactor (Mosbach 1987). Principally it can be distinguished between carrier-bound and carrier-free immobilised biocatalysts/methods. A large variety of methods and materials for enzyme immobilisation were developed and optimised in order to provide improvements for a given application.

Carrier-bound immobilised enzymes consist of two essential components: a non-catalytic structural component (matrix/carrier/support), which is designed to facilitate the separation and the process control, and a catalytic component, which converts the substrates into products (Tischer and Kasche 1999, Cao et al. 2003). Subsequently the immobilised biocatalyst can be described by two types of features: non-catalytic (physical, chemical and morphological parameters of the carrier) and catalytic (biochemical properties of the enzyme as its activity, selectivity; stability).

One of the most often used classifications of the enzyme immobilisation methods is shown in the Fig. 1. It is based on the combination of carrier nature and the nature of the immobilisation interactions (Buchholz and Kasche 1997). *Carrier-binding* methods are further divided into four groups with respect to the nature of the carrier-enzyme interaction: physical adsorption, ionic binding, metal-chelate binding and covalent binding. *Physical adsorption* is the simplest method and involves reversible surface interactions - van der Waals, hydrophobic and hydrogen, as well as stronger ionic bonds. Non-specific physical adsorption is the longest known immobilisation

procedure and involves simple mixing of the enzyme and the support. Subsequent techniques as electro-deposition, the reactor loading procedure, mixing or shaking bath loading became also known (Gemeiner 1992). The most largely used laboratory technique is the last one, where the carrier is continuously stirred with an enzyme solution in a shaking water bath, in order to obtain uniform distribution of the biocatalyst.

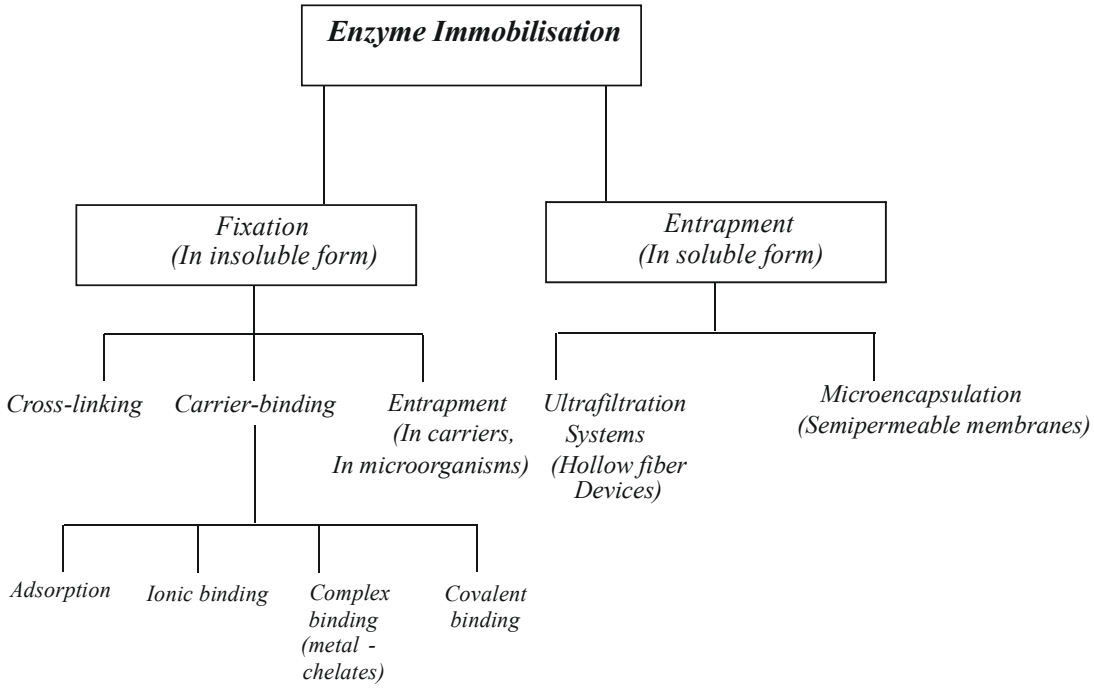

Figure 1: Classification of the enzyme immobilisation methods - (Buchholz and Kasche 1997).

The reactor loading procedure involves mixing of the biocatalyst and the matrix in the reactor (the agitation is throughout the reactor). By the electro-deposition the support is situated next to one of the electrodes in an enzyme bath and once the current is switched on the enzyme is transferred to the support. The hydrophobic interactions between the biocatalyst and the matrix can be obtained due to suitable changes in the pH, temperature, solvent and the ionic strength. Of course this binding depends on the hydrophobicities of both enzyme and support. The hydrophobicity of the "enzyme macromolecule surface" can be influenced by site-directed mutagenesis or by chemical modification of its primary structure. The advantages of the physical adsorption are: (i) no preliminary chemical modification of the support is required;

(ii) practically no conformational changes of the enzyme molecule are expected; (iii) simple and cheap procedure; (iv) reversibility - the carrier can be re-loaded with a fresh enzyme. On the other hand there are also disadvantages such as: (i) the bond enzyme-matrix is very weak and leakage of the biocatalyst can occur by changing the operational parameters as pH, ionic strength, flow rate in the reactor, more intensive agitation etc., (ii) unwanted non-specific binding can occur and (iii) an "over-charging" of the carrier with the biocatalyst is possible, which can cause steric hindrance and therefore can lower the enzyme activity. *Ionic binding* is another simple and effective manner for reversible enzyme immobilisation. Suitable for ionic binding carriers are commercial cation- and anion- exchangers. By this method the same advantages and disadvantages, as already described for the physical adsorption, can be observed. Non-specific binding can become problematic if substrate, product and/or residual contaminants are charged and interact with the carrier, causing thus diffusional limitations and alteration of the enzyme kinetic parameters (Bickerstaff 1997). Physical adsorption and the ionic binding represent the most natural manners of biocatalyst immobilisation.

By *metal-chelate binding* the chelating properties of a transition metal as titanium or zirconium are employed to attach biocatalysts to an organic (cellulose, alginate) or inorganic (glass) material (Ullmann's Encyclopedia of Industrial Chemistry 1989). Several works were carried out utilising iminodiacetic acid as metal ion chelator. Some amino acids and especially histidine, which is a strong electron donor at slightly alkaline pH can be bound to the metal-ion complexes at pH values greater than 6. The separation of the enzyme from the matrix could be done either by changes in the pH and/or ionic strength or by affinity elution (imidazole) (Morgan 1996, Hoffmann 2002).

High specific manner of binding is so called *bio-specific immobilisation*. Enzymes can be attached with extremely high affinity to matrices modified with antibodies (Gemeiner and references therein 1992). Lectins such as concanavalin A are glycoproteins of plant origin, which were employed for activation of cellulose and subsequent immobilisation of enzymes (invertase, L-ascorbate oxidase) (Ullmann's Encyclopedia of Industrial Chemistry 1989).

The *covalent immobilisation* requires formation of a covalent bond between the enzyme and the matrix. This implies presence of suitable functional groups/sites on the carrier surface, which can bind covalently the enzyme. The most important for the

covalent immobilisation amino acid residues (functional groups) are presented in Table 1 (Gemeiner 1992, Buchholz and Kasche 1997).

Table 1: Functional groups in the proteins which are important for covalent immobilisation ([a]Gemeiner 1992, [b]Buchholz and Kasche 1997). The p*Ka* values could be influenced by the micro-environment.

Functional groups	***pK_a***	***% in the proteins***
Amino-; Guanidino-:		
Lysine	10.5[b]	7[a]
Arginine	12.48[a]	7[b]
Carboxyl-:		
Aspartate	3.9[b]	4.8[b]
Glutamate	4.1[b]	4.8[b]
Hydroxyphenyl-:		
Tyrosine	10.07[a]	3.4[b]
Imidazole-:		
Histidine	6.1[a]	3.4/2.2[b]

Under normal conditions the covalent binding is stable and no enzyme leakage will take place. In order to prevent some loss of enzyme activity, it is essential to take care that the amino acids from the active- or substrate binding- sites do not participate in the reaction with the functional groups of the carrier.

Only a low number of matrices posses functional groups for direct covalent immobilisation of the biocatalyst. Usually the supports must be activated further for obtaining suitable reactive sites. Different methods for covalent bond formation between the carrier and the enzyme are summarised by Mosbach (1987), "Ullmann's Encyclopedia of Industrial Chemistry" (1989), Gemeiner (1992) as well as Buchholz and Kasche (1997). Important parameters influencing the immobilisation yield as well as the appearance of possible steric hindrances of the immobilised biocatalyst are the concentration of the functional sites and the spacer length, which will determine the distance between the support surface and the enzyme molecule. Having this in mind together with the carrier properties (porosity, size, specific surface area available, modifying options) an optimisation of the carrier activation reaction as well as the

immobilisation conditions (duration of the immobilisation process, pH and ionic strength of the immobilisation buffer) must become necessary.

Entrapment represents another immobilisation technique, where enzymes are included into the cross-linked structure of a gel, with pores large enough to be passed by the substrates and the products and in the same time small enough to prevent leakage of biocatalyst. Incorporation into cross-linked polymers is most efficient, when is combined with additional binding procedures (for example attachment of some monomers onto the enzyme surface and integration into growing polymeric chain) (Tischer and Kasche 1999). By *encapsulation* the enzyme macromolecules are enclosed into microcapsules (1-100 μm) permeable for the substrates and the products. As capsules nylon, cellulose nitrate as well as biological cells (erythrocytes) can be used.

The immobilisation procedures described above often decrease the biocatalyst activity and selectivity due to a possible modifying of the enzyme or its natural microenvironment. With respect to keep the enzyme in their native state, they can be separated from the educts and the products by a semi-permeable membrane. Microfiltration- and hollow-fiber- membrane utilising is described in "Ullmann's Encyclopedia of Industrial Chemistry" (1989). Enzymes can be also *cross-linked* employing different bi-functional agents (e.g. glutardialdehyde) and thus be converted into insoluble form (Cao et al. 2000, Cao et al. 2003). However the toxicity of such reagents may be an obstacle in applying such procedures to several enzymes (Bickerstaff 1997). Some of the discussed immobilisation methods are represented schematically in the Fig. 2.

In the recent years the dilemma concerning the choice between "carrier-bound or carrier-free enzyme" was subject of some publications. Tischer and Kasche (1999) discussed possible advantages/disadvantages of enzyme crystals compared to the immobilised onto support enzymes. Enzyme crystals and principally all carrier-free enzymes (also different types of cross-linked enzymes) are free of inactive mass of the carrier and have higher (than carrier-bound) volumetric activity of biocatalyst (Tischer and Kasche 1999, Cao et al. 2003).

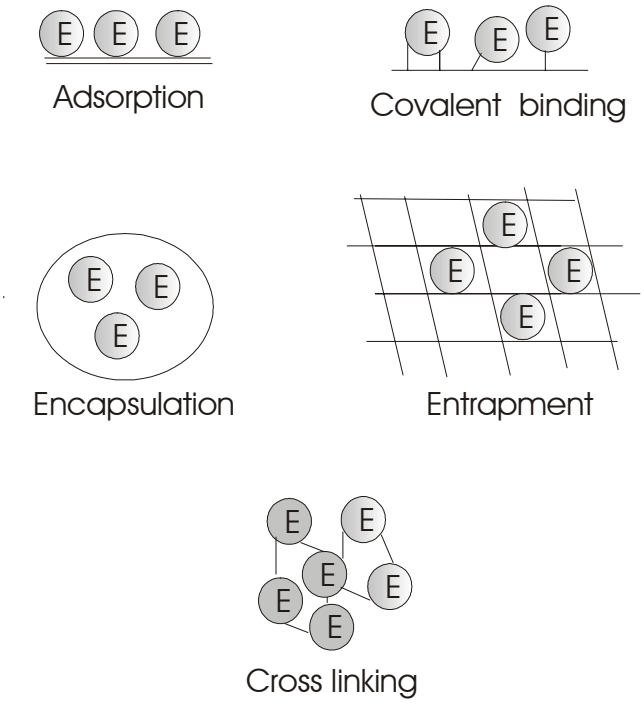

Figure 2: Enzyme immobilisation procedures - schematic representation.

Some disadvantages of the carrier-immobilised enzymes are: decreased mobility of the biocatalyst; possible steric hindrances; diffusional limitations (depends on the carrier size and its porosity); formation of pH gradients (can be observed also by enzyme-crystals); fouling of the carrier-pores with substrate and/or product; additional costs for carrier activation. The mathematical description of the diffusional and mass transfer effects of the enzyme kinetics is done by Buchholz and Kasche (1997). The extent of mass transfer control is often expressed by the stationary effectiveness factor η:

$$\eta = \frac{v_{imm.}}{v_{free}} \tag{2.1}$$

where $v_{imm.}$ and v_{free} are the reaction rates of the reaction catalysed by immobilised and free enzyme at the same concentrations of the active enzyme (Kasche 1983). The kinetic behaviour of immobilised-biocatalyst systems depends mainly on the carrier size and porosity, and also the enzyme density, but it is independent on whether carrier-bound or carrier-free biocatalyst is used (Tischer and Kasche 1999). The magnetic matrices used here as immobilisation carriers have sizes of several

micrometers and practically non-porous morphology. Therefore no internal diffusion limitations are expected during completion of the reaction with attached onto their surface enzyme.

1.2. Penicillin amidase

Penicillin amidase (PA, EC 3.5.1.11) (Fig. 3) catalyses the hydrolysis of Penicillin G (PenG) to phenylacetic acid (PAA) and 6-aminopenicillanic acid (6-APA), a starting material for the synthesis of semi-synthetic ß-lactam antibiotics (Fig. 4) (Vandamme 1983).

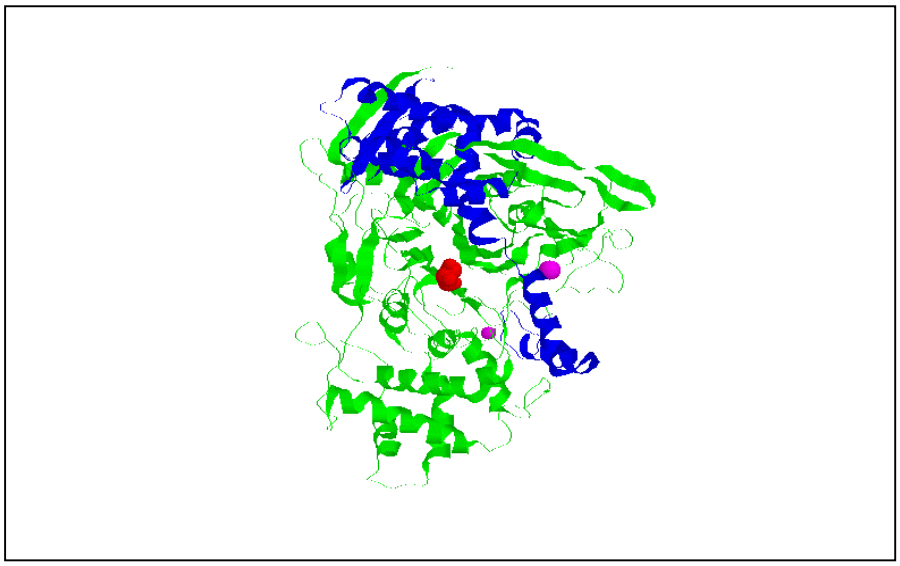

Figure 3: Three-dimensional structure of penicillin amidase from *E.coli*. * B chain - in green; A chain - in blue; the active center Ser B1 - in red; Ca^{2+} - in magenta. (Brookheaven Protein Data Bank: entry number 1pnk).

Penicillin amidase (called also penicillin acylase or penicillin amidohydrolase) is produced by several prokaryotic and eukaryotic microorganisms. The tertiary structure of PA has been solved for the penicillin amidase from *E.coli* (Duggleby et al. 1995) and *P.rettgery* (McDonough et al. 1999). All known penicillin amidases consist of shorter A-chains (~25 kDa) and long B-chains (~65 kDa). Penicillin amidase from *E.coli* (A-chain ~23 kDa and B-chain ~66 kDa) is formed through proteolytical processing of 90 kDa pro-enzyme, which is probably auto-catalytically transformed into the active form.

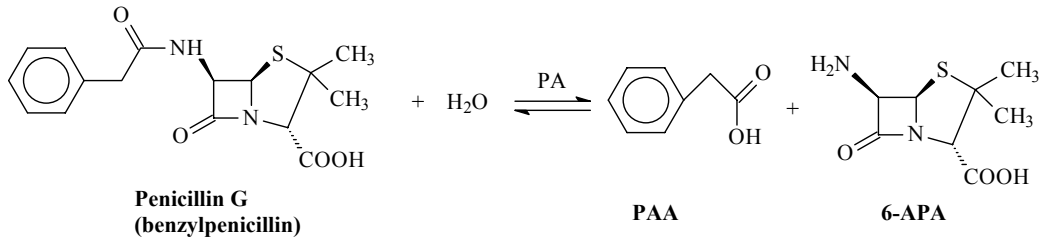

Figure 4: Hydrolysis of penicillin G catalysed by penicillin amidase.

The enzyme is a heterodimer (70*50*55 Å), which is kidney-shaped in cross section, with a deep cup-shaped depression in the middle, where the catalytically active site is situated (Duggleby et al. 1995). Penicillin amidase belongs to the N-terminal nucleophile (Ntn) hydrolase protein superfamily (Oinonen and Rouvinen 2000). The A-chain is built up mainly of α-helices, while B-chain contains so called Ntn fold-four layer α+β structure with two anti-parallel β-sheets.

The function of the calcium ion in the penicillin amidase molecule is not yet clear.

According to its structure, the catalytic mechanism of penicillin amidase from *E.coli* was described by Duggleby et al. (1995). Ser B1 performs with its hydroxyl group and N-terminal amino group the function of the nucleophile and indirectly of the base (Fig 5). The serine nucleophilic character is enhanced due to interaction, mediated by a bridging water molecule, with the adjacent N-terminal amino group. The tetrahedral intermediate is stabilised through hydrogen bridges to the main-chain amides of glutamine B23, alanine B69, and with N^{δ} of asparagine B241.

The biological function of PA is not yet known. It is speculated that its physiological activity *in vivo* could be involved in the metabolism of the aromatic compounds as a carbon source (Valle et al. 1991), as *pac* gene is present in the proximity of the 4-hydroxyphenilacetic acid cluster (Prieto et al. 1996).

Penicillin amidase catalysed reactions include hydrolysis of different amide bonds. The enzyme posses also esterase activity and can be used as a catalyst for kinetically controlled synthetic reactions. Preferred nucleophiles are aromatic S- amino acids. In kinetically controlled synthesis higher yields can be achieved than in equilibrium controlled processes (Kasche 1986).

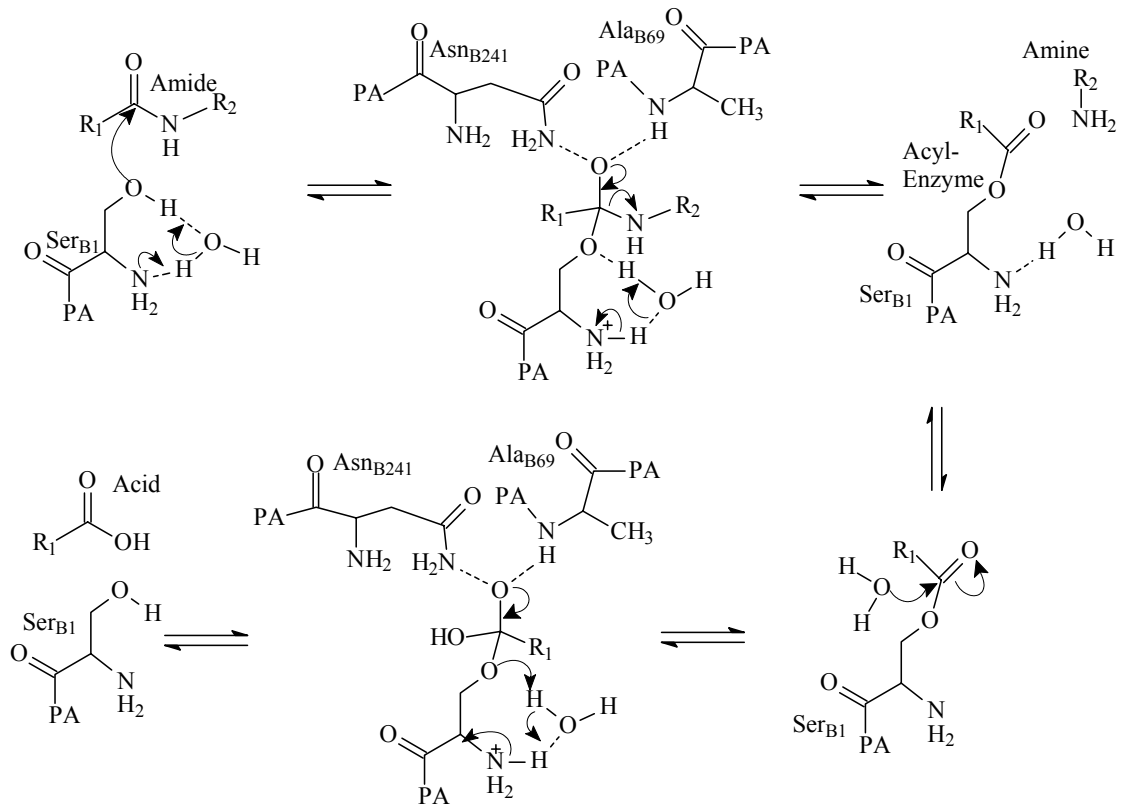

Figure 5: Catalytic mechanism of penicillin amidase *E.coli* for the hydrolysis of amide substrate - schematic representation (Duggleby et al. 1995) modified diagram.

Penicillin amidase from *E.coli* was found to be R-specific in the S_1-binding site and S-specific in S_1' binding site (Kasche et al. 1996). The enzyme was also employed to resolve racemic mixtures (Zmijewski et al. 1991) or for enzyme – catalysed cleavage of the amino-protection of nucleosides (Dineva et al. 1993).

1.3. Immobilisation of penicillin amidase

Enzymatic production of 6-APA is only economically viable in the case, where immobilised penicillin amidase is employed.

Penicillin amidases from *E.coli*, *B.megaterium* or *A.faecalis* were immobilised following different procedures, from attachment to pre-fabricated matrices to packing in enzyme crystals and powders (Shewale and Sivaraman 1989, Parmar et al. 2000, Arroyo et al. 2003) (Table 2). The use of immobilised biocatalysts, which show long life and higher stability leads to significant cost savings. Cross-linked enzyme crystals of penicillin G amidase from *E.coli*, which combine the properties of essentially pure

enzyme and high tolerance to organic solvents are available from Altus Biologics (Arroyo et al. 2003).

Table 2: Penicillin amidase immobilised on several matrices *via* various methods.

Enzyme	*Substrate*	*Immobilisation matrix*	*Immobilisation method*	*[a] K_m (M)*	*Enzyme loading of the matrix (U/g dry matrix)*	*Reference*
Penicillin G amidase from E.coli	Penicillin G	Chitosan	Adsorption-reticulation	$2.22\ 10^{-3}$	210	Braun et al. (1989)
Penicillin G amidase from E.coli	6-nitro-3-phenylacet-amido benzoic acid (NIPAB)	-Polygosil 500-1525 -Polygosil 100-2540	Adsorption on iminodiacetic acid:Cu(II) chelate sorbents	-	~[b]150 ~[b] 80	Anspach and Altmann-Haase (1994)
Penicillin V amidase from Chainia	Penicillin V	Kieselguhr Polyacrylamide gel	Adsorption Entrapment	$17.1\ 10^{-3}$	290 52.88	Chauhan et al. (1998)
Penicillin G amidase from E.coli	Penicillin G	Hollow fiber membrane	Entrapment	$8.04\ 10^{-3}$	[c] 100,000	Wenten and Widiasa (2002)
Penicillin G amidase from E.coli	Penicillin G	Amberlite-XAD-7	Covalent/ glutardialdehyde	$1.09\ 10^{-3}$	400	Bianchi et al. (1996)
Penicillin G amidase from E.coli	Penicillin G	Vinyl copolymers	Covalent/L-Lysine/ glutardialdehyde	-	123	Dhal et al. (1985)
Penicillin G amidase from E.coli	Penicillin G	Silica gel	Covalent/ silanisation	-	52.3	Fonseca et al. (1993)
Penicillin G amidase from E.coli	Penicillin G	Acrylic carriers	Covalent/ glutardialdehyde	-	[b] 10.83	Bryjak and Noworyta (1993)
Penicillin G amidase from E.coli	Penicillin G	Acrylic carriers	Covalent/ glutardialdehyde	-	[b] 4.0	Bryjak et al. (1989)
Penicillin G amidase from K.citrophila	NIPAB	Sepharose	Covalent/ different methods	-	[b] 200	Guisán et al. (1988)
Penicillin G amidase from B.megaterium	Penicillin G	Polyacrylo-nitrile fibers	Covalent/ glutardialdehyde	-	2330	Matsumoto et al. (1993)
Penicillin G amidase from E.coli	Penicillin G	α-glucan	Covalent/ BrCN	-	736	Matsumoto et al. (1993)
Penicillin G amidase from E.coli	Penicillin G	Sephadex G-200	Covalent/ BrCN	-	468	Matsumoto et al. (1993)
Penicillin G amidase from E.coli	Penicillin G	Eupergit® C	Covalent/ epoxy groups	-	587 [d] 974	Janssen et al. (2002)

[a] Michaelis-Menten constant; [b] in U/ml wet matrix; [c] in u.a/m^2; [d] after the carrier with the immobilised enzyme was crushed into smaller pieces.

Recently preparation of cross-linked enzyme aggregates (CLEAs) of penicillin G acylase from *E.coli* by physical aggregation under non-denaturing conditions, and subsequent cross-linking with glutardialdehyde, was reported (Cao et al. 2000). The CLEAs of penicillin G amidase were showed to be more efficient catalysts in the synthesis of ampicillin in organic solvents than cross-linked enzyme crystals of the same enzyme. Compared to the conventionally immobilised penicillin G amidase preparates CLEAs show higher productivity and synthesis/hydrolysis (S/H) ratio in the synthesis of semi-synthetic antibiotics in aqueous media (Cao et al. 2001).

Effect of different cross-linkers on the activity and stabilisation of penicillin G amidase from *E.coli* was studied also by Erarslan and Ertan (1995). Cross-linking with dimethyladipimidate increased significantly the thermostability of the enzyme, but causes only slight augmentation of the $*k_{cat}$ value, compared to the turnover number of the free penicillin amidase.

Penicillin amidase immobilisation on metal-chelate regenerable carriers (Sepharose and silica carriers) was reported by Anspach and Altmann-Haase (1994). The investigations revealed that adsorption of the enzyme on iminodiacetic acid:Cu(II) chelate matrices was possible only in the case, where a long spacer between the support and the iminodiacetic acid was included. This spacer was required to extend to the histidine residues buried below the enzyme molecule surface. Whole cells of *E.coli* contained penicillin G amidase activity were entrapped in porous gelatine beads, which were further cross-linked with glutardialdehyde (Norouzian et al. 2002). The kinetic parameters of the immobilized enzyme were changed (the observed K_m for penicllin G as a substrate, was lower than those reported by other authors) and immobilised penicillin G amidase showed a conversion rate of 85 % for penicillin G hydrolysis in continuous system, while the conversion rate in a batch system was 60 %. Immobilisation of penicillin G amidase onto commercial polymer epoxy-activated beads (Eupergit C) resulted in (a relative) improvement of the operational stability of the enzyme for industrial applications (Katchalsky-Katzir and Kraemer 2000). In spite of the stabilisation due to the penicillin amidase covalent attachment to the polymer beads, immobilised enzyme exhibited lower turnower rates in penicillin G hydrolysis than the free biocatalyst.

* k_{cat} - turnover number; number of substrate molecules, which are converted by one substrate saturated enzyme molecule per second

This fact can be explained by diffusion limitations of a substrate and product inhibition (Janssen et al. 2002). The effect of the multipoint covalent attachment on the stability of penicillin G amidase from *K.citrophila* onto aldehyde-agarose gels was studied by Guisán (1988). Later Fernàndez-Lafuente et al. (1992) observed different effects of chemical modification with formaldehyde as well as sodium borohydride reduction on activity/stability parameters of penicillin G amidase from *E.coli* and *K.citrophila* immobilised onto agarose-gels.

Previous multipoint attachment of the enzyme to the matrix allowed preparation of penicillin G acylase derivatives 50 000 folds more thermostable than the native enzyme.

A new epoxy-charged carrier called Sepabeads-EP was employed for the immobilisation of industrial enzymes (Mateo et al. 2002), with excellent results. In fact penicillin G amidase immobilised on this support was hundreds-fold more stable than Eupergit C derivatives, following the same immobilisation protocol (Mateo et al. 2000).

Aerogels consisting of more than 96 % air and 4 % silicone dioxide were described as interesting new matrices for penicillin G amidase immobilisation (Basso et al. 2000). Due to their porosity and therefore great ability to adsorb water, these supports are advantageous to be applied for entrapment of hydrolases to be used in organic media.

2. Materials and methods

2.1. Materials

The magnetic matrices used here were commercial (M-PVA, donated by chemagen Biopolymer Technologie AG; Baesweiler, Germany) or produced as described in Part A section 2 (PMMA - poly(methyl methacrylate); PMAb - big poly(methylacrylate); PMAs - small poly(methylacrylate); PVAc - poly(vinylacetate); ASMP - amino-silanised magnetic particles). Eupergit® C250 L was trade product of Röhm GmbH and Co. (Degussa). Penicillin amidase from *E.coli* (EC 3.5.1.11) with 56 $mg \cdot ml^{-1}$ active protein, phenylmethylsulfonyl fluoride (PMSF) (>99 %; GC), bovine serum albumin (1 $mg \cdot ml^{-1}$) solution, bicinchoninic acid and cooper (II) sulfate pentahydrate (4 % w/v), as well as the test description for the protein determination were obtained from Sigma Aldrich Chemie GmbH (Taufkirchen, Germany). 6-Nitro-3-phenylacetamido benzoic acid (NIPAB) was from GFB GmbH (Braunschweig, Germany) and from Sigma Aldrich Chemie GmbH (Taufkirchen, Germany). Polyethersulfone filters 0.45 μm were from PAL Gelman Lab. (PAL Corporation, USA). All other chemicals were analytical grade.

2.2. Immobilisation of penicillin amidase from E.coli onto epoxy-modified magnetic polymer matrices

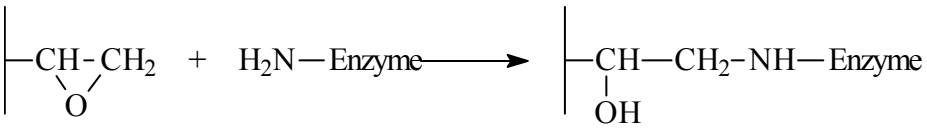

Figure 6: Immobilisation of penicillin amidase from *E.coli* onto epoxy-modified magnetic polymer matrices - schematic representation.

Epoxy-modified matrices are able to react with different nucleophiles on the protein molecule surface (e.g. amino-, hydroxyl-, or thiol- moieties) to form extremely strong linkages (secondary amino bonds, ether bonds, thioether bonds) with minimal chemical modification of the protein. In Fig. 6 the reaction of the epoxy-activated magnetic support with the amino groups of the enzyme is represented schematically.

Before the covalent attachment of the enzyme, all types of polymer magnetic beads were equilibrated with the immobilisation buffer. 60 mg active protein per gram dry carrier were used for immobilisation. After each immobilisation step the particles were separated from the supernatant magnetically. The polymer magnetic beads with immobilised PA were stored in a sodium phosphate buffer pH 7.5, I=0.2 M at 4°C. The amount of immobilised enzyme was calculated from the activity balances of the immobilisation (equation 2.2). Epoxy-activated polymer magnetic beads were suspended in a penicillin amidase solution in sodium phosphate buffer pH 7.5 with I=0.2 M, I=0.5 M or I=1 M and the immobilisation was performed at room temperature and gentle mixing (Rotator SB1; VWR International AG; Bruchsal, Germany) for 24 h (or for 72 h only in one case; to be discussed later). Once the reaction was completed, in order to remove the non-covalently attached enzyme, the magnetic matrix with immobilised PA was washed as follows: with 1 M phosphate buffer (pH 7.5), sodium acetate buffer (pH 4.0, I=0.1 M), sodium bicarbonate buffer (pH 9.0, I=0.2 M) and at the end for several times with sodium phosphate buffer pH 7.5, I=0.2 M until the washings showed no enzyme activity. Immobilised enzyme preparation was treated for 12 h with 1 M ethanolamine by gentle mixing (Rotator SB1; VWR International AG; Bruchsal, Germany), at pH 8.0 in order to block non-reacted epoxy groups. After completion of the reaction the immobilised penicillin amidase preparations were washed with sodium phosphate buffer pH 7.5, I=0.2 M and stored in it at 4 °C. The amount of bound enzyme (enzyme loading) was calculated from the enzyme activity balance:

$$IPA = \frac{C_i V_i - \left(C_s V_i + \sum_{i=1}^{n} C_{wi} V_{wi} \right)}{W} \tag{2.2}$$

where,

IPA - immobilised penicillin amidase, enzyme amount bound onto (dry) magnetic matrices [mg·g^{-1}]; C_i - initial concentration of the penicillin amidase [mg·ml^{-1}]; V_i - initial volume of the enzyme solution [ml]; C_s - final concentration of penicillin amidase in the supernatant buffer [mg·ml^{-1}]; C_{wi} - concentration of penicillin amidase

in the washing buffers [mg·ml^{-1}]; V_{wi} - volume of the washing buffers [ml]; i - number of the washing buffer (i = 1 to n) [-]; W - dry weight of the magnetic matrix [g].

The amount of immobilised protein was calculated in a similar manner, but using the concentrations of the total protein in the enzyme solution (before and after the immobilisation completion) and these in the washings.

The immobilisation yield was calculated as shown in equation (2.3):

$$IY = \frac{C_i V_i - \left(C_s V_i + \sum_{i=1}^{n} C_{wi} V_{wi} \right)}{C_i V_i} \cdot 100 \qquad (2.3)$$

where,

IY – immobilisation yield [%]; all other parameters the same as in equation (2.2).

2.3. Immobilisation of penicillin amidase from E.coli onto glutardialdehyde-modified (previously amino-charged) magnetic matrices

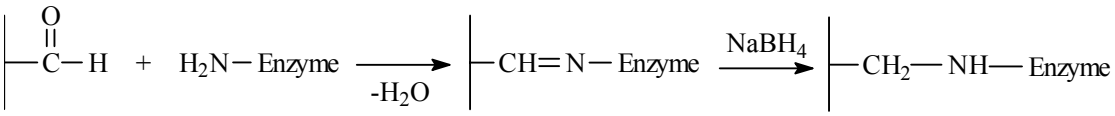

Figure 7: Immobilisation of penicillin amidase from *E.coli* onto glutardialdehyde-modified magnetic matrices - schematic representation.

Immobilisation of penicillin amidase on amino-functionalised and further glutaraldehyde-activated magnetic beads proceeded *via* a reaction of reductive amination (Fig. 7). As already described above for the epoxy-matrices, before the covalent binding of the enzyme, all types of magnetic beads were equilibrated with the immobilisation buffer. 60 mg active protein per gram dry carrier were used for immobilisation (in the case of amino-silanised magnetic particles (ASMP) 100 mg active protein were per gram beads were used for immobilisation; to be discussed later). After each immobilisation step the particles were separated from the supernatant magnetically. Aldehyde-activated (Part A section *2.2.3.)* amino-magnetic beads were suspended in the solution of PA in a sodium phosphate buffer pH 7.5 with

I=0.2 M, *I*=0.5 M or *I*=1 M and the immobilisation was performed at room temperature and gentle mixing (Rotator SB1; VWR International AG; Bruchsal, Germany) for 24 h to 72 h. After the reaction completion, the magnetic matrix with covalently bound enzyme was washed as already described for epoxy-activated magnetic matrices. The formed Schiff´s base linkages were reduced with sodium borohydride. The procedure described by Bianchi et al. (1996) was slightly modified: the magnetic carrier with the immobilised penicillin amidase was suspended in 2.5 $mg \cdot ml^{-1}$ sodium borohydride solution in a sodium phosphate buffer pH 7.5 with *I*=0.2 M and the reaction was conducted for 45 min at room temperature in a fume cupboard. The immobilised enzymes were washed and stored in a sodium phosphate buffer pH 7.5 *I*=0.2 M at 4 °C.

The amount of the immobilised enzyme was calculated as described in equations (2.2) and (2.3).

2.4. Immobilisation of penicillin amidase from E.coli onto N,N'-carbonyl diimidazole (CDI)-modified magnetic matrices

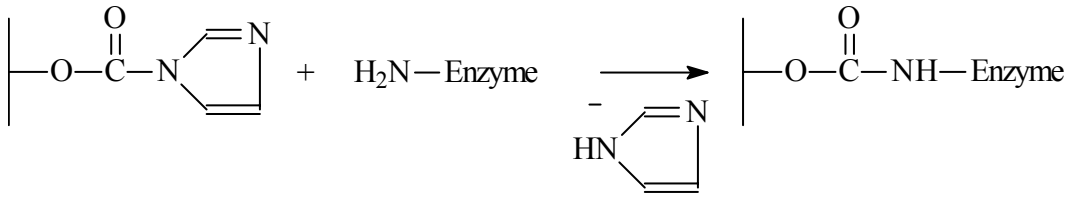

Figure 8: Immobilisation of penicillin amidase from *E.coli* onto *N,N'*-carbonyl diimidazole-modified magnetic matrices - schematic representation.

Immobilisation proceeds *via* a reaction between the imidazolyl carbamate (see Part A section *2.2.4*.) which can react with the N-nucleophiles (α-amino and lysine side-chain (ε-amino) functionalities in the proteins) to give an N-alkyl carbamate linkage (Hermanson et al. 1992) Fig. 8.

As already described, before covalent attachment of the enzyme, all types of magnetic matrices were washed for several times with distilled water and then equilibrated with the immobilisation buffer. 60 mg active protein per gram dry carrier were used for immobilisation. After each immobilisation step the particles were separated from the supernatant magnetically. The magnetic beads were suspended in penicillin amidase solution (in a sodium phosphate buffer pH 7.5 *I*=0.2 M or *I*=1 M) and the

immobilisation was conducted for 24 h at room temperature and gentle mixing. After reaction completion, the magnetic matrix with immobilised enzyme was washed as already described for epoxy-activated magnetic matrices and stored in a sodium phosphate buffer pH 7.5, *I*=0.2 M, at 4 °C. The amount of the immobilised enzyme was calculated as described in equations (2.2) and (2.3).

2.5. Analytical methods

2.5.1. Penicillin amidase activity assay

The activity of free penicillin amidase was measured by a spectrophotometric assay with the chromogenic substrate 6-nitro-3-phenylacetamido benzoic acid (NIPAB) (Kasche et al. 1987) (Fig. 9). The test was performed as follows: the spectrophotometer was reset to zero with 125 μM NIPAB solution in sodium phosphate buffer pH 7.5, *I*=0.2 M, and the reaction was initiated by the addition of the enzyme at 25°C, then the absorbance change at λ=380 nm was measured for 1 minute. PA amount was calculated per ml stock solution.

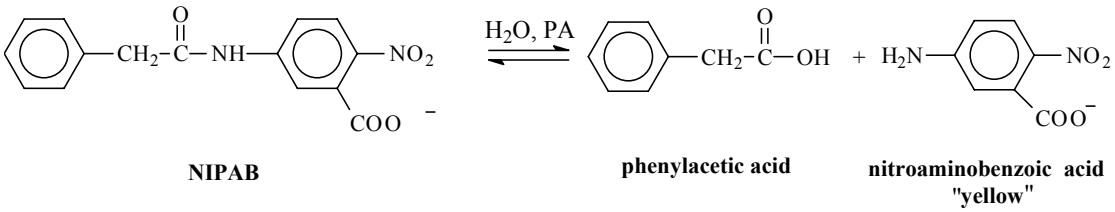

Figure 9: Penicillin amidase catalysed hydrolysis of NIPAB.

Under the conditions of the chromogenic test, stock solution of 1 mg PA·ml^{-1} causes an absorbance change of 3,0 (± 10% standard deviation) per minute, which corresponds to 42 U·ml^{-1}.

The activity measurement of the immobilised PA was performed as described by Galunsky et al. (1994). The assay was modified as follows: The spectrophotometer was reset to zero with 125 μM NIPAB solution in sodium phosphate buffer pH 7.5, *I*=0.2 M. The reaction was initiated by addition of immobilised enzyme suspension under intensive vortex-mixing (Vortex Genie 2T; VWR International AG, Bruchsal,

Germany) at 25 °C. The absorbance change at λ=380 nm in the supernatant was measured after one minute reaction (including the separation of the immobilised biocatalyst by centrifugation).

2.5.2. Penicillin amidase active site titration

Active site titration (AST) is a well known technique for the determination of the (active) enzyme concentration. For the PA this is done using the reversible inhibitor phenylmethylsulfonyl fluoride (PMSF) (Svedas et al. 1977) (Fig. 10). One molecule PMSF acylates selectively the active site serine B1 in the PA and thus deactivates the enzyme. This acyl-enzyme is deacylated extremely slowly and other substrates cannot be hydrolysed. Samples containing equal PA amounts were incubated with different PMSF concentrations for 20 min (free enzyme) and 2 h (immobilised penicillin amidase) by gentle mixing at room temperature. After incubation the residual activity of the enzyme was measured with the NIPAB test as described above. As the concentration of the inhibitor increases, the residual enzyme activity decreases. The reaction rate in the sample without inhibitor was used as a reference (100%). The reaction rates in the samples with different PMSF concentrations were calculated relative to the reference. These were plotted against the PMSF concentration. The concentration of the enzyme is equal to the concentration of the inhibitor where the relative activity equals zero.

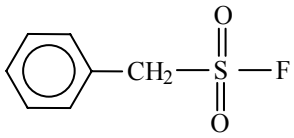

Figure 10: Phenylmethylsulfonyl fluoride – chemical structure.

2.5.3. Protein assay

The total protein amount was determined by bicinchoninic acid assay (BCA assay; Pierce Ltd., Rockford, Illinois, USA). The assay is based on the formation of a Cu^{2+}-protein complex in alkaline media, followed by reduction of Cu^{2+} to Cu^{1+}. The amount of reduced Cu^{2+} is proportional to the protein content (it has been shown that

cysteine, cystine, tryptophane, tyrosine, and the peptide bond are able to reduce Cu^{2+} to Cu^{1+}). BCA forms a purple-blue complex with Cu^{1+} under alkaline conditions, thus providing a basis for monitoring the reduction of alkaline Cu^{2+} by the proteins. As a standard protein bovine serum albumin was used. The protein measurements were performed with a "Cobas Mira Plus" - spectrophotometric-roboter from Roche (Basel, Switzerland).

2.5.4. Spectrophotometric measurements

The spectrophotometric measurements were performed with a spectrophotometer "Shimadzu UV 1202" (Shimadzu, Japan).

2.5.5. Separation of the magnetic matrices

During different procedures the matrices were separated from the liquid phase using a Nd-Fe-B block magnet (48×28×15 mm, 850 mT) from Steinert Elektromagnetbau GmbH (Germany). For centrifugation a 5415 D-Eppendorf centrifuge (Eppendorf AG, Germany) was utilised.

2.5.6. Method for determination of the dry-weight of the magnetic particles

The dry weight of the magnetic matrices was determined as they were filtered on 0.45 μm polyethersulfone filters, washed with copious amounts of distilled water, dried for 8 min. in a microwave oven at 350 W, then cooled for 24 h in desiccator. The masses of the filters were evaluated on an analytical balance Sartorius BP 221S (Sartorius AG, Germany), and the dry-weight content was calculated from the difference in masses before and after sample application.

3. Results and discussion

3.1. Immobilisation of penicillin amidase from E.coli onto M-PVA magnetic matrices

Penicillin amidase from *E.coli* was immobilised onto M-PVA beads modified with different spacers, varying also the ionic strength of the immobilisation buffer. The results are summarised in Table 3.

The table shows that for the activated with longer spacers M-PVA E02 and M-PVA N12 amino-matrices with increasing spacer length the immobilisation yield increases, in comparison to M-PVA E02 and M-PVA 012 beads, which were modified with shorter epoxy- or imidazolyl carbamate- spacers. Similar results for other carriers and enzymes are reported by Manecke and Polakowski (1981). A possible reason for this effect is that unfavourable interactions (steric repulsions) between the carrier and the enzyme molecule might be reduced (Dhal et al. 1985). Additionally, particular modification of the epoxy groups with HMDA provides moieties able to promote the initial physical adsorption (e.g. by ionic exchange) of the proteins and thus supporting the following covalent immobilisation (Mateo et al. 2000). Higher ionic strength of the immobilisation buffer can reduce unfavourable charge-charge interactions between the magnetic carrier surface and the enzyme molecule and therefore may also contribute to obtain higher enzyme loadings (Table 3).

The effect of the ionic strength is more pronounced in the case of epoxy- and CDI-modified M-PVA 012 beads than in the case of modified with longer amino-spacers M-PVA 02 and M-PVA N12 matrices. In order to validate this assumption one must look into section *3.3*. of Part A, where it can be seen that M-PVA epoxy-modified beads have negative ξ potentials at pH 7.5 (the pH of the immobilisation buffer), where penicillin amidase from *E.coli* is also negatively charged. With increasing the ionic strength of the immobilisation phosphate buffer, the potential will fall to its bulk value within a short distance (Atkins 1990). Thus the electrostatic repulsion to hinder a close approach of the enzyme molecule to the matrix can be diminished, thus allowing easier covalent binding to the shorter (compared to the amino-spacers) epoxy spacer of the magnetic beads. One possible mechanism of such salt induced

covalent attachments of the proteins was reported by Wheatley and Schmidt (1993, 1999).

Table 3: Influence of the type of chemical modification of the matrix and ionic strength of the immobilisation buffer on the amount of penicillin amidase from *E.coli* immobilised onto M-PVA magnetic beads.

All immobilisations were performed in sodium phosphate buffer pH 7.5, for 24 h at room temperature. 60 mg active protein per gram dry beads were used for immobilisation. Standard deviation ± 20 %.
ECH - epichlorohydrine; CDI - *N,N'*-carbonyl diimidazole; HMDA - hexamethylene diamine; GA - glutardialdehyde.

Type of M-PVA beads	***Active group/ Modification method***	***Active group concentration (µmol·g^{-1}dry beads)***	***Length of the spacer (Å)***	***Ionic strength of the immobilisation buffer (M)***	***Immobilisation yield (%)***	***Amount of bound protein (mg·g^{-1} dry beads)***	
						Calculated [a]	***Directly determined*** [b]
M-PVA 012	*Imidazolyl carbamate/* CDI method	n.d.	~2.4	0.2 1.0	7 17	4 10	4 9
M-PVA 012	*Epoxy/* ECH method	400	~6.0	0.2 1.0	13 37	4[c] 11[c]	4 11[d]
M-PVA E02	*Aldehyde/* ECH/ HMDA/GA method	100[e]	~20.8	0.2 0.5 1.0 1.0	38 55 67 79	23 33 40 63[f]	22 33 39[d] 32
M-PVA N12	*Aldehyde/* toluene-2,4-diisocyanate/ GA method	650[e,g]	~13.7	0.2 1.0	42 50	25 30	20 25

[a] - determined from the activity balance of the immobilisation (section *2.2.* equation (2.2)).
[b] - by direct NIPAB test with immobilised penicillin amidase (section *2.5.1.*).
[c] - in the case of epoxy-beads 30 mg active protein per gram dry beads were used for immobilisation.
[d] - directly determined by AST enzyme concentration on the matrix (section *2.5.2.*).
[e] - concentration of the amino groups of the carrier was determined.
[f] - 80 mg active protein (instead of 60 mg) per gram dry beads were used for immobilisation.
[g] - data from manufacturer.

They considered a dependence of immobilisation on the salt concentration, which is interpreted as a salt induced hydrophobic interaction on the equilibrium formation of the non-covalent protein-matrix complex.

For all studied magnetic M-PVA beads, the directly determined bound active protein per gram dry carrier was in a good agreement with the calculated values from the activity balance of the respective immobilisation.

The only case, where the amount of the active protein found by activity balance was higher than the directly determined penicillin amidase activity was where 80 mg (instead of 60 mg) active protein per gram dry beads were used for immobilisation. The M-PVA E02 magnetic beads showed higher (than in the case where only 60 mg active protein per gram dry beads were offered for immobilisation) loading capacities (see Table 3), but only 32 mg per gram active protein from immobilised 63 mg per gram were found to be active. Similar effects are reported also by Kolarz et al. (1996). This may be due to a "dence packing" of the enzyme molecules (Bryjak et al.1989), which can cause steric hindrances (also in the active site) and thus lower the enzyme activity.

Penicillin amidase from *E.coli* was immobilised onto epoxy M-PVA 012 beads following the procedure already described in section *2.2*. The process was conducted with 10 mg enzyme per gram dry carrier for 72 h. The study was done for comparison to the immobilisation of the same enzyme onto larger porous carrier Eupergit® C250 L at the same immobilisation conditions. The samples from the supernatant were taken as the immobilisation was on going and the penicillin amidase activity was determined relatively to the total active protein offered for covalent attachment at the beginning of the reaction (Fig. 11). The diagram shows that for M-PVA 012 (1-3 μm) magnetic beads the immobilisation process is completed in 24 h, while in the case of the larger (approx. 100 μm) Eupergit® C250 L for 72 h. This is due to the fact that the enzyme needs longer times in order to diffuse inside the large internal pore-net of the matrix. For the significantly smaller and practically non-porous M-PVA matrices covalent binding occurs practically only on the particle surface and it can be completed in shorter times.

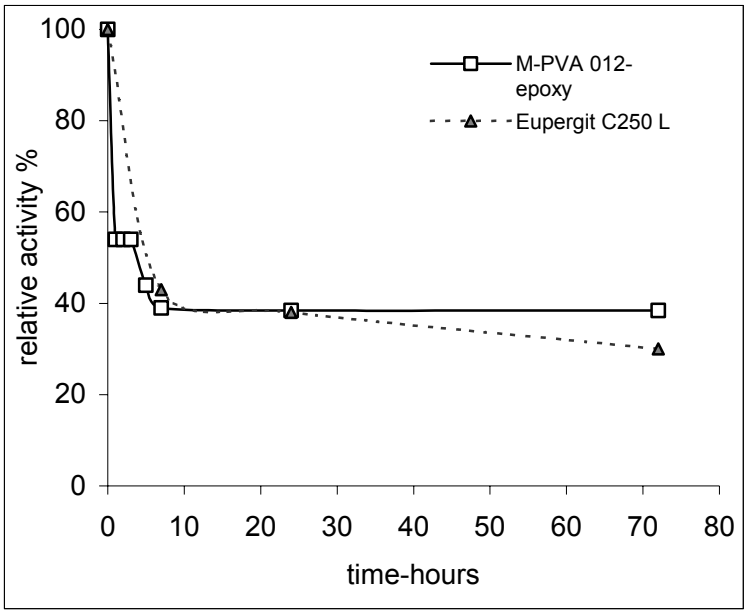

Figure 11: Comparison of the time-course of penicillin amidase (*E.coli*) immobilisation on two different types of matrices: M-PVA 012 and Eupergit® C250 L.

Immobilisation conditions: phosphate buffer pH 7.5, *I*= 0.2 M; duration 72 h; 10 mg enzyme per gram dry carrier used for immobilisation.

3.2. Immobilisation of penicillin amidase (E.coli) onto PVAc and PMMA magnetic matrices

In Table 4 the immobilisation results obtained with PMMA epoxy-modified and PVAc epoxy- and amino/glutardialdehyde- modified magnetic beads are represented.

For the same ionic strength (*I*=0.2 M), comparable spacer length and amount of the functional groups of the matrix, PMMA magnetic beads immobilised more than two-fold higher amount of active protein per gram dry carrier compared to PVAc epoxy-beads. Considering the hydrophobic nature of PMMA, some hydrophobic interactions between the polymer matrix and the penicillin amidase molecule can be expected, which will facilitate the following covalent binding. This results in more efficient immobilisation of the biocatalyst to the epoxy ligands of the magnetic matrix. Similar favourable adsorption interactions with hydrophobic matrices are described by Hermanson et al. (1992), discussed also in Part A section *1.2*. They probably support the following covalent binding of the enzyme to the matrix.

Higher ionic strength of the immobilisation buffer augments (most probably due to the same reasons already discussed for M-PVA in section *3.1*.) the amount of the

immobilised enzyme ranges up to 34 mg per gram dry epoxy-PVAc magnetic beads, although the amount of the active protein found by AST was only 8 mg per gram dry matrix. This can be due to the higher specific concentration of epoxy-sites, which are able to bind at these conditions larger enzyme amount. The obtained high enzyme density on the carrier surface can cause steric hindrances or deformation of the active centre (Kolarz et al.1996). Similar effects are described by Bryjak and Kolarz (1998).

Table 4: Influence of the type of matrix chemical modification and ionic strength of the immobilisation buffer on the amount of penicillin amidase from *E.coli* immobilised onto PVAc and epoxy-PMMA magnetic beads.

All immobilisations were performed in sodium phosphate buffer pH 7.5, for 24 h at room temperature. 60 mg active protein per gram dry beads were used for immobilisation. Standard deviation ± 20 %.
ECH - epichlorohydrine; HMDA - hexamethylene diamine; GA - glutardialdehyde.

Type of the magnetic beads	***Active group/Modification method***	***Concentration of the active groups (μmol·g^{-1}dry beads)***	***Length of the spacer (Å)***	***Ionic strength of the immobilisation buffer (M)***	***Immobilisation yield (%)***	***Amount of bound protein (mg·g^{-1} dry beads)***	
						Calculated [a]	***Directly determined*** [b]
PMMA	*Epoxy*/glycidol method	500	~7.1	0.2	30	9[c]	7
PVAc	*Epoxy*/ECH method	700	~6.0	0.2 1.0	5 57	3 34	3 8[d]
PVAc	*Aldehyde*/ECH/ HMDA/GA method	135[e]	~21.0	0.2 1.0	47 77	28 46	24[d] 33[d]

[a] - determined from the activity balance of the immobilisation (section *2.2.* equation (2.2)).
[b] - by direct NIPAB test with immobilised penicillin amidase (section *2.5.1*).
[c] - 30 mg active protein per gram dry beads used for immobilisation.
[d] - directly determined by AST enzyme concentration (section *2.5.2.)*.
[e] - concentration of the amino groups of the carrier was determined.

Here as well as for M-PVA matrix (section *3.1.*), the effect of the ionic strength on the immobilisation yield is more obvious for the modified with shorter spacer epoxy-PVAc magnetic beads. Expanding the spacer length for PVAc magnetic beads caused substantial increase in the immobilisation yields. Similar results were obtained for

M-PVA beads and reported also for other immobilisation matrices (Nouaimi et al. 2001).

3.3. Immobilisation of penicillin amidase (E.coli) onto amino / glutardialdehyde modified PMAb and PMAs magnetic beads

Penicillin amidase from *E.coli* was covalently bound onto amino-modified PMAb (10-20 μm) magnetic beads at two different ionic strengths and amino-modified PMAs (5-10 μm) magnetic beads varying the duration of the immobilisation procedure (Table 5). Both types of magnetic beads were functionalised with amino-sites through ammonolysis reaction with ethylene diamine, followed by glutardialdehyde activation as described in Part A sections *2.2.2.* and *2.2.3.*.

Table 5: Influence of ionic strength (PMAb) and duration of the immobilisation (PMAs) on the immobilisation yield of penicillin amidase from *E.coli*.
Immobilisation conditions as described in section *2.3*. Standard deviation ± 20 %.

Type of the magnetic beads	***Concentration of the amino groups (μmol.g^{-1}dry beads)***	***Length of the spacer (Å)***	***Duration of the immobilisation (h)***	***Ionic strength of the immobilisation buffer (M)***	***Immobilisation yield (%)***	***Amount of bound protein (mg.g^{-1} dry beads)***	
						Calculated [a]	***Directly determined [b]***
PMAb	640	~12.4	24	0.2	98	59	37
			24	1.0	95	57	55
PMAs	440	~12.4	24	1.0	58	35	30
			48	1.0	70	42	29
			72	1.0	90	54	42

[a] - determined from the activity balance of the immobilisation (section *2.2.* equation (2.2)).
[b] - directly determined by AST enzyme concentration (section *2.5.2.*).

The immobilisation results are summarised in Table 5. Increasing the ionic strength (from 0.2 to 1 M) in the case of PMAb magnetic carrier did not increase the amount of the immobilised enzyme at the same duration of the process. The positive ξ potential (Part A section *3.3.*) determined for the matrix implies favourable charge-

charge interactions between the PMA magnetic beads and the enzyme molecule, which has a negative charge at this pH. Therefore the increase of the ionic strength did not lead to significant augmentation in the amount of the immobilised enzyme. The longer duration of the immobilisation process in the case of PMAs magnetic beads leads to an increase of the amount of covalently bound protein.

The high immobilisation yields in a range of 70-98 % obtained with these magnetic particles can suppose an increase in the enzyme loadings (mg per gram carrier) in case where more than 60 mg penicillin amidase are going to be offered at the beginning of the reaction. Therefore the reached high amounts of bound protein per g magnetic beads can be considered as optimal yields for the described experimental conditions.

3.4. Immobilisation of penicillin amidase from E.coli onto amino-activated / glutardialdehyde modified ASMP (poly(glutaraldehyde) coated matrices

The influence of the spacer length on the immobilisation yields for two different "spacer units" - ethylene diamine/glutardialdehyde (EDA/GA) and hexamethylene diamine/glutardialdehyde (HMDA/GA) attached to ASMP/PGA carriers was studied (Table 6).

The attachment of a spacer to the surface of the immobilisation matrix could prevent undesirable side interactions between the large enzyme molecule and the surface of the magnetic support (Arica et al. 2000). In the case of the HMDA/GA modified ASMP/PGA coated matrix it was found that introduction of a longer spacer increases the enzyme loadings. The magnetic carrier showed maximal binding capacity in the case where four spacer HMDA/GA units were covalently attached to its surface. Comparable data for trypsin immobilised onto polymer carriers with different spacer lengths were reported by Manecke and Polakowski (1981). Their results indicated that if an enzyme with relatively low molecular weight is immobilised the amount of bound, but not the retained enzyme activity is affected by the spacer length.

In the case of this work this effect was also more pronounced for the amount of the immobilised (calculated from the activity balances) than for the directly measured onto the carrier penicillin amidase activity (Fig. 12 and Table 6).

Table 6: Influence of the spacer length for two different types of spacer units (EDA/GA and HMDA/GA) on immobilisation yields of the penicillin amidase from *E.coli* for poly(glutaraldehyde) (PGA) coated ASMP particles.

Immobilisation conditions as described in section *2.3* (in all cases phosphate buffer pH 7.5, *I*=0.2 M was used as immobilisation media). Standard deviation ± 20 %.

HMDA - hexamethylene diamine; EDA - ethylene diamine; GA - glutardialdehyde; PGA - poly(glutaraldehyde).

Type of the magnetic beads	***Number of the covalently attached to the matrix spacer units*** [a]	***Length of the spacer (Å)***	***Concentration of the amino groups ($\mu mol \cdot g^{-1}$ dry particles)***	***Immobilisation yield (%)***	***Amount of bound protein ($mg \cdot g^{-1}$ dry beads)***	
					Calculated [b]	***Directly determined*** [c]
ASMP-PGA coated	0	-	310[d]	65	65	54
ASMP-HMDA/GA modified	1	~16.2	425	63	63	59
	2	~32.5	315	67	67	61
	3	~48.7	313	95	95	66
	4	~64.9	380	93	93	74
	5	~81.1	370	90	90	65
	6	~97.4	350	82	82	64
ASMP-EDA/GA modified	3	~33.9	75	66	66	37
	6	~67.9	23	72	72	33

[a] - defined as one HMDA/GA or EDA/GA " spacer unit".
[b] - determined from the activity balance of the immobilisation (section *2.2.* equation (2.2)).
[c] - by direct NIPAB test with immobilised penicillin amidase (section *2.5.1*).
[d] - amino groups from the amino-silane coating of the iron oxide particles (Part A section *2.1.6.*).

For EDA/GA modified ASMP with increasing the spacer length no significant augmentation in the enzyme loadings was observed. In both cases (of 3 and 6 spacer units) the amount of the covalently bound enzyme was in the same order of magnitude, however the penicillin amidase activity directly measured onto the carrier was lower than the one calculated from the activity balance of the immobilisation

reaction. This might be due to the possible steric hindrances of the immobilised enzyme.

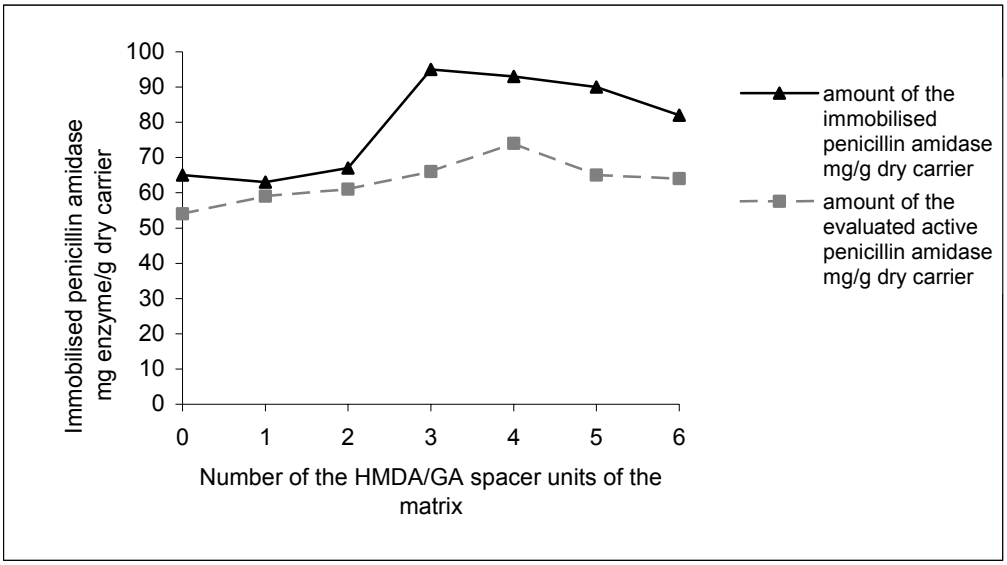

Figure 12: Immobilisation results for penicillin amidase from *E.coli* obtained for ASMP/PGA coated magnetic matrices for varied spacer lengths (different number of hexamethylene diamine/glutardialdehyde spacer units attached to the particles surface).

For these matrices very high immobilisation yields in a range up to 95 % were obtained. However, it could be expected that with an increase of the penicillin amidase amount used for immobilisation, the enzyme loadings (mg enzyme per gram dry carrier) of the supports will further rise.

The ASMP particles have a larger (compared to other carriers here) positive ξ potentials (Part A section *3.3*.) at the pH (7.5) of the immobilisation buffer. Therefore no "negative" electrochemical interactions between the enzyme and the matrices are expected. Considering this the "positive effect" of the longer immobilisation spacers must be more pronounced for magnetic matrices, which posses a negative ξ potential at pH 7.5.

4. Summary and conclusions

Penicillin amidase from *E.coli* was covalently immobilised onto magnetic matrices modified with different functional sites. The results showed that the amount of covalently bound enzyme depends on: the type of the matrix, the spacer type, and in most cases on the ionic strength of the immobilisation buffer.

- In the case of the most extensively studied here M-PVA beads, with increasing the spacer length an increase of the amount of covalently attached active protein was observed: from 4 mg active protein per gram dry beads for epichlorohydrine (ECH) and *N,N'*-carbonyldiimidazole (CDI) modified M-PVA 012 beads to up to 22 mg active protein per gram dry beads for hexamethylene diamine/glutardialdehyde (HMDA/GA) M-PVA 02 beads and up to 20 mg active protein per gram dry beads for toluene-2,4-diisocyanate/GA activated M-PVA N12 beads (data for immobilisation buffer with I=0.2 M, pH 7.5).
- The effect of the ionic strength of the immobilisation buffer on the amount of the protein covalently bound to the matrix (Fig. 13) is more pronounced in the case of modified with shorter spacers (CDI and ECH) M-PVA magnetic beads. This can be due to avoiding possible unfavorable charge-charge interactions or steric hindrances between the magnetic support surface and the enzyme molecule.

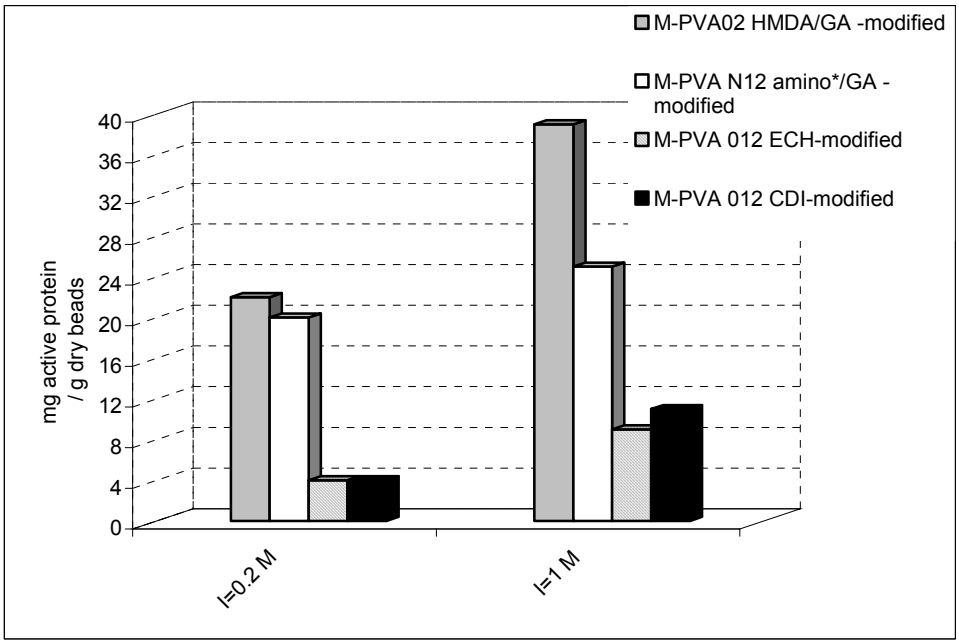

Figure 13: Immobilisation results for penicillin amidase from *E.coli* obtained for M-PVA carriers modified with four different spacers at two different ionic strengths of the immobilisation sodium phosphate buffer (pH 7.5).

All other immobilisation conditions as described in section *2*. The amount of the directly measured onto the carrier immobilised enzyme activity (mg active protein per gram dry matrix) is represented. * - amino modification with toluene-2,4-diisocyanate (manufacturer). Standard deviation ± 20 %.

CDI - *N,N'*-carbonyl diimidazole; ECH - epichlorohydrine; HMDA - hexamethylene diamine; GA - glutardialdehyde.

- Immobilisation results for epoxy-modified PMMA (glycidol-activated) and PVAc (ECH-activated) magnetic matrices (Table 4) were similar to those obtained for M-PVA 012 ECH-epoxy-charged beads. The higher amount of active protein per gram dry beads in the case of PMMA carrier can be due to hydrophobic interactions with the matrix, which make subsequent covalent immobilisation of the enzyme easier.
- Amino-modified PMAs and PMAb magnetic beads (Table 5) show similar to amino-charged M-PVA particles immobilisation capacities for penicillin amidase from *E.coli*. The ESEM images as well as the determined BET specific surface areas did not show pores large enough to be entered by the enzyme molecule. The higher enzyme loadings obtained with increasing the duration of the immobilisation process (for PMAs beads) can be due to high

specific concentration of the amino/(aldehyde) groups on the particles surface. Although the “denser packing” of the biocatalyst on the matrix surface did not lead to a significant increase in the amount of the active protein bound to the beads.

- For ASMP/PGA coated matrices with increasing spacer length (the number of HMDA/GA spacer units) the amount of immobilised as well as the amount of active protein found on the magnetic support increased (Table 6). An maximum of the immobilisation yield of 74 mg active protein per gram dry carrier was found in the case of four HMDA/GA spacer units (Fig. 12). This result presents the maximal immobilisation capacity of magnetic matrices for the chosen experimental conditions.

5. Symbols and abbreviations

Symbols

C_i	initial concentration of the penicillin amidase [mg·ml^{-1}]
C_s	final concentration of penicillin amidase in the supernatant buffer [mg·ml^{-1}]
C_{wi}	concentration of penicillin amidase in the washing buffers [mg·ml^{-1}]
i	number of the washing buffer (i =1-n) [-]
I	ionic strength [M]
IPA	immobilised penicillin amidase, enzyme amount bound onto (dry) magnetic matrices [mg·g^{-1}]
IY	immobilisation yield [%]
k_{cat}	turnover number [s^{-1}]
K_m	Michaelis-Menten constant [M]
M	concentration [mol·L^{-1}]
V_i	initial volume of the enzyme solution [ml]
V_{wi}	volume of the washing buffers [ml]
W	dry weight of the magnetic matrix [g]
U	enzyme unit [μmol·min^{-1}]

Greek Symbols

$\nu_{imm.}$	initial reaction rate of the reaction catalysed by an immobilised enzyme [M·s^{-1}]
ν_{free}	initial reaction rate of the reaction catalysed by a free enzyme [M·s^{-1}]
η	stationary effectiveness factor [-]
ξ	zeta potential [mV]

Abbreviations

AST	active site titration
BCA	bicinchoninic acid assay
CDI	*N,N'*-carbonyl diimidazole
CLEA	cross-linked enzyme aggregate
ECH	epichlorohydrine
EDA	ethylene diamine
GA	glutardialdehyde
HMDA	hexamethylene diamine
Ntn-hydrolase	N-terminal hydrolase
NIPAB	6-nitro-3-phenylacetamido benzoic acid
PA	penicillin amidase
Pen G	penicillin G (benzylpenicillin)
PAA	phenylacetic acid
6-APA	6-aminopenicillanic acid
7-ACA	7-aminocephalosporanic acid
7-ADCA	7-aminodeacetoxycephalosporanic acid
PGA	poly(glutaraldehyde)
PMSF	phenylmethylsulfonyl fluoride
S/H ratio	synthetic/hydrolytic ratio
ASMP	amino-silanised magnetic particles
M-PVA 012	magnetic poly(vinylalcohol) beads (non-functionalised)
M-PVA E02	magnetic poly(vinylalcohol) beads (epoxy-functionalised)
M-PVA N12	magnetic poly(vinylalcohol) beads (amino-functionalised)
PVAc	magnetic poly(vinylacetate) beads
PMAs	magnetic poly(methylacrylate) small beads
PMAb	magnetic poly(methylacrylate) big beads
PMMA	magnetic poly(methyl methacrylate) beads

6. References

Atkins, P.W. (1990) *Physical Chemistry* (fourth edition), Oxford University Press

Anspach, F.B., Altmann-Haase, G. (1994) *Biotechnol. Appl. Biochem*., **20**, 313-322

Arica, M.Y., Yavuz, H., Patir, S., Denizli, A. (2000) *J. Mol. Catal. B: Enzymatic*, **11**, 127-138

Arroyo, M., de la Mata, I., Acebal, C., Castillón, M.P. (2003) *Appl. Microbiol. Biotechnol.*, **60**, 507-514

Braun, J., Le Chanu, P., Le Goffic, F. (1989) *Biotechnology and Bioengineering*, **33**, 242-246

Bryjak, J., Trochimczuk, A., Noworyta, A. (1989), *Bioprocess Engineering*, **4**, 159-162

Bryjak, J., Noworyta, A. (1993) *J. Chem. Tech. Biotechnol*., **57**, 79-85

Bianchi, D., Golini, P., Bortolo, R., Cesti, P. (1996) *Enzyme Microb. Technol*., **18**, 592-596

Bickerstaff, G.F. (1997) *Immobilization of Enzymes and Cells*, Humana Press Inc. New Jersey

Buchholz, K., Kasche, V. (1997) *Biokatalysatoren und Enzymtechnologie*, VCH Verlagsgesellschaft mbH Weinheim

Bryjak, J., Kolarz, B.N. (1998) *Process Biochemistry*, **33** (4), 409-417

Basso, A., De Martin, L., Ebert, C., Gardossi, L., Tomat, A., Casarci, M., Rosi, O.L. (2000) *Tetrahedron Lett*., **41**, 8627-8630

Chauhan, S., Nichkawade, A., Iyengar, M.R.S., Chattoo, B.B. (1998), *Current Microbiology*, **37**, 186-190

Cao, L., van Rantwijk, F., Sheldon, R.A. (2000) *Organic Letters*, **2** (10), 1361-1364

Cao, L., van Langen, L.M., van Rantwijk, F., Sheldon, R.A. (2001) *J. Molecular Catalysis B: Enzymatic*, **11**, 665-670

Cao, L., van Langen, L., Sheldon, R.A. (2003) *Current Opinion in Biotechnology*, **14**, 1-8, *article in press*

Dhal, P.K., Babu, G.N., Sudhakaran, S., Borkar, P.S. (1985) *Makromol. Chem., Rapid Commun.*, **6**, 91-95

Duggleby, H.J., Tolley, S.P., Hill, C.P., Dodson, E.J., Dodson, G., Moody, P.C.E. (1995) *Nature*, **373**, 264-268

Dineva, M.A., Galunsky, B., Kasche, V., Petkov, D.D. (1993) *Bioorganic and Medical Chemistry Lett*., **3** (12), 2781-2784

Erarslan, A., Ertan, H. (1995) *Enzyme Microb. Technol*., **17**, 629-635

Fernández-Lafuente, R., Rosell, C.M., Alvaro, G., Guisán, J.M. (1992) *Enzyme Microb. Technol*., **14**, 489-495

Fonseca, L.P., Cardoso, J.P., Cabral, J.M.S., (1993) *J. Chem. Technol. Biotechol*., **58**, 27-37

Guisán, J.M. (1988) *Enzyme Microb. Technol*., **10**, 375-382

Gemeiner, P. (1992) *Enzyme Engineering: immobilized biosystems*, Ellis Horwood Ltd. and Alfa Publishers

Galunsky, B., Schlothauer, R.C., Böckle, B., Kasche, V. (1994) *Anal. Biochem*., **221**, 213-214

Hermanson, G.T., Mallia A.K., Smith, P.K. (1992) *Immobilized Affinity Ligand Techniques*, Academic Press, Inc.

Hoffmann, C. (2002) *PhD Thesis*, Forschungszentrum Karlsruhe- in der Helmholtz Gemeinschaft, University Fridericiana, Karlsruhe, Germany

Janssen, M.H.A., van Langen, L.M., Pereira, S.R.M., van Rantwijk, F., Sheldon, R.A. (2002) *Biotechnology and Bioengineering*, **78** (4), 425-432

Kasche, V. (1983) *Enzyme Microb. Technol*., **5**, 2-13

Kasche, V. (1986) *Enzyme Microb. Technol*., **8**, 4-16

Kasche, V., Haufler, U., Markowsky, D., Melnyk, S., Zeich, A, Galunsky, B. (1987) *Annals of the New York Academy of Sciences*, **501**, 97-102

Kasche, V., Galunsky, B., Nurk, A., Piotraschke, E., Rieks, A. (1996) *Biotechnology Letters*, **18** (4), 455-460

Kolarz, B.N., Bryjak, J., Wojaczyńska, M., Pawlów, B. (1996) *Polymer*, **37** (12), 2445-2449

Katschlaski-Katzir, E., Kraemer, D.M. (2000) *J. Mol. Catal. B: Enzymatic*, **10**, 157-176

Mosbach, K. (1976) *FEBS Lett.*, **62**, 80-95

Manecke, G., Polakowski, D. (1981) *J. Chromatography*, **215**, 13-24

Mosbach, K. (1987) *Methods in Enzymology*, Vol. 135: *Immobilised Enzymes and Cells* (Colowick, S.P. and Kaplan, N.O., eds.), Academic Press, Inc.

Matsumoto, K. (1993) *Industrial Applications of Immobilized Biocatalysts; Production of 6-APA, 7-ACA, and 7-ADCA by Immobilized Penicillin and Cephalosporin Amidases*, (Tanaka, A., Tosa, T., Kobayashi, T., eds.), Dekker, New York

Morgan, P.E. (1996) *PhD Thesis*, University College London, London, Great Britain

McDonough, M.A., Klei, H.E., Kelly, J.A. (1999) *Protein Science*, **8**, 1971-1981

Mateo, C., Fernández-Lorente, G., Abian, O., Fernández-Lafuente, R., Guisán, J.M. (2000) *Biomacromolecules*, **1**, 739-745

Mateo, C., Abian, O., Fernández-Lorente, G., Pedroche, J., Fernández-Lafuente, R., Guisán, J.M. (2002) *Biotechnol. Prog*., **18**, 629-634

Nouiami, M., Möschel, K., Bisswanger, H. (2001), *Enzyme Microb. Technol*., **29**, 567-574

Norouzian, D, Javadpour, S., Moazami, N., Akbarzadeh, A. (2002), *Enzyme Microb. Technol*., **30**, 26-29

Oinonen, C., Rouvinen, J. (2000) *Protein Science*, **9**, 2329-2337

Prieto, M.A., Díaz, E., García, J.L. (1996) *Journal of Bacteriology*, **178** (1), 111-120

Parmar, A., Kumar, H., Marwaha, S.S., Kennedy, J.F. (2000), *Biotechnology Advances*, **18**, 289-301

Svedas, V.K., Margolin, A.L., Sherestyuk, C.F., Klyosov, A.A., Berezin, I.V. (1977) *Biorg. Khim*., **3**, 547-553

Shewale, J.G., Sivaraman, H. (1989*) Process Biochemistry*, 146-154

Tischer, W., Kasche, V. (1999) *TIBTECH*, **17**, 326-335

Ullmann`s Encyclopedia of Industrial Chemistry (1989) (Gerhartz, W., exec. ed.), Vol. A14: *"Immobilized Biocatalysts to Isoprene"*

Vandamme, E.J. (1983) *Enzyme Microb. Technol*., **5**, 403-416

Valle, F., Balbàs, P., Merino, E., Bolivar, F. (1991) *TIBS*, **16**, 36-40

Wheatley, .B., Schmidt, D.E., (1993) *J. Chromatography*, **644**, 11-16

Wheatley, .B., Schmidt, D.E., (1999) *J. Chromatography A*, **849**, 1-12

Wenten, I.G., Widiasa, I.N. (2002) *Desalination*, **149**, 279-285

Zmijewski, M.J.Jr., Briggs, B.S., Thompson, A.R., Wright, I.G. (1991) *Tetrahedron Lett.*, **32** (13), 1621-1622

Part C: Evaluation of the selectivity and stereoselectivity of penicillin amidase from *E.coli* immobilised onto magnetic micro-matrices

1. Knowledge basis

1.1. Enzyme catalysis and kinetics

Enzymes are catalysts of unique properties, which allow them not only to speed up one defined reaction, but also to minimise the yield of undesired side products. Generally the mechanism of the enzyme catalysis includes:

- Non-covalent binding of the substrates in the substrate-binding sub-sites. According to the convention employed to describe the substrate specificity of proteolytic enzymes (Schlechter and Berger 1967), the substrate-binding sub-sites are assigned as S_i and S'_i (Fig.1). This description can be applied also for transformation of non-peptides as substrates.
- After the correct substrate binding, the catalytic site C interacts with the part of the substrate, causing thus chemical reaction to convert it into product(s).
- Finally the product formed, dissociate from the enzyme-product complex. The binding of the product in the active site may cause product inhibition (hampers the binding of the substrate). This cannot be avoided in the enzyme-catalysed reaction. Therefore in biocatalytic processes larger substrate concentrations (up to 1 M) are used compared to those in the living systems (< 10^{-3} M) (Buchholz and Kasche 1997).

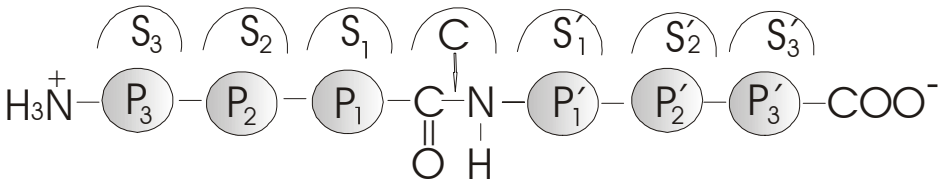

Figure 1: Convention, which describes the substrate specificity of the enzymes, represented for peptidases (Schlechter and Berger 1967) – modified diagram. C - catalytic site; S_i and S'_i – binding sub-sites before and after the chemical bond, which is going to be changed during the reaction.

The substrate-binding sub-sites and the catalytic-site form the *active site/centre*. The structure of the penicillin amidase active site, as well as the catalytic mechanism were described by Duggleby et al. (1995).

In the complex, where the substrate(s) are bound into the active site (by electrostatic or hydrophobic interactions), both the structure of the substrate(s) and the enzyme active centre are changed in a way that they can interact with a precision within 10^{-2} nm (Buchholz and Kasche 1997). This leads to a decrease in the activation energy compared to the non-catalysed reaction. Thus, the rate of the enzyme-catalysed process can be accelerated by a factor of up to 10^{10}.

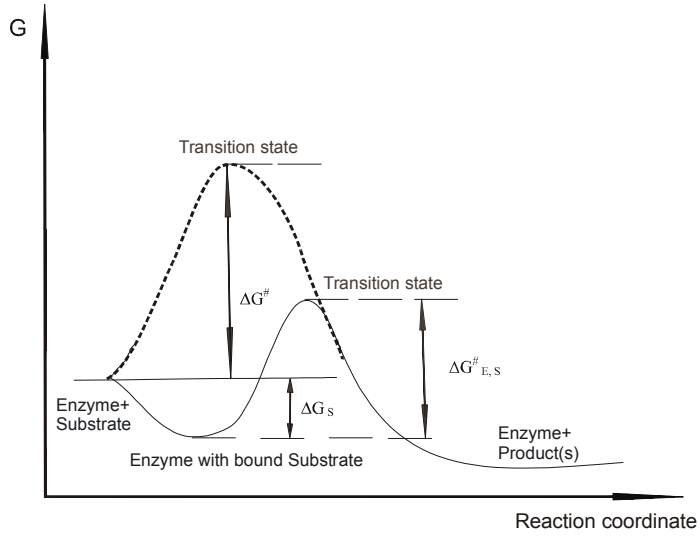

Figure 2: Free energy diagram for an enzyme catalysed (—) and non-catalysed (---) reaction.

Fig. 2 presents schematically the free energy diagram for enzyme-catalysed and non-catalysed processes. The diagram shows, that the (apparent) activation energy of the enzyme-catalysed reaction ($\Delta G^{\#}_{E,S}$) is much smaller than this for non-catalysed reaction ($\Delta G^{\#}$), where ΔG_S is the free energy of binding.

For amide (peptide) bond hydrolysis, which involves formation of covalent acyl-enzyme intermediate the diagram in the Fig. 3. can be used.

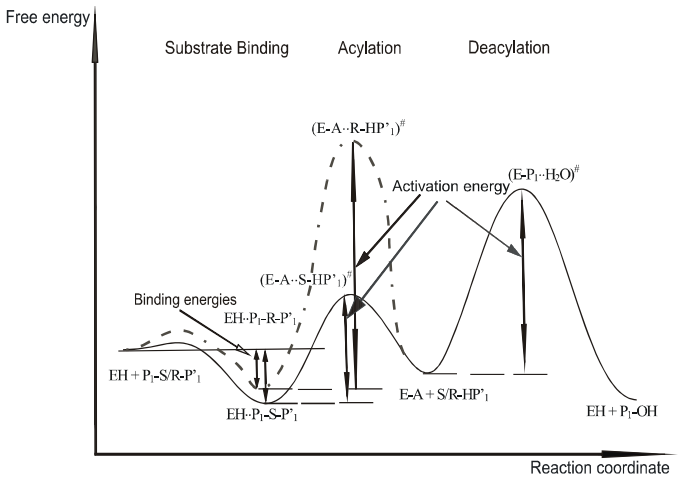

Figure 3: Free energy diagram for an enzyme catalysed process with the formation of an acyl-enzyme intermediate. One binding and two chemical reactions with an S- (—) and R- (---) amino acid in the P_1 position are demonstrated (Buchholz and Kasche 1997).

The free energy of binding ΔG_S determines a dissociation constant K_S from which the Michaelis-Menten constant K_m, employed as a quantitative measure for the substrate binding, can be derived. The activation energy $\Delta G^{\#}_{E,S}$ defines the turnover number assigned as k_{cat}. It is a first order rate constant, which refers to the properties and reactions of the enzyme-substrate, enzyme-intermediate and enzyme-product complexes (Fersht 1985). For the mechanism shown in Fig. 3 the turnover number depends on the first order rate constants for both reactions.

Many enzymes are able to catalyse the conversion of different substrates, which results in different K_m and k_{cat} values. They reflect the thermodynamic understanding of the enzyme substrate specificity. The above-mentioned constants will vary also for the same substrate using enzymes with the same function, but from diverse sources.

Kinetic description of the enzyme-catalysed reactions

The enzyme-catalysed reactions can be: one-substrate processes (in the case of lyases in one direction and isomerases in both directions) and two-substrate processes (for all other enzymes classes) (Buchholz and Kasche 1997). In the case of two-substrate reactions, two possible manners of the substrate-binding can be described (Fig. 4).

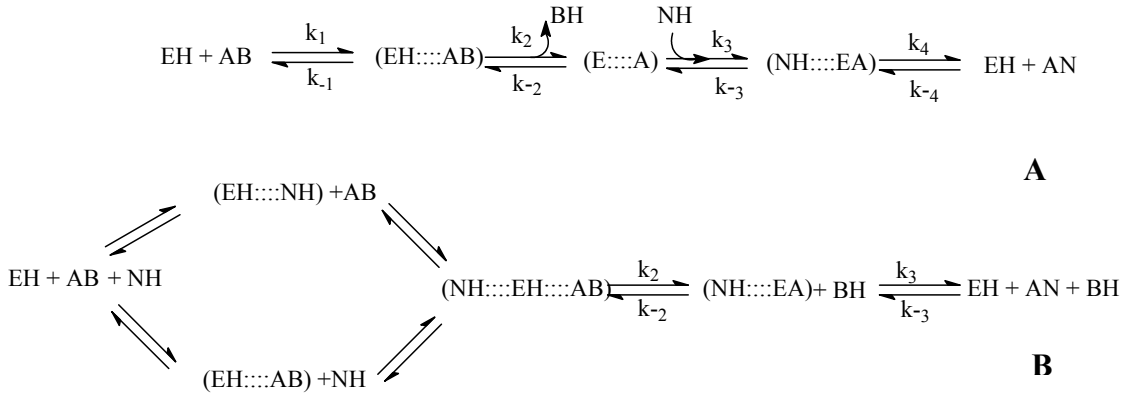

Figure 4: Schematic representation of two-substrates enzyme-catalysed reactions. **A**- both substrates cannot be bound simultaneously in the active centre; **B**- both substrates can be bound simultaneously in the active centre (Buchholz and Kasche 1997). EH-enzyme; AB-substrate; NH-substrate; AN, BH-products; (::::) - denotes non-covalent binding.

System of equations that describes quantitatively the enzyme properties and the rate of the enzyme reaction can be derived assuming that:

-the substrate concentration is much higher than the enzyme concentration at the beginning of the reaction (t = 0);

-only the initial rate of the reaction is measured;

-equilibrium in the binding of the substrates is achieved;

-steady-state in the concentrations of the intermediates EH··AB, NH··EH··AB, NH··EA, EA. [(··) - denotes non-covalent interactions, EA - covalent acyl-enzyme intermediate)].

The rate of the product formation for the reaction represented in Fig. 4 **A** is:

$$\nu = d[AN]/dt = k_4\,[EA\cdot\cdot NH] \qquad (3.1)$$

An expression for [EA··NH] from the known $[EH]_0$, $[AB]_0$, $[NH]_0$ concentrations and the rate constants, can be derived from linear set of equations (Buchholz and Kasche 1997). After insertion in (3.1) the following relation for one-substrate reaction is derived:

$$\nu = \frac{V_{\max}[AB]_0}{K_m + [AB_0]} \qquad (3.2)$$

This expression for the rate of enzyme-catalysed reaction was first described by Michaelis and Menten in 1913. In this equation $V_{max}= k_{cat,AB}\,[EH_0]$.

Turnover number - k_{cat} [s^{-1}] denotes the number of substrate molecules, which can be converted from one "substrate-saturated" enzyme molecule per second.

K_m is an apparent dissociation constant, that may be assigned as the overall dissociation constant of all enzyme-bound species (Fersht 1985). It has dimension [M] and denotes the concentration of the substrate, at which 50 % from the maximal velocity V_{max} has been reached.

If the initial concentration of NH is large (the case where NH = H_2O), k_{cat} and K_m are expressed as follows:

$$k_{cat,AB} = \frac{k_2 k_4}{k_2 + k_4} \tag{3.3}$$

$$K_{m,AB} = \frac{k_4\left(k_{-1} + k_2\right)}{k_1\left(k_2 + k_4\right)} \tag{3.4}$$

For smaller initial NH concentrations these constants will depend on $[NH]_0$. Both parameters k_{cat} and K_m depend on pH, temperature and ionic strength, and are employed to describe the kinetic properties of the enzyme. k_{cat}/K_m ratio [$M^{-1}\cdot s^{-1}$] – assigned as specificity constant is an apparent second-order rate constant, that refers to the properties and the reactions of the free enzyme and free substrate (Fersht 1985).

With respect that $V_{max}= k_{cat}[E]_0$ the equation (3.2) could be rearranged to give:

$$\nu = V_{max} - \frac{K_m \nu}{[AB]_0} \tag{3.5}$$

Plotting of ν as a function of $\nu/[AB]$ gives an intercept of V_{max} on the y axis as $\nu/[AB]$ tends towards zero. The slope of the line is equal to $-K_m$. This linear dependence is known as Eadie-Hofstee plot. Another frequently used method is to plot $1/\nu$ against 1/[S], called Lineweaver-Burk-Plot. It was shown that the Eadie-Hofstee plot is in general more accurate than the Lineweaver-Burk one (Fersht 1985, Bisswanger 2000).

Although the immobilised biocatalysts offer a lot of advantages (discussed already in Part B) compared to the free ones, several undesirable effects as diffusional and mass transfer limitations can appear during the reaction catalysed by immobilised enzyme. The substrate(s) and the product(s) must diffuse through the bulk solution to the carrier surface and furthermore inside the matrix-pores (in the case of large porous matrices >100 μm in diameter) in order to reach the enzyme. This diffusion may become a rate-limiting step. A measure for the relative magnitude of the diffusion and the maximal reaction rate is the dimensionless number Thiele modulus φ:

$$\varphi^2 = \frac{R^2 V'_{\max}}{D'_S K'_m} \tag{3.6}$$

where:

R - radius of the carrier-particles [m]; $V'_{\max}$ - maximal velocity of the reaction, catalysed with immobilised enzyme [M·s^{-1}]; D'_S - diffusion coefficient in the particles [m^2·s^{-1}]; K'_m - Michaelis-Menten constant for the immobilised enzyme [M].

For comparison of free and immobilised biocatalysts the ratio of the immobilised and free enzyme activity called stationary effectiveness factor is employed (Kasche 1983):

$$\eta = \frac{\nu_{obs,i}}{\nu_{obs,f}} \tag{3.7}$$

where,

$\nu_{obs,i}$ - initial reaction rate with immobilised enzyme [M·s^{-1}] and $\nu_{obs,f}$ - initial reaction rate with free enzyme [M·s^{-1}] (both reactions for the same substrate concentration).

The above equation is valid for Michaelis-Menten reactions in flat carriers.

For the practical purposes the operational effectiveness factor η_0 is used:

$$\eta_0 = \frac{\tau_f}{\tau_i} \tag{3.8}$$

where,

τ_f and τ_i [s] are the times to convert the same amount of substrate with the free and respectively with the immobilised enzyme.

Due to mass-transfer limitations in many biotechnological processes, especially hydrolysis reactions, where an acid is formed, the pH value in- and out- side the

carrier can differ considerably and thus influences the biocatalyst activity, selectivity and stability, and the reaction equilibrium (Tischer and Kasche 1999, Spiess et al. 1999).

Both effectiveness factors introduced above can be employed to characterise the immobilised biocatalysts.

1.2. Chirality. Chiral molecules. Racemic resolutions

Chiral is an object, which is not superimposable upon its mirror image. Common examples of chiral objects are the left and the right hands. Molecules, which contain a tetrahedral carbon atom attached with four different substituents (called stereogenic centre) are chiral. These molecules can exist as two different stereoisomers that are non-superimposable mirror-images of each other, called *enantiomers* (Greek: enantio- opposite). They have identical chemical and physical properties, but they differ in their ability to rotate the plane-polarized light. The enantiomers rotate the plane-polarized light to an equal, but opposite extent. The first convention, to distinguish between the enantiomers was suggested by Emil Fischer in 1919 and consequently replaced by the Cahn-Ingold-Prelog convention (Cahn et al. 1966). It is based on rules, which allow a hierarchal assignment of the substituents at any asymmetric centre (Fig. 5):

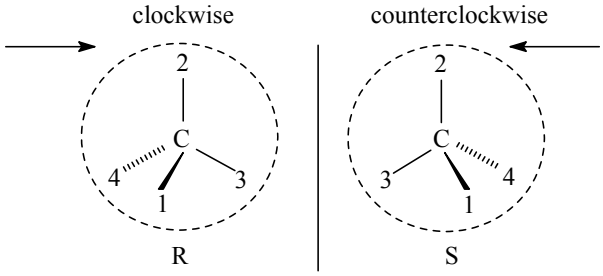

Figure 5: The Cahn-Ingold-Prelog convention of rules for determination of the enantiomer configuration.

If the path of the sequence with decreasing priority ($1 \Rightarrow 2 \Rightarrow 3$) is clockwise, the configuration is denoted as *R* (Latin: rectus - right), and if it is counterclockwise as *S* (Latin: sinister - left).

Stereoisomers, which are not mirror images of each other, are known as diastereomers. The physical and chemical properties of diastereomers differ, and furthermore their optical rotation can vary in both: sign and magnitude.
The optical purity can be defined by the term enantiomeric excess (*ee*), which is given by (for $R > S$):

$$\%ee = \frac{(R-S)}{(R+S)} \cdot 100 \tag{3.9}$$

In the chemical reactions one of the enantiomers might be preferred. In the case where the %*ee* has a value between 0 and 100 (-100) the reaction is defined as stereoselective. Processes, in which only one enantiomer is converted (%*ee* = 100 or –100) are assigned as stereospecific.
Due to their high substrate specificity and stereoselectivity, the enzymes have a steadily increasing role in the production of pure enantiomers. The strength of the substrate binding can vary for the enantiomers due to possible sterical hindrances. The formed during the catalytic process diastereomeric transition states as well as diastereomeric products have different contributions to the free energy. The chemical resolution of racemates can be controlled in different stereochemical manners (Fig. 6). In the case, where pure enantiomers are irreversibly transformed by a chiral reagent *via* diastereomeric transition states into their products the process is assigned as kinetically controlled (Lummer 2000). The stereoselectivity is then quantified by the difference between the free activation energies of the diastereomeric transition states:

$$\Delta\Delta G_{SR}^{\#} = \Delta G_S^{\#} - \Delta G_R^{\#} = -RT \ln \frac{k_S}{k_R} \tag{3.10}$$

By reversible processes the ratio between the products is determined from the free energies of their ground state.

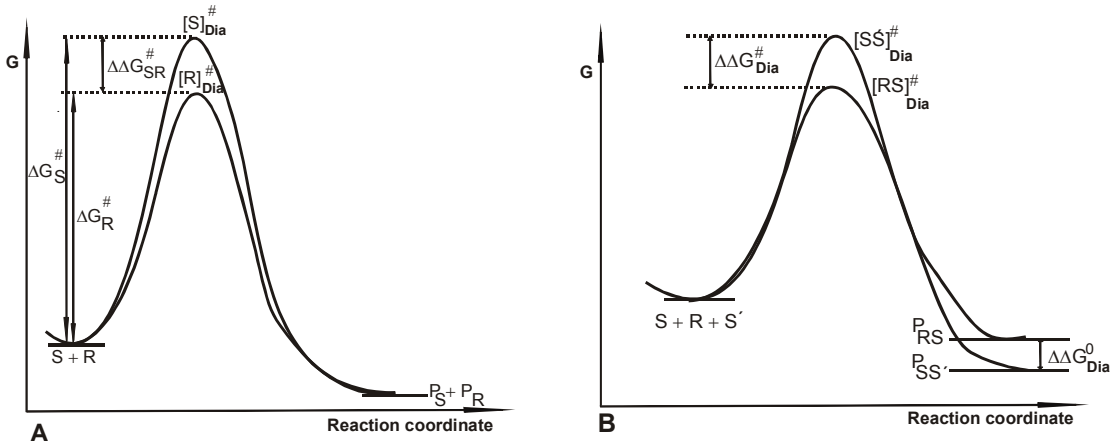

Figure 6: Free energy diagrams: **A** kinetically controlled racemic resolution with pure enantiomeric products and **B** thermodynamically controlled racemic resolution with diastereomeric products (Lummer 2000).

Such reactions are thermodynamically or equilibrium controlled:

$$\Delta\Delta G_{Dia}{}^{0} = \Delta G_{SS'}{}^{0} - \Delta G_{RS'}{}^{0} = -RT \ln \frac{k_{SS'}}{k_{RS'}} \qquad (3.11)$$

Due to the fact that the differences between the free energies of the ground states are in general less than the ones between the transition states, the equilibrium-controlled processes are in the most cases disadvantageous for racemic resolutions.

1.3. Kinetically and equilibrium controlled processes catalysed by hydrolases. Enantioselectivity of penicillin amidase

In general hydrolases can be used to catalyse the synthesis of condensation products (β-lactam antibiotics, peptides, etc), which can be carried out either as an equilibrium controlled or kinetically controlled processes (Fig. 7).

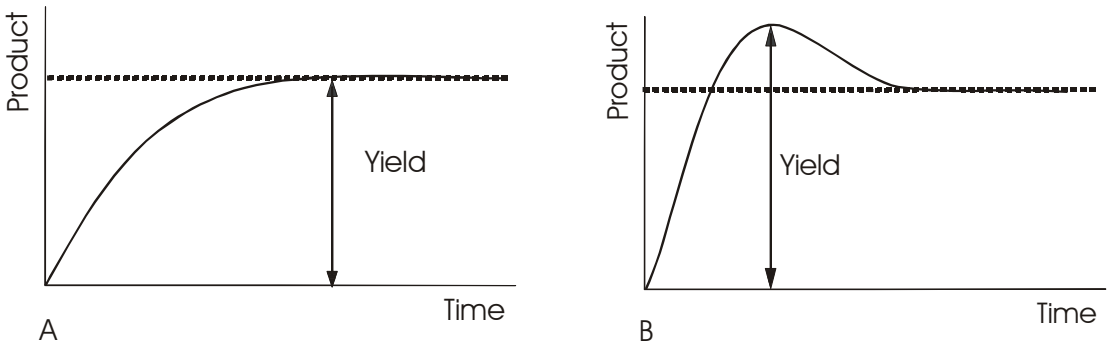

Figure 7: Schematic presentation of the reaction course of an equilibrium (A) and kinetically (B) controlled process. The dotted line indicates the thermodynamic equilibrium between the substrate and the product.

The yield (the molar ratio of formed product to invested substrate) in the kinetically controlled processes can be influenced not only by the chemical equilibrium (i.e. the reaction conditions), but also additionally (contrary to the equilibrium controlled reactions) by the enzyme properties. In the kinetically controlled reactions higher than in the equilibrium controlled processes yields can be obtained (Kasche 1986).

In the case, where the acyl-enzyme intermediate is going to be deacylated by other than the water nucleophiles, the hydrolases act as transferases (transfer of the acyl group to the nucleophile). These reactions require an activated substrate (Kasche 1986).

The enzyme-catalysed production of pure chiral substances in the pharmaceutical and fine chemical industry steadily increases (Sheldon 1993, Bossi et al.1998, Gröger et al. 2001, Landis et al. 2001, Turner 2003).

Quantitative measure for the enzyme enantioselectivity in these processes is the enantiomeric ratio. It is evaluated from the rate constants of the enzyme-catalysed reaction for the *S*- and *R*-enantiomer (Chen et al. 1982):

$$\mathrm{E} = \frac{k_S}{k_R} \tag{3.12}$$

With regard to obtain high steric purity of the products E should be > 100 for an S-specific enzyme or < 0.01 for an R-specific enzyme.

In Fig. 3 above is shown the free energy diagram for an enzyme-catalysed process (hydrolysis of a dipeptide) involving formation of acyl-enzyme intermediates for *R*- and *S*- enantiomer of the substrate. Both the binding and the activation energies for the enatiomers can differ.

For equilibrium controlled enzyme-catalysed reactions (i.e. hydrolysis by hydrolases) the enantioselectivity is defined as the ratio of the specificity constants for both enantiomeric substrates (Chen et al. 1982):

$$\mathrm{E}_{hyd} = \frac{\left(\frac{k_{cat}}{K_m}\right)_S}{\left(\frac{k_{cat}}{K_m}\right)_R} \tag{3.13}$$

Equation (3.13) shows that the enantiomeric ratio in this case is an intrinsic enzyme property (Galunsky et al. 2002), which determined with isolated enantiomers will give the information of how the binding and activation energies are employed by the biocatalyst to discriminate between the enantiomers and will allow to study the influence of different factors (temperature, pH etc.) on the enzyme stereoselectivity (Kasche et al. 1996, Galunsky et al. 1997, Lummer et al. 1999). For kinetically controlled synthesis catalysed by amidases and peptidases, the stereoselectivity in the S'_1 binding sub-site was initially defined as the ratio of the transferase to hydrolase rate constants for the enantiomeric nucleophiles (Kasche 1986):

$$\mathrm{E}_{syn} = \frac{\left(\frac{k_T}{k_H}\right)_S}{\left(\frac{k_T}{k_H}\right)_R} \tag{3.14}$$

where,

$$\left(\frac{k_T}{k_H}\right)_{app} = \frac{\nu_T[\mathrm{H_2O}]}{\nu_H[\mathrm{NH}]} \tag{3.15}$$

ν_T - initial rate of the condensation product formation [M·s^{-1}]; ν_H - initial rate of hydrolysis product formation [M·s^{-1}]; [H_2O] - concentration of the water [M]; [NH] - concentration of the nucleophile [M].

If the initial concentrations of the nucleophiles are equal and considering the equation (3.12), E determined with racemic nucleophile is:

$$E_{syn,rac} = \frac{\nu_{T,S}}{\nu_{T,R}} \tag{3.16}$$

Galunsky and Kasche (2002) showed that $E_{syn} = E_{syn,rac}$ only in the case when deacylation of the acyl-enzyme-nucleophile complexes for the both enantiomeric nucleophiles can be neglected ($k_{h,N,R} = k_{h,N,S} = 0$) (Fig. 8). According to this mechanism for the equilibrium in NH binding (neglecting the AN hydrolysis) and for reaction with an isolated enantiomer the k_T/k_H ratio determined form the initial rates is (Kasche 1986):

$$\left(\frac{k_T}{k_H}\right)_{app} = \frac{k_t}{\left(k_h K_N + k_{h,N}[\mathrm{NH}]\right)} \tag{3.17}$$

where K_N is the equilibrium constant for nucleophile binding to the acyl-enzyme, k_t is the deacylation rate constant of the acyl-enzyme-nucleophile complex, k_h is the deacylation rate constant of the acyl-enzyme by water, and $k_{h,N}$ is the deacylation rate constant of the acyl-enzyme-nucleophile complex by water.

Assuming equation (3.14) the enantiomeric ratio E is:

$$E_{syn} = \frac{k_{t,S}\left(k_h K_{N,R} + k_{h,N,R}[\mathrm{NH}_R]\right)}{k_{t,S}\left(k_h K_{N,S} + k_{h,N,S}[\mathrm{NH}_S]\right)} \tag{3.18}$$

The equation (3.18) shows that in the case, where the E is determined with isolated enantiomers, it depends on the nucleophile concentration and it is not an intrinsic property of the enzyme. In case where racemic nucleophiles are converted, they compete for the acyl-enzyme and according to Fig. 8 can be derived:

$$E_{syn,rac} = \frac{k_{t,S} K_{N,R}}{k_{t,R} K_{N,S}} \tag{3.19}$$

which is an intrinsic property of the enzyme (Galunsky and Kasche 2002).

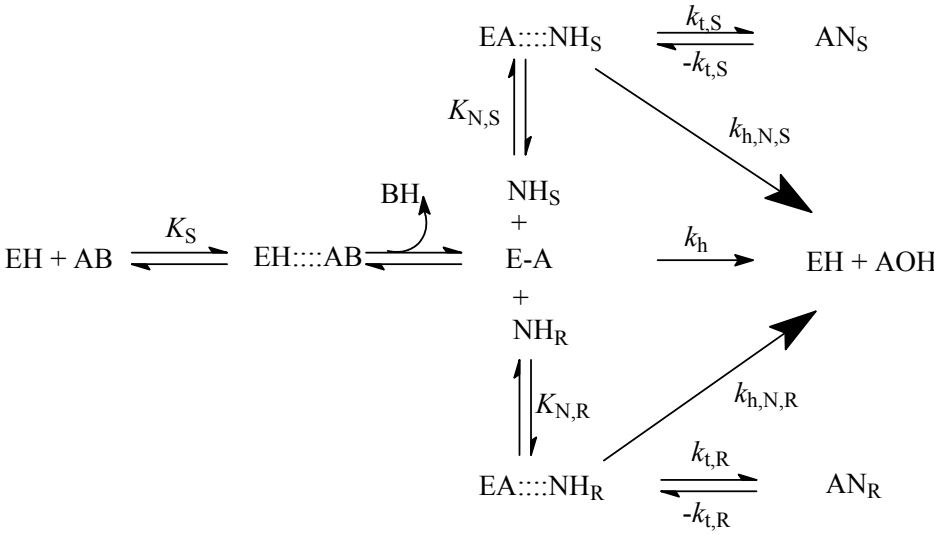

Figure 8: Schematic* presentation of the mechanism for the hydrolase catalysed synthesis of condensation product AN from an activated substrate AB and a racemic nucleophile NH.
*For simplification the binding of the nucleophile to the enzyme and enzyme-substrate complex is neglected.

The best-characterised penicillin amidase from *E.coli* was found to be R-specific in the S_1-binding site and S-specific in S'_1 binding site (Kasche et al. 1996). Observed stereoselectivities of the penicillin amidase are much larger in the S'_1 than in S_1-subsite (Galunsky et al. 2000). Being a ratio of rate constants, E depends on the temperature and the pressure (Rieks 1997). The enzyme enantioselectivity was generally found to decrease with temperature, but for substances that are bound very strongly, the opposite temperature dependence has been found (Galunsky et al. 1997). When the enzyme contains in the active site basic or acidic groups, which must be charged or uncharged during the catalysis the pH-dependence of the stereoselectivity is possible. The pK_a values of these groups can be disturbed when the S- or R-substrate enantiomer is bound into the active site leading to a pH dependence of E (Lummer 2000).

The enantioselective properties of the penicillin amidase were employed largely in the recent years: enantioselective acylation of β-lactam intermediate for the synthesis of loracarbef (Zmijewski et al. 1991); preparation of chiral beta amino acids (Landis et al. 2001); amines-resolution (van Langen et al. 2000); enantoselective acylation of amines (in aqueous medium (Guranda et al. 2001).

1.4. Penicillin amidase in the synthesis of semi-synthetic β-lactam antibiotics

After the discovery of the antibacterial activity in the mold *Penicillium notatum* (Fleming 1929), penicillin G was characterised and largely employed in the clinical practice. Later, due to the fact that an increased number of bacterial strains became resistant to penicillin G, in the 1960's it was replaced by various semi-synthetic penicillins (derived from acylated by various side-chains 6-aminopenicillanic acid; 6-APA) (Wegman et al. 2001). Introduced later in the medical practice semi-synthetic cephalosporins are derived from acylated by different side-chains 7-aminodeacetoxycephalosporanic acid; 7-ADCA. The industrial synthesis of β-lactam antibiotics and their intermediates is undergoing remarkable transformation: the traditional chemical methods (requirement of hazardous chemicals and solvents; extreme conditions; long reaction times) are going to be replaced by environmentally and economically more viable enzyme-catalysed reactions (Bruggink et al.1998, Wegman et al. 2001, Arroyo et al. 2002).

As discussed in section 1.3 enzyme-catalysed condensation reactions can be performed under equilibrium or under kinetic control (Kasche 1986, Kasche et al. 1987b). The equilibrium controlled processes involve direct acylation of the nucleophilic compound (6-APA; 7-ADCA) by free acids at low pH values. The known penicillin amidases do not accept charged functions, and therefore if the phenylglycine is used as substrate, the carboxyl function must be uncharged. However, when this is reached, the amino group will be charged and the enzyme catalytic function is therefore not possible (Bruggink et al. 1998). Because the direct condensations are thermodynamically limited (Schroën et al. 1999, Youshko et al. 2001), an efficient production of the semi-synthetic β-lactam antibiotics can only be completed by a kinetically controlled acyl-transfer reaction with activated substrates (e.g. amides, esters). The mechanism of the kinetically controlled synthesis, in which

non-equilibrium concentrations of the desired condensation product (antibiotic) can be obtained, was described by Nam et al. (1985) for the formation of cephalexin (from 7-ADCA and phenylglycine methyl ester), catalysed by *Xanthomonas citri*, but it holds equally well for other antibiotics (Bruggink et al. 1998). The yield in these type of processes depends not only on the reaction conditions, but also on the enzyme properties (Buchholz and Kasche 1997), and it is determined from the rate of three different reactions catalysed by the enzyme: (i) the synthesis of β-lactam compound, (ii) the hydrolysis of the activated acyl donor and (iii) the hydrolysis of the synthesised antibiotic. Fig. 9 presents a simplified mechanism of the kinetic controlled synthesis of β-lactam antibiotics (cephalexin in the case of this work) carried out with penicillin amidase.

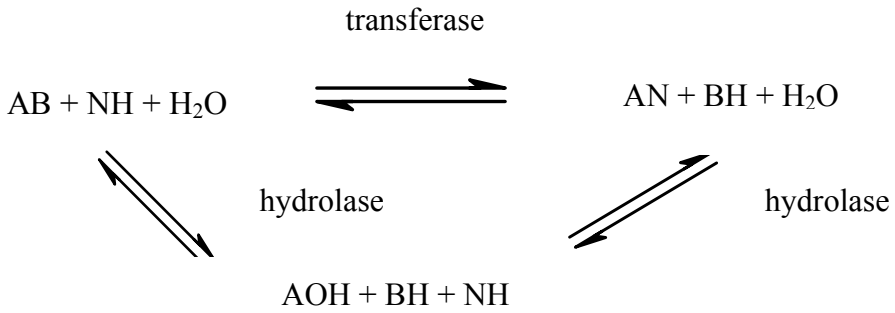

Figure 9: Schematic representation of the β-lactam antibiotics synthesis catalysed by penicillin amidase. AB-activated substrate, NH-nucleophile, AOH- hydrolysis-product, AN-condensation product (Kasche 1986).

In this reaction first the activated substrate (AB) is going to be bound to the free enzyme forming thus an acyl-enzyme complex. The last complex is then either hydrolysed to AOH or reacts with the nucleophile to produce the desired antibiotic (AN). In the case where cephalexin is going to be synthesised the activated substrate is most often phenylglycine amide or phenylglycine esters. The formed condensation product (antibiotic) can be also hydrolysed. In the last process reversible inhibition of the enzyme by phenylacetic acid that maybe present in the nucleophile (7-ADCA) is described by Schroën et al. (2001). Kasche describes inhibition by the nucleus (Kasche et al. 1984, Kasche 1986). The synthesis/hydrolysis ratio (S/H: mole ratio between the condensation product (antibiotic) and the hydrolysed side-chain donor formed) is used as a parameter to evaluate the viability of the condensation process

(Wegman et al. 2001). Different attempts to inhibit the undesired hydrolytic activity of the penicillin amidase were described: by selective removing of the product from the reaction mixture (Bruggink et al. 1998, Wegman et al. 2001); side-directed enzyme mutagenesis (Arroyo et al. 2003); improvement analogous to enzymatic peptide synthesis (Hänsler and Jakubke 1996) was observed also by performing the reaction at subzero temperatures with free biocatalyst (van Langen et al. 1999); by "lowering" the water activity due to the use of water-organic mixtures (Kasche 1986, Shewale et al. 1990). The catalytic behaviour and the stability of the penicillin amidase in systems with low water content was studied by Youshko et al. (1999). The yield determining factors as the type of the substrate activation, ionic strength, temperature, pH, organic solvents, substrate recycling were studied extensively (Kasche and Galunsky 1982, Kasche 1986, 1987a, Bruggink et al. 1998, Youshko et al. 2001, Wegman et al. 2001)

The development of the immobilised penicillin amidase techniques makes the industrial production of the semi-synthetic β-lactam antibiotic economically feasible. Possible advantages as well as the limitations, using the immobilised enzyme in the antibiotics synthesis, were studied extensively in the recent years (De Vroom 1997, Cao et al. 2001, Ilhan and Kraemer 2001, Schroën et al. 2001, 2002).

Driven by the economic and environmental needs, traditional chemical methods for the production of semi-synthetic β-lactam antibiotics are increasingly being replaced by shorter biocatalytic transformations. Combining the above-mentioned advantages of the enzymatic processes with the opportunities of the easier operation (separation of the immobilised biocatalyst) and control (stopping the reaction when the maximal yield is reached) offered by the immobilised penicillin amidase technology serves new advantageous manners of the antibiotics manufacturing.

2. Materials and methods

2.1. Materials

Benzylpenicillin (penicillin G; Pen G) was from Sigma (Heisenhofen, Germany), 7-aminodeacetoxycephalosporanic acid (7-ADCA) and *R*-phenylglycine amide were from DSM Research (Geleen, The Netherlands). *S*- , *S*,*R* - phenylalanine (Phe) and methanol (LiChrosolv®) gradient grade for liquid chromatography were from Merck (Bruchsal, Germany), *R*-Phe was from Lancaster (Mühlheim am Mein, Germany). Phenylacetyl-*R,S*-phenylalanine (PAA-*R,S*-Phe) was kindly provided by Dr. M. Guncheva (Institute of Organic Chemistry, Bulgarian Academy of Sciences, Sofia, Bulgaria). Phenylmethylsulfonyl fluoride (PMSF) (>99 % GC purity) was obtained from Sigma Aldrich Chemie GmbH (Taufkirchen, Germany). 6-Nitro-3-phenylacetamido benzoic acid (NIPAB) was from GFB GmbH (Braunschweig, Germany) and from Sigma Aldrich Chemie GmbH (Taufkirchen, Germany). Penicillin amidase (*E.coli*) immobilised onto different magnetic matrices, obtained as described in Part B of this work were investigated in the model reactions studied here. Nalgene® cellulose acetate 4 mm filters (pore size 0.2 μm) were from Sybron Int. Corp. (USA). All other chemicals were analytical grade.

2.2. Penicillin amidase catalysed equilibrium and kinetically controlled model processes

Penicillin amidase catalysed benzylpenicillin hydrolysis

The hydrolysis of Pen G catalysed by immobilised onto different magnetic matrices PA from *E.coli* (Part B section *1.2*. Fig. 4) was performed at 37°C and pH 7.8 (phosphate buffer *I*=0.2 M). The used substrate concentrations were in the range 10-500 μM. The concentration of the immobilised enzyme in the reaction mixture was $8\text{-}10.10^{-10}$ M, determined by active site titration. Periodically aliquots were withdrawn, filtered (Nalgene® cellulose acetate filters) and immediately analysed by HPLC (section 2.3.). The initial rates (about 10% substrate conversion) were determined on the basis of the increase of phenylacetic acid (PAA) concentration as a

function of time. Five to six points were measured. The initial hydrolysis rates were calculated by linear regression analysis. The values of the steady-state kinetic parameters K_m (determined from the slope of the linear plot) and k_{cat} (calculated as $V_{max}/[E]_0$; Part C section *1.1.*) were evaluated using reversed Eadie-Hofstee plots.

Penicillin amidase (E.coli) catalysed kinetically controlled synthesis of cephalexin

The experiment was done with 100 mM 7-ADCA and 400 mM *R*-phenylglycine amide at 5°C or 200 mM 7-ADCA and 200 mM *R*-phenylglycine amide at 25°C and at pH 7.5 (0.05 M phosphate buffer) (Fig. 10). The reaction was started by addition of immobilised onto M PVA 02 (1,6-diaminohexane / glutardialdehyde modifying method) magnetic beads penicillin amidase from *E.coli*. The enzyme concentration in the reactor was 3.9×10^{-6} M in both cases. The pH in the reactor was kept constant by addition of H_3PO_4 (40 %) or NaOH (5 M). At time intervals samples were withdrawn, filtered (Nalgene® cellulose acetate filters) and analysed by HPLC (section 2.3.). The measured initial rates of formation of the condensation (cephalexin) and the hydrolysis (phenylglycine) products were used to calculate the selectivity v_{syn}/v_{hyd} of the immobilised biocatalyst in the kinetically controlled condensation reaction (Kasche 1986).

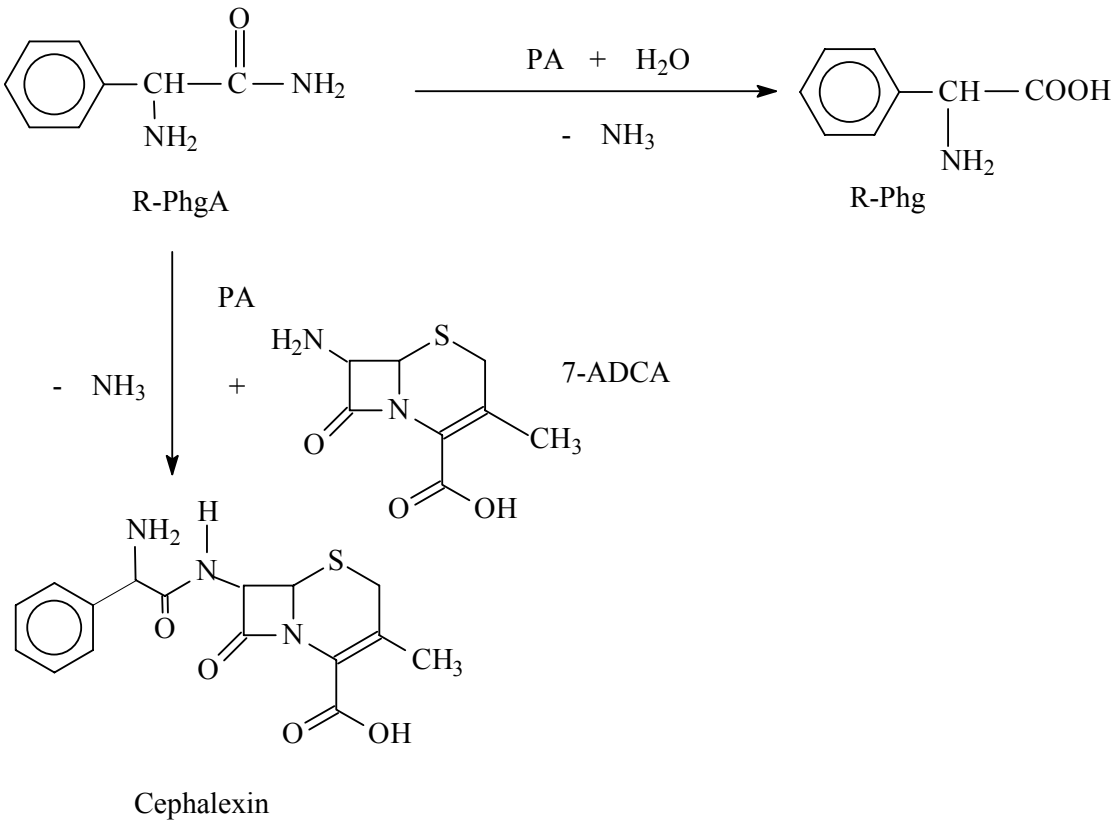

Figure 10: Penicillin amidase catalysed cephalexin synthesis.

Determination of the stereoselectivity of penicillin amidase from E.coli in equilibrium and kinetically controlled reactions

The kinetically controlled condensations of 10 mM *R*-phenylglycine amide with 100 mM *S*-, *R*- or *S,R*- Phe were performed in bicarbonate buffer pH 9.0, *I*=0.2 M at 25°C (Fig. 11). After the reactions were started by addition of immobilised PA, periodically samples were withdrawn, filtered (Nalgene® cellulose acetate filters) and analysed by HPLC (section 2.3.). The initial rates of formation of the condensation and hydrolysis products were used to calculate the transferase to hydrolase ratios k_T/k_H for the enantiomeric nucleophiles. The apparent enantiomeric ratios E_{syn} (for isolated enantiomeric substrates) and $E_{syn,rac}$ (for racemic substrate) were evaluated as described in section *1.3*.

Stereoselectivity was studied also for equilibrium controlled hydrolytic process. 50 mM racemic phenylacetyl-Phe was hydrolysed at pH 7.5 (0.2 M phosphate buffer) and at 25°C (Fig. 12). After the reaction was initiated by an addition of free or immobilised PA, at time intervals samples were withdrawn, filtered in the case of the

immobilised catalyst (Nalgene® cellulose acetate filters) and analysed by HPLC with the use of chiral separation column (section 2.3.). The initial rates of formation of *S*- and *R*- Phe were measured and used to estimate the enantiomeric ratio $E_{hyd,rac} = v_S/v_R$ (Galunsky and Kasche 2002).

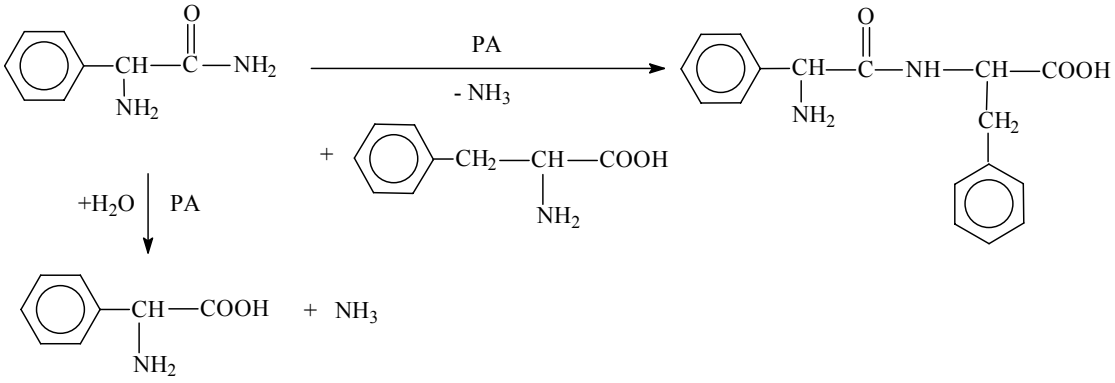

Figure 11: Penicillin amidase catalysed condensation of *R*-phenylglycine amide with phenylalanine.

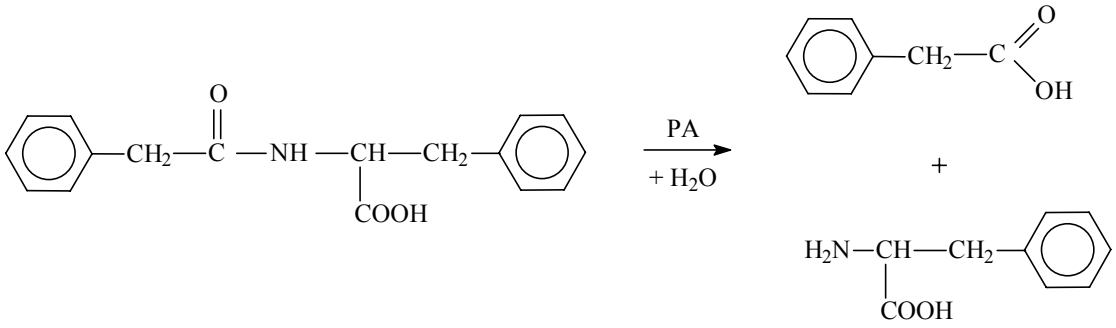

Figure 12: Penicillin amidase catalysed hydrolysis of racemic phenylacetyl-phenylalanine.

2.3. HPLC methods, used for the identification and analysis of the substrates and the products in the penicillin amidase catalysed model reactions

Separation of the products and substrates in penicillin amidase catalysed kinetically controlled synthesis of cephalexin

The substrates and the products were identified and analysed by HPLC using a Pharmacia LKB 2249 solvent delivery system and LKB Bromma 2151 variable wavelength detector. For all measurements the peak integration was done with Chrom

Star software 1994 (Bruker). For the kinetically controlled synthesis of cephalexin the substances were quantified using reversed phase column RP 18, 5 μm, 125/4 mm (Merck) thermostatted at 30°C and calibration curves for the peak areas at λ = 225 nm. The flow rate was 2 ml·min^{-1}. The elution system for resolution of the substrates and the products was: methanol / 67 mM KH_2PO_4 (pH 6.0) (5:95 v/v) for 2 minutes followed by a step gradient with methanol / 67 mM KH_2PO_4 (pH 6.0) (30:70 v/v) for further 3 minutes. For determination of v_{syn}/v_{hyd} only the peaks for cephalexin and the hydrolysis product (R-Phg: *R*-phenylglycine) were integrated. The chromatogram with the retention times for all components in the reaction mixture is represented in appendix II.

Separation of the products and substrates in penicillin amidase catalysed equilibrium controlled hydrolysis of phenylacetyl-R,S-phenylalanine (PAA-R,S-Phe)

The racemic substrate and the products were identified and analysed by HPLC using a Hewlett Packard 1100 series liquid chromatography system, equipped with Hewlett Packard ChemStation software (Agilent Technologie GmbH, Waldbronn, Germany) for the integration of the reactants peaks.

For the hydrolysis of the racemic phenylacetyl-phenylalanine (PAA-*R,S*-Phe) the enantiomeric products were quantified using a chiral column Chirobiotic TAG, 5 μm, 250/4.6 mm (Astec, USA) thermostatted at 30°C and calibration curves for the peak areas at λ = 210 nm. The isocratic elution at flow rate 1.4 ml·min^{-1} was with methanol / 20 mM ammonium acetate (pH 4.0) (10:90 v/v). The chromatogram with the retention times of the reaction components is represented in appendix V.

Separation of the products and substrates in penicillin amidase catalysed kinetically controlled condensations of R-phenylglycine amide with S-, R- or R,S-phenylalanine (Phe)

The substrates and the products were identified and analysed by HPLC using a Hewlett Packard 1100 series liquid chromatography system, equipped with Hewlett Packard ChemStation software (Agilent Technologie GmbH, Waldbronn, Germany) for the integration of the reactants peaks. For the penicillin amidase (PA) catalysed condensation between the *R*-phenylglycine amide and *R*-, *S*-, or *R,S*- Phe the

substrates were quantified using RP 8, 5 μm, 125/4 mm (Merck) column thermostatted at 56 °C and calibration curves for the peak areas at λ = 225 nm obtained with reference compounds of known concentrations. The response factor for the diastereomeric *R*-Phg-*S*-Phe and *R*-Phg-*R*-Phe was inferred from the response factors for the *R*-phenylglycine amide and *R*-Phg and assuming the constant sum of the concentration of the activated substrate, condensation and hydrolysis products during the reaction. The elution media for the resolution of *R*-Phg, *R*-phenylglycine amide, *S*-, *R*-, or *S,R*- Phe and the distereomeric products *R*-Phg-*S*-Phe and *R*-Phg-*R*-Phe was: 67 mM KH_2PO_4 (pH 4.5) for the first three minutes followed by a step gradient methanol / 67 mM KH_2PO_4 (pH 4.5) (35:65 v/v) and elution for further 5 minutes. The flow rate was 2 ml·min^{-1}. The chromatogram with the retention times of the reaction components is represented in appendix III.

Separation of the products and substrates in penicillin amidase catalysed benzylpenicillin hydrolysis

The substrate – Pen G and its hydrolysis products were identified, and analysed by HPLC using a Hewlett Packard 1100 series liquid chromatography system, equipped with Hewlett Packard ChemStation software (Agilent Technologie GmbH, Waldbronn, Germany) for the integration of the reactants peaks. For the penicillin amidase (PA) catalysed benzylpenicillin hydrolysis the reactants were separated and analysed using RP 8, 5 μm, 125/4 mm (Merck) column thermostatted at 56 °C and calibration curves for the peak area of PAA at λ = 210 nm. The elution media for the resolution of the reactants was: methanol / 67 mM KH_2PO_4 (pH 4.7) (30:60 v/v). The flow rate was 2 ml·min^{-1}. The chromatogram with the retention times of the reaction compounds is represented in appendix IV.

2.4. Other analytical methods

Determination of the surface charge density of the matrices

The charge density on the carrier particles (M-PVA E02) was determined by acid-base titration. 500 mg particles were suspended in 500 μl 0.2 M KCl and 10 μl 1M NaOH were added. Then the suspension was titrated with 25 μl portions of 0.1 M HCl to pH 3. After each portion HCl the suspension was shaken for 30 s, the particles were magnetically separated or allowed to sediment for 2 min and the pH was measured. A

reference sample without particles was titrated in the same way. From the difference between the amounts of 0.1 M HCl used to titrate the suspension with carriers and the blank was estimated the charge density in μmole·m^{-2} surface area.

Penicillin amidase activity assay

The enzyme assay was performed as described in Part B section *2.5.1*.

Penicillin amidase active site titration

The active site titration (AST) of the enzyme was performed as described in Part B section *2.5.2*.

3. Results and discussion

3.1. Apparent kinetic parameters of the immobilised penicillin amidase (E.coli) for benzylpenicillin hydrolysis

Kinetic constants of the reactions catalysed by immobilised enzymes differ in general from those obtained with the free one. K_m and k_{cat} are sensitive to even slight changes in the accessibility of the active sites and conformational modifications in the proteins. The processes catalysed by immobilised enzymes are often mass-transfer limited. This is detected by the increased apparent K_m value compared to the free biocatalyst. Mass-transfer limitations can be avoided when $(R^2V_{max}/DK_m) \leq 10$ (see equation (3.6)) (Kasche 1983). This can be achieved by decreasing the particle size.
Table 1 represents the apparent K_m and k_{cat} constants for benzylpenicillin hydrolysis, catalysed by penicillin amidase - free or immobilised onto different matrices.

Table 1: Kinetic parameters for benzylpenicillin hydrolysis catalysed by free and immobilised onto different magnetic and non-magnetic carriers penicillin amidase from *E.coli*. [a] Data from Bozhinova et al. 2004. The reaction conditions were the same in all cases (section *2.2.*).

Type of the magnetic beads	***Matrix functionalisation method***	***Spacer length (Å)***	***Particle size (μm)***	K_m ***(μM)***	k_{cat} (s^{-1})
[a] *none*	-	-	-	10	50
PVAc	ECH/HMDA/GA modified	20.9	2 - 5	140	90
PMA	EDA/GA modified	12.4	10 - 20	60	18
ASMP/PGA coated	HMDA/GA modified	16.2	1 - 3	100	90
M-PVA E02	HMDA/GA modified	20.8	1 - 3	55	20

ECH - epichlorohydrine; EDA - ethylene diamine; HMDA - hexamethylene diamine; GA - glutardialdehyde; PGA - poly(glutaraldehyde).

The effect of the particle size on the apparent K_m is demonstrated in Table 1 where the kinetic constants for benzylpenicillin hydrolysis, catalysed by free and immobilised on different magnetic matrices are compared.

Penicillin amidase bound to larger and porous Eupergit C has apparent K_m value two orders of magnitude higher compared to the free enzyme (Bozhinova et al. 2004). For the same enzyme immobilised on practically non-porous magnetic beads the apparent K_m is only several fold (five for M-PVA E02 and six for PMA) to up to one order of magnitude (for PVAc and ASMP) higher compared to the free penicillin amidase.

The intrinsic molecular property of penicillin amidase for the hydrolysis of the charged substrate benzylpenicillin - k_{cat} can be influenced (increased or decreased) due to the changes in the protein structure caused by interactions with the carrier during the covalent immobilisation (Kasche et al.1991). The observed values for the turnover numbers for some of the magnetic carriers were higher compared to the value obtained for the free penicillin amidase from *E.coli*. Similar effects were reported also by other authors (Buchholz and Kasche 1997, Ivanov et al. 2003). Slight increase in the k_{cat} value for some cross-linked with bifunctional agents penicillin amidase aggregates was reported by Erarslan and Ertan (1995). The order of magnitude of the turnover numbers for the studied here immobilised enzymes and those attached on larger matrices (Bozhinova et al. 2004) was similar. This implies better specificity constant and catalytic efficiency of the penicillin amidase immobilised onto studied here magnetic particles.

3.2. Penicillin amidase catalysed equilibrium and kinetically controlled processes

3.2.1. Study of the penicillin amidase S'$_1$ enantioselectivity in equilibrium controlled hydrolysis of racemic phenylacetylphenylalanine and kinetically controlled condensation of R-phenylglycine amide with R-, S-, or R,S- phenylalanine

The enzyme enantioselectivity in an equilibrium controlled hydrolysis of racemic substrate - phenylacetylphenylalanine (PAA-*R,S*-Phe) was quantified by the ratio of the initial rates of enantiomeric products formation (Galunsky and Kasche 2002). In Table 2 are presented the results obtained with penicillin amidase from *E.coli* immobilised onto different magnetic matrices, compared to the enantioselectivity of the free enzyme. The penicillin amidase from *E. coli* was found to be *R*-specific in

S_1- and *S*-specific in S'_1-binding subsites (Kasche et al. 1996). The S'_1 specificity reflects the ability of the enzyme to catalyse acyl transfer reactions (Kasche 1986). It is quite broader and varies from penem and cephem nuclei to different amino acids, peptides, aromatic and aliphatic amines. The substrate binding in the S'_1-binding subsite depends on the electrostatic interactions (Svedas et al. 1996) and S'_1 enatioselectivity of penicillin amidase was found to be more pronounced and more relevant for the enantiomer discrimination (Galunsky et al. 2000).

Table 2: Comparison of S'_1 enantioselectivity of free and immobilised penicillin amidase from *E.coli* for the equilibrium controlled hydrolysis of racemic phenylacetylphenylalanine. The reaction conditions were the same for all studied enzyme preparations (section *2.2*.).

Type of the matrix	***Matrix functionalisation method***	***Particle size (μm)***	v_R $(M \cdot s^{-1})$	v_S $(M \cdot s^{-1})$	[b] $E_{hyd,rac}$
none	-	-	[a] n.o.	-	>1000
PVAc	ECH/HMDA/GA modified	2 - 5	[a] n.o.	6.10^{-6}	>1000
PMA	EDA/GA modified	10 - 20	[a] n.o.	4.10^{-6}	>1000
PMA	EDA/GA modified	5 - 10	[a] n.o.	3.10^{-6}	>1000
ASMP/PGA coated	HMDA/GA modified	1 - 3	[a] n.o.	1.10^{-5}	>1000
M-PVA E02	HMDA/GA modified	1 - 3	3.10^{-9}	7.10^{-7}	230
Eupergit® C 250 L	Epoxy	150	2.10^{-7}	5.10^{-6}	25

[a] no formation of *R*-Phe was observed. [b] $E_{hyd,rac} = \nu_S/\nu_R$. ECH - epichlorohydrine; EDA - ethylene diamine; HMDA - hexamethylene diamine; GA - glutardialdehyde; PGA - poly(glutaraldehyde).

The S'_1 enatioselectivity of the enzyme was studied also for penicillin amidase catalysed condensation of R-phenylglycine amide (*R*-phenylglycine amide) with isolated enantiomers of phenylalanine (Phe) (Table 3). The enantioselectivity of the immobilised enzymes is generally lower than that of the free enzyme. When an enzyme is attached to the matrix, in addition to external mass transfer effects there is diffusion of the substrate to the carrier in order to reach the biocatalyst. For charged carriers the electrical double layer may cause concentration gradients of the substrate. In the case of the condensation reaction between *R*-phenylglycine amide and *R*- or *S*-Phe this gradient will be greater for the more specific enantiomeric nucleophile. This

difference in the concentration gradients for the enantiomeric substrates results in an decrease in enantioselectivity compared to that of the free penicillin amidase from *E.coli*. The influence on the structural changes in the enzyme molecule caused by the covalent immobilisation should also be considered as a reason for the reduced stereoselectivity of the immobilised enzyme.

Table 3: Comparison of S'_1 enantioselectivity of free and immobilised penicillin amidase from *E.coli* for the kinetically controlled condensation/hydrolysis of *R*-phenyglycineamide with *R*- or *S*- phenylalanine. The surface charges of the magnetic beads expressed as ξ-potentials are shown in Table 4 (Part A); the enzyme loading of the carriers can be found in Part B section 3. The reaction conditions were the same for all studied enzyme preparations (section *2.2*.).

Type of the magnetic beads	***Matrix functionalisation method***	***Particle size (μm)***	[a] E_{syn}
none	-	-	>1000
PVAc	ECH/HMDA/GA modified	2 - 5	40
PMA	EDA/GA modified	10 - 20	50
PMA	EDA/GA modified	5 - 10	55
ASMP/PGA coated	HMDA/GA modified	1 - 3	142
M-PVA E02	HMDA/GA modified	1 - 3	460

[a] $E_{syn} = (k_T/k_H)_S /(k_T/k_H)_R$ (see equation (3.14) and (3.15) in *1.3*). ECH - epichlorohydrine; EDA - ethylene diamine; HMDA - hexamethylene diamine; GA - glutardialdehyde; PGA - poly(glutaraldehyde).

For the enzyme bound onto the smaller magnetic beads (M-PVA E02 and ASMP/PGA coated) the decrease in the enantioselectivity was less stronger.

Table 3 shows that penicillin amidase immobilised onto M-PVA E02 beads showed the highest enantioselectivity (E_{syn}=460) for the studied condensation reaction, but lower compared to the other immobilised enzymes (Table 2) enantiomeric ratio ($E_{hyd,rac}$) for the hydrolysis of racemic phenylacetylphenylalanine.

The immobilised enzymes, which were found to exhibit “the best” (PA immobilised onto M-PVA E02 beads) and “the worst” (PA immobilised onto PVAc beads) (Table 3) enantioselectivity in the condensation of *R*-phenyglycine amide with *R*- or

S- phenylalanine, were investigated in the condensation of *R*-phenyglycine amide with racemic nucleophile (Table 4). The enantioselectivity of the penicillin amidase immobilised onto magnetic PVAc beads determined with racemic nucleophile as a substrate was higher compared to the one determined with isolated phenylalanine enantiomers ($E_{syn,rac} \neq E_{syn}$). For the enzyme immobilised onto M-PVA E02 beads the observed enantioselectivities were of the same order of magnitude in both cases ($E_{syn,rac} \approx E_{syn}$). It can be concluded that the immobilisation may affect the enzyme enantioselectivity in a different way.

Table 4: Comparison of S'_1 enantioselectivity of free and immobilised penicillin amidase from *E.coli* for the kinetically controlled condensation/hydrolysis of *R*-phenyglycine amide with *R,S*- phenylalanine. The reaction conditions were the same for both studied enzyme preparations (section *2.2.*).

Type of the magnetic beads	***Matrix functionalisation method***	$v_{T,S}$ $(M \cdot s^{-1})$	$v_{T,R}$ $(M \cdot s^{-1})$	[a] $E_{syn,rac}$ (-)
none	-	-	-	>1000
PVAc	ECH/HMDA/GA modified	1.10^{-6}	2.10^{-9}	500
M-PVA E02	HMDA/GA modified	1.10^{-6}	2.10^{-9}	500

[a] $E_{syn,rac} = v_{T,S} / v_{T,R}$, where $v_{T,S}$ and $v_{T,R}$ are the initial rates of the formation of the diastereomeric condensation products (*R*-Phg-*S*-Phe and *R*-Phg-*R*-Phe). ECH - epichlorohydrine; EDA - ethylene diamine; HMDA - hexamethylene diamine; GA - glutardialdehyde.

3.2.2. Penicillin amidase selectivity in the kinetically controlled synthesis of cephalexin

During the kinetically controlled synthesis of β-lactam antibiotics (in the case of this work cephalexin) two products are formed: condensation (cephalexin) and hydrolysis (phenylglycine) (Fig. 12). The selectivity of the penicillin amidase in this process is quantified by the ratio of the initial rates (v_{syn}/v_{hyd}) of formation of the condensation and the hydrolysis side-product. The decreased selectivity of immobilised PA from *E.coli* (compared to that of the free enzyme) (Table 5) is probably due to the impeded binding of 7-ADCA to PA at high ionic strength (Kasche 1986), whereas it does not influence the hydrolysis of phenylglycine amide. The observed higher selectivity of

the biocatalyst immobilised onto magnetic micro-beads, compared to this of the penicillin amidase covalently attached onto larger matrices (Bozhinova et al. 2004) can be attributed to the difference in the charge density. The lower charge density of the magnetic micro-matrices implies that the ionic strength near to the carrier surface with the immobilised enzyme, where cephalexin synthesis occurs, is lower in comparison to this for the larger Eupergit C particles, which have higher surface charges (Table 5). Therefore the binding of the negatively charged, at the reaction conditions, nucleophile (7-ADCA) into the positively charged S'_1 binding subsite of the enzyme will be more impeded for the carriers with larger surface charge (Eupergit C) and subsequently the synthetic reaction rate will be stronger reduced for these matrices. The observed effects can not be due only to the charge-charge interactions in the electric double layer around the matrix-particle, where the process occurs, but possible changes in the protein molecule structure due to the covalent immobilisation should also be considered (Kasche et al. 1991).

Table 5: Penicillin amidase from *E.coli* (free and immobilised) selectivity in kinetically controlled synthesis of cephalexin. The reaction conditions as described in section *2.2*.

Type of the magnetic beads	***Mole ratio 7-ADCA : R-phenylglycine amide***	***T (°C)***	***Specific surface charge density (µmol·m^{-2} surface area)***	***v_{syn}/v_{hyd} (-)***
[a]*none*	1 : 4	5	-	13
[b]*M-PVA E02*	1 : 4	5	1.2	8
[a]*Eupergit C*	1 : 4	5	5	3
[b]*M-PVA E02*	1 : 1	25	1.2	5

[a] reference Bozhinova (2004), [b] hexamethylene diamine / glutardialdehyde modified.

For biotechnological applications substrate concentrations larger than 100 mM are desirable (Kasche et al. 1987b). One possibility to overcome the excessive production of the hydrolysis product is to perform the cephalexin synthesis with practically equimolar amounts of substrates and design the process in which the degree of conversion is kept relatively low (Bruggink et al. 1998). At low temperatures the higher yields and synthetic / hydrolytic ratios are due to the fact that the hydrolytic

reaction is suppressed (in the case of a free enzyme) or the synthesis reaction is less sensitive to the temperature than the hydrolysis reaction (in the case of immobilised enzymes) (Schroën et al. 2002).

4. Summary and conclusions

The kinetic properties (apparent kinetic parameters K_m and k_{cat}) of the penicillin amidase covalently immobilised onto the magnetic matrices (described in Part A and Part B) were investigated here for the hydrolysis of penicillin G. The selectivity of the immobilised enzyme preparations was studied in kinetically controlled synthesis of semi-synthetic β-lactam antibiotic - cephalexin, and the enantioselectivity in equilibrium controlled hydrolysis and in kinetically controlled condensation processes.

- The evaluated apparent K_m constants for Pen G hydrolysis catalysed by the enzyme, immobilised onto investigated here magnetic supports were higher compared to the one for the free penicillin amidase from *E.coli*, but were one or two orders of magnitude lower compared to those for the same enzymes attached onto larger (>100 μm) porous carriers. Considering the same order of magnitude of the turnover numbers for the compared immobilised enzymes (Table 1) this implies better specifity constant and catalytic efficiency.
- The selectivity of the immobilised onto M-PVA E02 beads penicillin amidase from *E.coli* was studied in kinetically controlled synthesis of cephalexin from *R*-phenylglycine amide and 7-ADCA. It was found that the enzyme immobilised onto the magnetic micro-beads shows better synthetic abilities (higher v_{syn}/v_{hyd} ratios) compared to the same biocatalyst immobilised onto larger, porous matrices.
- Enantioselectivity of the penicillin amidase from *E.coli* immobilised onto different magnetic matrices was investigated in equilibrium controlled hydrolysis of racemic PAA-Phe and kinetically controlled condensation of *R*-phenylglycine amide with *R*-, *S*-, or *R,S*- Phe. The immobilised enzymes studied here showed $E_{hyd,rac}$ >100 for investigated hydrolytic process, which is a precondition for their successful application as catalysts for racemate resolution. The enzyme immobilised onto M-PVA E02 beads was found to possess the highest enantioselectivity (E_{syn}= 460) for the condensation reaction with isolated enantiomeric substrates. In the case where the same process was conducted with racemic nucleophile, the two studied immobilised enzymes

onto PVAc and M-PVA E02 beads showed different stereoselective behaviour.

The experimental data gave that penicillin amidase from E.coli covalently bound to PVAc beads has enantiomeric ratio one order of magnitude larger than those determined with isolated enantiomers. Although for the same enzyme immobilised onto M-PVA E02 beads the calculated $E_{syn,rac}$ was of the same order of magnitude as E_{syn}. Having this in mind, further investigations of how the carrier properties influence these enzyme properties should be performed.

5. Symbols and abbreviations

Symbols

k_{cat}	turnover number [s^{-1}]
K_m	Michaelis-Menten constant [M]
k_{cat}/K_m	specificity constant [$M^{-1} \cdot s^{-1}$]
M	concentration [$mol \cdot L^{-1}$]
V_{max}	maximal velocity of the enzyme catalysed reaction [$M \cdot s^{-1}$]
$E_{hyd,rac}$	enantiomeric ratio for the hydrolysis reaction determined with racemic substrate [-]
$E_{syn,rac}$	enantiomeric ratio for the synthesis reaction determined with racemic substrate [-]
E_{syn}	enantiomeric ratio for the synthesis reaction determined with isolated enantiomers [-]

Greek symbols

φ	Thiele modulus [-]
η_0	operational effectiveness factor [-]
η	stationary effectiveness factor [-]

Abbreviations

ASMP	amino-silanised-magnetic-particles
AST	active site titration
6-APA	6-aminopenicillanic acid
7-ADCA	7-aminodeacetoxycephalosporanic acid
ECH	epichlorohydrine
EDA	ethylene diamine
GA	glutardialdehyde
HMDA	hexamethylene diamine

M PVA E02	magnetic poly(vinylalcohol) beads
NIPAB	6-nitro-3-phenylacetamidobenzoic acid
PAA	phenylacetic acid
PAA-Phe	phenylacetylphenylalanine
PA	penicillin amidase
Pen G	penicillin G (benzylpenicillin)
Phe	phenylalanine
Phg	phenylglycine
PGA	poly(glutaraldehyde)
PMSF	phenylmethylsulfonyl fluoride
PVAc	magnetic poly(vinylacetate) beads
PMA	magnetic poly(methylacrylate) beads

6. References

Arroyo, M., de la Mata, I., Acebal, C., Castillón, M.P. (2003) *Appl. Microbiol. Biotechnol.*, **60**, 507-514

Buchholz, K., Kasche, V. (1997) *Biokatalysatoren und Enzymtechnologie*, VCH Verlagsgesellschaft mbH Weinheim

Bossi, A., Cretich, M., Righetti, P.G. (1998) *Biotechnology and Bioengineering*, **60** (4), 454-461

Bruggink, A., Roos, E.C., de Vroom, E. (1998) *Organic Process Research and Development*, **2**, 128-133

Bisswanger, H. (2000) *Enzymkinetik: Theorie und Methoden*, Wiley-VCH, Weinheim

Bozhinova, D., Galunsky, B., Yueping, G., Franzreb, M., Köster, R., Kasche, V. (2004) *Biotechnol. Lett.*, **26**, 343-350

Cahn, R.S., Ingold, C., Prelog, V. (1966) *Angew. Chem*., **78** (8), 413-447

Chen, C.-S., Fujimoto, Y., Girdaukas, G., Sin, C.J. (1982) *J. Am. Chem. Soc.*, **104**, 7294-7299

Cao, L., van Langen, L.M., van Rantwijk, F., Sheldon, R.A. (2001) *J. Molecular Catalysis B: Enzymatic*, **11**, 665-670

Duggleby, H.J., Tolley, S.P., Hill, C.P., Dodson, E.J., Dodson, G., Moody, P.C.E. (1995) *Nature*, **373**, 264-268

De Vroom, E. (1997) *WO Patent* 97/04086

Erarslan, A., Ertan, H. (1995) *Enzyme Microb. Technol*., **17**, 629-635

Fleming, A. (1929) *Br. J. Exp. Pathol.*, **10**, 226-236

Fersht, A. (1985) *Enzyme structure and Mechanism*, W.H. Rreeman and Company, New York

Galunsky, B., Schlothauer, R.C., Böckle, B., Kasche, V. (1994) *Anal. Biochem*., **221**, 213-214

Galunsky, B., Ignatova, S., Kasche, V. (1997) *Biochim. Biophys. Acta*, **1343**, 130-138

Galunsky, B., Lummer, K., Kasche, V. (2000) *Chemical Monthly*, **131**, 623-632

Guranda, D.T., van Langen, L.M., van Rantwijk, F., Sheldon, R.A., Švedas, V.K. (2001) *Tetrahedron: Asymmetry*, **12**, 1645-1650

Gröger, H., Capan, E., Barthuber, A., Vorlop, K.-D. (2001) *Organic Letters*, **3** (13), 1969-1972

Galunsky, B., Kasche, V. (2002) *Adv. Synth. Catal.*, **344** (10), 1115-1119

Hänsler, M., Jakubke, H.-D. (1996) *J. Peptide Science*, **2**, 279-289

Ilhan, F., Kraemer, D. (2001) *US Patent* 6,218,138 B1

Ivanov, A.E., Edink, E., Kumar, A., Galaev, I.Yu., Arendsen, A.F., Bruggink, A., Mattiasson, B. (2003) *Biotechnol. Prog.* , **19**, 1167-1175

Kasche, V., Galunsky, B. (1982) *Biochemical and Biophysical research Commun.*, **104** (4), 1215-1222

Kasche, V. (1983) *Enzyme Microb. Technol*., **5**, 2-13

Kasche, V., Haufler, U., Zöllner, R. (1984) *Hoppe-Seyler's Z. Physiol. Chem.*, **365**, 1435-1443

Kasche, V. (1986) *Enzyme Microb. Technol*., **8**, 4-16

Kasche, V. (1987a) *Advances in the Biosciences*, **65**, 151-158

Kasche, V., Haufler, U., Riechmann, L. (1987b) *Immobilized Enzymes/Cells in Organic Synthesis In "Methods in Enzymology"* (ed. by K. Mosbach), Vol. **136,** 280-292

Kasche, V., Michaelis, G., Galunsky, B. (1991) *Biotechnology Letters*, **13** (2), 75-80

Kasche, V., Galunsky, B., Nurk, A., Piotraschke, E., Rieks, A. (1996) *Biotechnology Letters*, **18** (4), 455-460

Lummer, K., Rieks, A., Galunsky, B., Kasche, V. (1999) *Biochim. Biophys. Acta*, **1433**, 327-334

Lummer, K. (2000) *PhD Thesis,* Technical University Hamburg-Harburg, Germany

Landis, B.H., Ng, J.S., Topgi, R.S., Yonan, E.E., Wang, P.T. (2001) *US Patent* 6,214,609

Nam, D.H., Kim, C., Ryu, D.D.Y. (1985) *Biotechnology and Bioengineering*, **27**, 953-960

Rieks, A. (1997) *PhD Thesis,* Technical University Hamburg-Harburg, Germany

Schlechter, I., Berger, A. (1967) *Biochem. Biophys. Res. Commun.*, **27**, 157

Švedas, V.K., Margolin, A.L., Sherestyuk, C.F., Klyosov, A.A., Berezin, I.V. (1977) *Biorg. Khim*., **3**, 547-553

Shewale, J.G., Deshpande, B.S., Sudhakaran, V.K., Ambedkar, S.S. (1990) *Process Biochemistra International*, 97-103

Sheldon, R.A. (1993) C*hirotechnology*, Marcel Dekker, Inc.

Švedas V.K., Savchenko M.V., Beltser A.I., Guranda D.F. (1996) *Ann. N.Y. Acad. Sci*., **799**, 659-669.

Schroën, C.G.P.H., Nierstrasz, V.A., Kroon, P.J., Bosma, R., Janssen, A.E.M., Beeftink, H.H., Tramper, J. (1999) *Enzyme Microb. Technol.*, **24**, 498-506

Spieβ, A., Schlothauer, R.-C., Hinrichs, J., Scheidat, B., Kasche, V. (1999) *Biotechnology and Bioengineering*, **62** (3), 267-277

Schroën, C.G.P.H., Nierstrasz, V.A., Moody, H.M, Hoogschagen, M.J., Kroon, P.J., Bosma, R., Beeftink, H.H., Janssen, A.E.M., Tramper, J. (2001) *Biotechnology and Bioengineering*, **73** (3), 171-178

Schroën, C.G.P.H., Fretz, C.B., deBruin, V.H., Berendsen, W., Moody, H.M, Roos, E.C., van Roon, J.L., Kroon, P.J., Strubel, M., Janssen, A.E.M., Tramper, J. (2002) *Biotechnology and Bioengineering*, **80** (3), 331-340

Tischer, W., Kasche, V. (1999) *TIBTECH*, **17**, 326-335

Turner, N.J. (2003) *Current Opinion in Biotechnology*, **14**, 1-6

Van Langen, L.M., de Vroom., E., van Rantwijk, F., Sheldon, R. (1999) *FEBS Letters*, **456**, 89-92

Van Langen, L.M., Oosthoek, N.H.P., Guranda, D.T., van Rantwijk, F., Švedas, V.K., Sheldon, R.A. (2000) *Tetrahedron: Asymmetry*, **11**, 4593-4600

Wegman, M.A., Janssen, M.H.A., van Rantwijk, F., Sheldon, R.A. (2001) *Adv. Synth. Catal.*, **343** (6-7), 559-576

Youshko, M.I., Sinev, A.V., Švedas, V.K. (1999) *Biochemistry (Moscow)*, **64** (10), 1415-1419

Youshko, M.I., van Langen, L.M., de Vroom, E., van Rantwijk, F., Sheldon, R.A., Švedas, V.K. (2001) *Biotechnology and Bioengineering*, **73** (5), 426-430

Zmijewski, M.J.Jr., Briggs, B.S., Thompson, A.R., Wright, I.G. (1991) *Tetrahedron Lett.*, **32** (13), 1621-1622

Part D: Summary. Outlook and future work

SUMMARY

Driven mainly by economical reasons the immobilisation and reuse of many enzymes is necessary. Magnetic carrier technology, which serves many convenient separation methods, was in recent years widely employed in biotechnology, molecular biology and medicine.

The subject of this work was to develop and characterise magnetic micro-matrices for covalent immobilisation of enzymes. As a model biocatalyst penicillin amidase from *E.coli* - an enzyme of high industrial importance for the production of semi-synthetic β-lactam antibiotics, was used.

Poly(vinylacetate) (PVAc) and poly(methylacrylate) (PMA) magnetic beads of sizes in a range 2-20 μm were synthesised by an oil-in-water suspension polymerisation method. Cross-linked poly(methyl methacrylate) (PMMA) beads of 6 μm diameter were converted into magnetic particles by a swell-deswell manufacturing procedure in a toluene-based magnetic fluid comprising of nano-crystals of magnetite covered by a bi-layer of surfactant. Amino-silanised magnetic particles of 1-2 μm diameter were produced by co-precipitation of Fe(II) and Fe(III) salts at high alkaline pH and covered by amino-silane and finally by poly(glutaraldehyde) layers. Poly(vinylalcohol) beads under the trade name M-PVA, of 1-3 μm diameter, were donated by chemagen Biopolymer Technologie AG and largely studied here.

All of the magnetic matrices investigated had sizes in a range of 1-20 μm and showed superparamagnetic behaviour e.g. no magnetic memory effects once they were set out of an external magnetic field. The measured magnetic saturation values of the immobilisation matrices were in a range of 11-40 $A \cdot m^2 \cdot kg^{-1}$. The obtained Environmental Scanning Electron Microscopy (ESEM) images for poly(vinylacetate), poly(methylacrylate) and poly(methyl methacrylate) beads showed no pores large enough to be entered by the chosen enzyme during the covalent immobilisation. BET evaluations for these magnetic carriers gave specific surface areas of 3-15 $m^2 \cdot g^{-1}$ values, which are in a good correlation with the theoretically calculated ones, assuming smooth surface relief. For poly(vinylalcohol) and amino-silanised magnetic particles the specific surface areas values determined by BET measurements were larger compared to the theoretically expected ones. A simplified self-scaling model,

which describes “the surface relief roughness” was suggested here in order to explain the appeared differences for M-PVA beads. According to the above-mentioned model the calculated diameter of the surface convexities was approximately 1 Å, which is one order of magnitude smaller than the dimensions of the studied enzyme (70*50*55 Å; Duggleby et al. 1995). This practically means that the specific surface area accessible for the enzyme molecules was smaller then the BET-determined one. For the amino-silanised magnetic particles the evaluated high specific surface area is most probably due to the fact that by the pre-heating of the samples to up to 60 °C the poly(glutaraldehyde) and amino-silane coatings can be disrupted, which cause surface area increase.

The zeta potential of the matrices surface in an aqueous solution was determined in the pH range between 7-7.5. This parameter was of significant meaning later for the immobilisation of the enzyme on some magnetic beads modified with shorter spacers.

Modification of the magnetic bead surfaces mainly with epoxy-, or amino- and subsequent aldehyde- spacers, was done in order to create sites, suitable for the covalent immobilisation of enzymes. M-PVA (epichlorohydrine - modified), poly(methyl methacrylate) (glycidol - modified) and poly(vinylacetate) (epichlorohydrine - modified) magnetic beads showed high epoxy-loading capacities (400-700 μmol groups g^{-1} dry carrier). The highest amino-loadings were determined for the commercial amino- M-PVA N12 magnetic beads and obtained for poly(methylacrylate) (ethylene diamine - modified) magnetic particles - 650 and respectively 640 μmol groups per gram dry carrier.

Penicillin amidase from *E.coli* was covalently immobilised onto magnetic matrices investigated in this work *via* different spacers/reactions.

For M-PVA commercial beads, with increasing of the ***spacer length*** an increase in the amount of the covalently bound active protein, of up to 22 mg enzyme per gram dry beads for the functionalised with hexamethylene diamine / glutardialdehyde (20.8 Å length) spacer matrix at low (0.2 M) ionic strength of the immobilisation buffer was observed. For comparable immobilisation conditions, the same carrier with shorter (6.0 Å length) epoxy-spacer immobilised only 4 mg enzyme per gram dry beads. Comparable results were obtained for subsequently modified amino-silanised magnetic particles with a different number of hexamethylene diamine / glutardialdehyde “spacer units” at the above-mentioned low ionic strength of the immobilisation buffer. For the last matrix an immobilisation maximum of 74 mg

enzyme per gram dry beads at four spacer units (64.9 Å length) was evaluated. This result was also the *maximum enzyme loading* obtained with the magnetic matrices studied here for the chosen biocatalyst and immobilisation conditions. For poly(vinylacetate) magnetic beads with increasing spacer length from 6.0 Å (epoxy-spacer) to up to 21.0 Å (hexamethylene diamine / glutardialdehyde spacer), the amount of the immobilised active penicillin amidase increased from 3 to up to 24 $mg \cdot g^{-1}$ dry beads.

Furthermore, for M-PVA magnetic beads the influence of the ***immobilisation buffer ionic strength*** on the achievable enzyme loadings was more pronounced for the matrices modified with shorter epoxy- (epichlorohydrine) and imidazolyl-carbamate (N,N´-carbonyl diimidazole) spacers. For both spacers a significant increase - of almost three folds of the amount of the covalently bound enzyme, with rising ionic strength of up to 1 M, was observed. This can be due to minimising of un-desirable charge-charge interactions between the matrix surface (negative zeta potential at pH 7.5 determined) and the enzyme molecule (negative charge at pH 7.5) during the immobilisation process. It is logical, that the effect of the ionic strength was more significant in the case of the above-mentioned shorter spacers, which means shorter distances and stronger electrostatic repulsions between the matrix and the enzyme. Comparable results were also obtained for poly(vinylacetate) magnetic matrix.

Amino-modified and further glutardialdehyde-functionalised poly(methylacrylate) magnetic beads showed enzyme loading capacities comparable to those obtained with the commercial M-PVA matrices at similar immobilisation conditions. With a prolongation of the immobilisation reaction time from 24 h to 72 h, the amount of bound penicillin amidase increased from 35 to 54 mg per gram dry beads.

The apparent kinetic constants K_m and k_{cat} of the penicillin amidase from *E.coli* covalently immobilised onto the studied magnetic matrices were investigated here for the hydrolysis of penicillin G. The evaluated apparent K_m constants were several fold higher compared to the one for the free enzyme, but were one or two orders of magnitude lower compared to those for penicillin amidase bound onto larger (>100 μm) porous carriers.

The selectivity of the enzyme immobilised onto M-PVA beads was investigated in kinetically controlled synthesis of cephalexin from *R*-phenylglycine amide and 7-aminodeacetoxycephalosporanic acid at 5 °C and an excess of nucleophile. The

observed immobilised enzyme selectivity, calculated as ν_{syn}/ν_{hyd}= 8 was comparable to this of the free penicillin amidase from *E.coli* e.g. ν_{syn}/ν_{hyd}= 13.

Enantioselectivity of the penicillin amidase from *E.coli* immobilised onto different magnetic matrices was studied for the equilibrium controlled hydrolysis of racemic phenylacetylphenylalanine and kinetically controlled condensation of *R*-phenylglycine amide with pure enantiomers or racemic mixture of phenylalanine. All studied enzymes, immobilised onto magnetic micro-particles, showed $E_{hyd,rac}$ >100 for the investigated hydrolysis reaction.

For the condensation reaction studied here with isolated enantiomeric substrates (phenylalanine) the enzyme immobilised onto M-PVA E02 beads was found to possess the highest enantioselectivity (E_{syn}= 460). In the case where the same process was conducted with racemic nucleophile as a substrate the enzymes immobilised onto PVAc and M-PVA E02 beads exhibited different behaviour with respect to their enantioselectivity. Penicillin amidase from *E.coli* covalently attached to the PVAc beads had enantiomeric ratio $E_{syn,rac}$= 500, which was one order of magnitude larger than those determined with isolated enantiomers (E_{syn}= 40). For the same enzyme immobilised onto M-PVA E02 beads the observed $E_{syn,rac}$= 500 was of the same order of magnitude as E_{syn}= 460. Obviously the electrical double layer of the supports with the attached enzyme may influence the enantioselectivity of the biocatalyst, which requires further studies of the interactions matrix-enzyme on the nano-level and detailed mechanism of the carrier influence on the enzyme properties.

OUTLOOK AND FUTURE WORK

The magnetic beads synthesised and characterised in this study were evaluated as immobilisation matrices for one chosen model enzyme - penicillin amidase from *E.coli*. Further investigations of other hydrolytic or biocatalysts from other enzymes classes should be performed.

In this work covalent immobilisation *via* different spacers was performed. The influence mainly of two parameters - the spacer length and the ionic strength of the immobilisation buffer, on the enzyme loading capacities of the matrices was investigated. Future experimental work, in order to study the detailed mechanism of the increase in the amount of the bound to the matrix enzyme at higher ionic strengths should be conducted. The spacer length can be vary e.g. increased until it is "longer" than the width of the electrical double layer around the beads, where the electrostatic effects matrix-enzyme molecule are playing a significant role during the immobilisation process. Thus the enzymes immobilised onto practically non-porous magnetic supports as studied here, modified with such spacers are going to be prevented from unfavourable interactions e.g. electrostatic repulsions from the matrices. Moreover the kinetic parameters (K_m and k_{cat}), which describe the catalytic properties of the enzyme can be influenced due to the changes in the protein structure caused by interactions with the carrier during the covalent immobilisation. Therefore in the above-mentioned case, where the enzyme is immobilised practically only on the beads surfaces, and spacer length exceeds the width of the electrical double layer around the matrices, this influence might be reduced.

The enantioselectivity of the penicillin amidase from *E.coli* immobilised onto different magnetic micro-sized carriers, was studied for two model processes: kinetically controlled condensation of R-phenylglycine amide with R-, S-, or racemic-phenylalanine and equilibrium controlled hydrolysis of racemic phenylacetylphenylalanine. Further investigations of the enzyme enantioselectivity should be done for other processes and nucleophilic substrates. In the kinetically controlled condensation reaction, performed with isolated enantiomeric nucleophilic substrates, the enzyme behaviour was studied only for one concentration of the nucleophile. More experimental work can be performed in order to describe the influence of this parameter on the evaluated enantiomeric ratios.

The selectivity of one immobilised penicillin amidase from *E.coli* was evaluated for the kinetically controlled synthesis of cephalexin. Comparative studies should be conducted with immobilised on the other magnetic carriers enzymes as well as for other synthetic reactions (other antibiotics).

All studied magnetic matrices appeared to be practically non-porous for the large enzyme molecules, and therefore covalent immobilisation occurred on the matrix surface. In this context the diffusional limitations, during completion of processes catalysed by these immobilised enzymes, are expected to be significantly reduced in comparison to biocatalysts immobilised on large porous matrices. Therefore the magnetic matrices studied in this work can be especially favourable for the reactions with substrates of high molecular weights, where the above-described effects are of significant importance.

Error discussion

1. Particle size measurements

During the size determination of the synthesised magnetic matrices by employment of a Cis 100 particle sizer (Part A section *2.3.7.*) errors appear due to the presence of the particles with sizes below 1 μm. The working principle of the apparatus is based on the "time of-transition theory" - practically He-Ne beam is scanned circularly by a rotating wedge prism and focused down to a 1.2 μm spot, which scans the sample measurement volume. Therefore particles of sizes below this critical value are "not visible" for the laser and therefore not included into the total size-distribution calculated in the end of the measurement. For some of the carriers (ASMP) the ESEM images showed presence of such particles. Although application of a different separation procedures (for example sieving) in order to obtain a uniform size-distribution was difficult because of the small diameter of the carriers. That is why in all cases only the approximate mean particle diameter range was determined from at least two independent size-evaluation techniques.

2. BET specific surface area (SSA) measurements

The errors during these evaluations are generated due to three main reasons: (i) pre-heating of the samples to up to 60 °C in order to keep the chemical structure of the polymers compact, which can not avoid the presence of "some humidity" in the magnetic carrier-particles; (ii) relative low amount (masse) of the matrix used for the measurements, which leads to errors as the surface area is calculated per masse (dry material); (iii) errors during the measurement and obtaining the BET isotherm. Summing all these relative errors a total error of max. 50 % could be expected for some of the evaluations (Dr. P. Weidler - personal communications). Therefore the determined SSA must be interpreted as approximate values. This explains also the obtained higher SSA compared to the ones theoretically calculated using the ESEM determined mean diameter of the particles (Part A section *3.1*)

3. Determination of the concentration of the dry magnetic particles in suspension

The weighting error (Part A section *2.3.4*) was minimised to ±1 % as the amount of the dry particles used in all cases was >1-2 mg and the concentration was determined by weighting of three independent dry samples.

4. Penicillin amidase activity assay

The spectrophotometric assay employed for monitoring of the enzyme activity (Part B section *2.5.1*) leads to an error of maximal ±2 % in the case, where the measurements were performed with a free enzyme. The dilution errors are also included into this value. In the case where the evaluations were performed with immobilised enzyme in order to transfer the "eppendorf cup" out of the centrifuge after separation of the carrier with immobilised penicillin amidase from the supernatant and to transfer the last one into the cuvette for determination of $A_{380\ nm}$ an additional time error of ±5 s was generated. The maximal error in this case was ±20 %.
The penicillin amidase concentration determined from active site titration (Part B section *2.5.2*) in all cases was calculated from three independent measurements. The maximal error was ±20 %.

5. HPLC analysis

In the penicillin amidase catalysed hydrolysis of racemic phenylacetylphenylalanine (Part C section *2.3.*), the substrate was contaminated by the presence of R- and S-phenylalanine of concentrations in the range 3 - 4.5 mM. Generally the enzyme is more specific towards the transformation of a S-enantiomer of the substrate in S'_1 binding sub-site. Therefore the production of S-phenylalanine during the reaction is faster and the evaluation rate of the same is better compared to the one of the R-enantiomer. It was difficult to evaluate the small increment in the R-phenylalanine during the course of the reaction, due to the presence of a large amount of this compound as impurity in the substrate. With regard to evaluate the minimal measurable increase in the concentration of R-phenylalanine during the hydrolytic

reaction the method of the external HPLC standard was applied. Different amounts R-phenylalanine were added to 50 mM substrate solution, starting from 0.25 mM up to 5 mM total concentration of the compound into the substrate solution. The samples were analysed by HPLC in order to determine “the minimal increase” in the R-phenylalanine concentration, which was detectable by the used HPLC evaluation method. The experimental data showed that even 0.25 mM increase in the concentration of the above-mentioned compound was “measurable”. Due to the fact that only the initial formation rates (about 10 % substrate conversion e.g. 5 mM) of the enantiomeric products were evaluated, it can be concluded that the formation of R-phenylalanine in the above-mentioned concentration range was detectable. Concerning the pipeting and dilutions errors a total error of ±5-10 % can be assumed.

APPENDIX I:

Basis of the magnetism. Types of magnetism

Magnetic fields are created by moving of electrical charges. The effect of a magnetic field is defined by the theoretical force acting on 1 m wire length (within the field) with a current of 1 Ampere. The ratio between the force, F, and the product of the current, I; and the wire length, l, is a measure of the field intensity and is called magnetic flux density, B:

$$B = \frac{F}{I \cdot l} \tag{A.1}$$

where,
B - flux density [Tesla]; F - force [N]; I - current [A]; l - wire length [m].
In the case of a long coil the magnetic field strength is defined as:

$$H = I.\frac{n}{l} \tag{A.2}$$

where,
H - magnetic field strength [$A \cdot m^{-1}$]; I - current [A]; n - number of the windings (if the wire is coiled into a long cylinder) [-]; l - wire length [m].
The relationship between B and H is given by:

$$B = \mu_0 \cdot \mu_r \cdot H \tag{A.3}$$

where,
H - magnetic field strength [$A \cdot m^{-1}$]; μ_r - permeability, dimensionless number characterising the influence of the matter inside the coil. Is equal to 1 in a vacuum and in air (with approximation); μ_0 - permeability of free space, proportionality factor and in SI system has a value of $4 \cdot \pi \cdot 10^{-7} \cdot V \cdot s \cdot A^{-1} \cdot m^{-1}$.
With regard to their magnetic behaviour in an external magnetic field the magnetic materials can be separated into: *diamagnetic*, *paramagnetic* - ferromagnetic,

ferrimagnetic, antiferromagnetic, superparamagnetic, speromagnetic. Diamagnetism is a basic property of all substances to slightly repulse by a magnetic field (Cornell and Schwertmann, and references therein 1996).

The magnetic susceptibility - χ (the dependence of the magnetisation on the external field strength) of these materials is in the range $-10^{-4} < \chi < -10^{-9}$ (Thomas and Franzreb will be published).

$$M = \chi \cdot H_{outside} \qquad \text{(A.4)}$$

where,

M - magnetisation - the difference between the apparent magnetic field strength inside and outside the material [$A \cdot m^{-1}$]; χ - magnetic susceptibility [-]; $H_{outside}$ - magnetic strength of the external field, into which the material is introduced [$A \cdot m^{-1}$].

For paramagnetic materials, in which every atom, ion or molecule can be visualised as a small magnet with its own inherent magnetic moment, the application of an external magnetic field causes an alignment of these "magnets" parallel to the field (Cornell and Schwertmann 1996), the magnetic susceptibility is in the range $10^{-6} < \chi < 10^{-3}$. Ferro- and ferri- magnetic materials are characterised by higher magnetisation, but also by saturation behaviour at high field strengths. The magnetic susceptibility can reach high values (χ - up to 10^5) at small fields and $\chi < 1$ at higher field strengths (Thomas and Franzreb will be published). Ferro- and ferri- magnetic particles contain domains - regions in which the magnetic moments of the atoms are aligned in the same direction and during the magnetisation process, domains pointing the direction of the external magnetic field grow, until all domains are aligned and the material is magnetically saturated. The magnetisation curve (plot of the material magnetisation against the external field strength) for such materials has a typical outlook and is called hysteresis loop (Fig. 1).

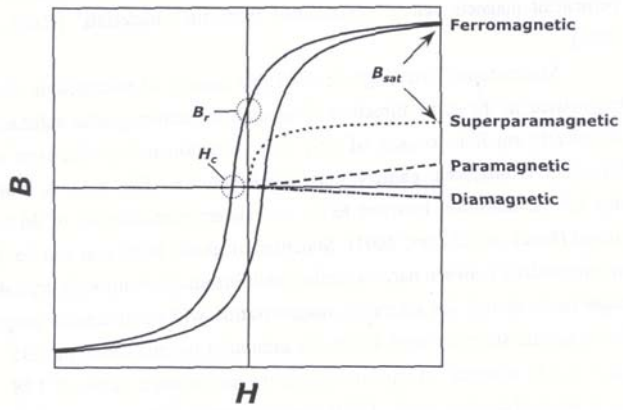

Fig. 1: Magnetisation curves for dia-, para-, superpara- and ferro- magnetic materials.

If it starts from a value where the saturation polarization/magnetisation is reached B_{sat}, and then the magnetic filed strength is reduced down to zero, the magnetisation does not disappear completely (a certain remanence B_r is left) and therefore to bring it back to zero a magnetic field of opposite direction to the original one is required. The magnetic strength of this field is known as coercivity, H_c [A·m^{-1}]. For small nano- and micro- particles the magnetisation could depend on their size. Below a certain particle size (~100 μm in case of magnetite Fe_3O_4), the coercivity field strength rises the susceptibility falls, as the number of the magnetic domains decreases. At a size where only a single domain is left (~1 μm in the case of magnetite), the coercivity reaches a maximum and the susceptibility respectively a minimum. If the particle size is decreased furthermore, the coercivity reaches zero at a certain critical particle size (10-20 nm for magnetite) and the ferro- and ferri- magnetic materials smaller than this size behave paramagnetically with respect to the coercivity, but the absolute value of their magnetisation is quite higher. Species composed of primary nanoparticles of this size are called *superparamagnetic*. In contrast to ferromagnetism these materials show very little remanent magnetisation, which means that superparamagnetic particles have essentially no "magnetic memory", once the external magnetic field is removed. For the magnetic iron oxides with crystal sizes >50 nm this feature is lost.

APPENDIX II:

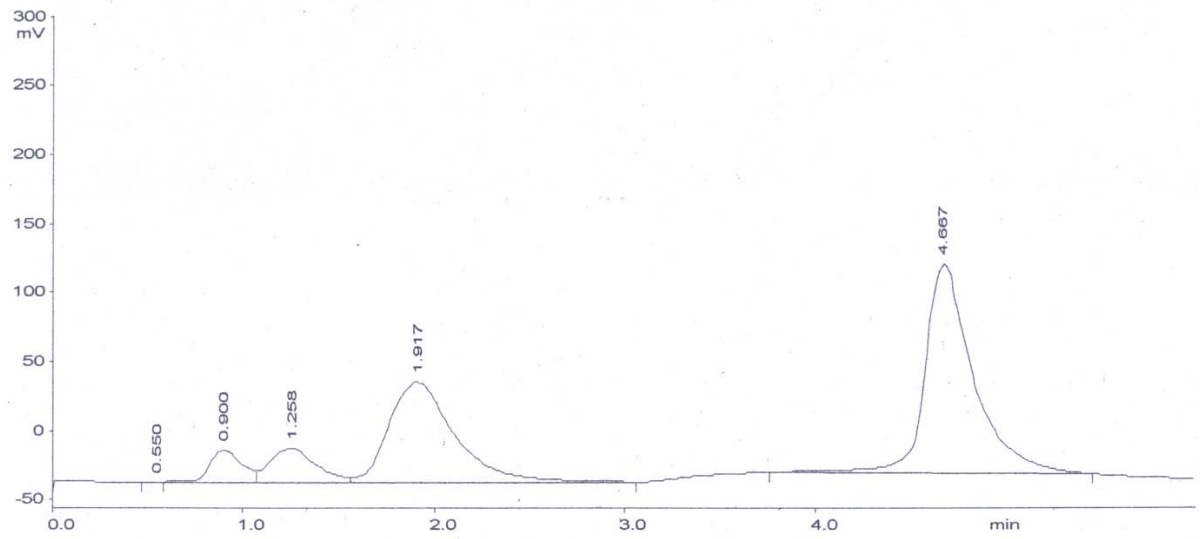

HPLC chromatogram to demonstrate the separation of the compounds during the penicillin amidase catalysed synthesis of cephalexin.

Retention times: 0.9 min phenylglycine; 1.2 min 7-ADCA; 1.9 min R-phenylglycine amide; 4.6 min cephalexin

HPLC separation conditions:

Separation column: RP 18, 5 µm, 125/4 mm (Merck)

Column temperature: 30 °C

Flow rate: 2 ml·min^{-1}

Detection: absorbance at 225 nm

Injection volume: 10 µl

Eluent: methanol / 67mM KH_2PO_4 (pH 6.0) (5:95 v/v) for 2 minutes followed by a step gradient with methanol / 67mM KH_2PO_4 (pH 6.0) (30:70 v/v) for further 3 minutes

APPENDIX III:

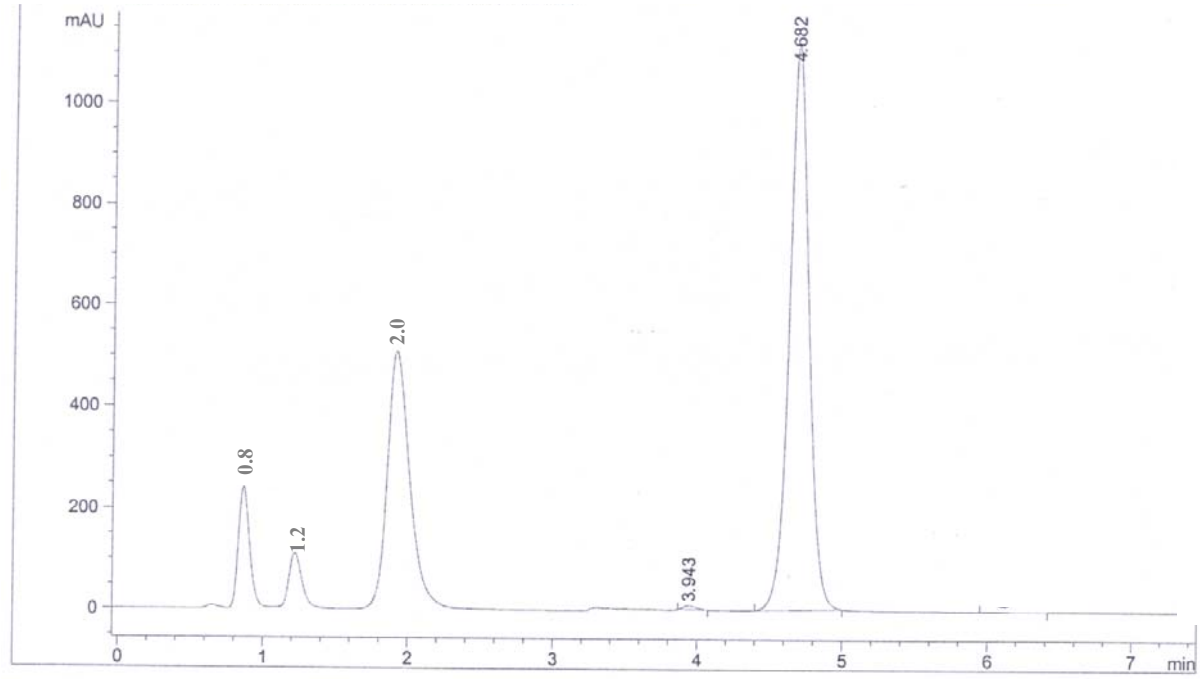

HPLC chromatogram to demonstrate the separation of the compounds during the penicillin amidase catalysed condensation/hydrolysis of R-phenylglycine amide with S-, R-, or R,S- phenylalanine.

Retention times: 0.8 min phenylglycine; 1.2 min R-phenylglycine amide; 2.0 min S-, R- phenylalanine; 3.9 min R-phenylglycine-R-phenylalanine; 4.6 min R-phenylglycine-S-phenylalanine.

HPLC separation conditions:

Separation column: RP 8, 5 µm, 125/4 mm (Merck)

Column temperature: 56 °C

Flow rate: 2 $ml \cdot min^{-1}$

Detection: absorbance at 225 nm

Injection volume: 100 µl

Eluent: 67 mM KH_2PO_4 (pH 4.5) for the first three minutes followed by a step gradient with methanol / 67 mM KH_2PO_4 (pH 4.5) (35:65 v/v) for further 5 minutes

APPENDIX IV:

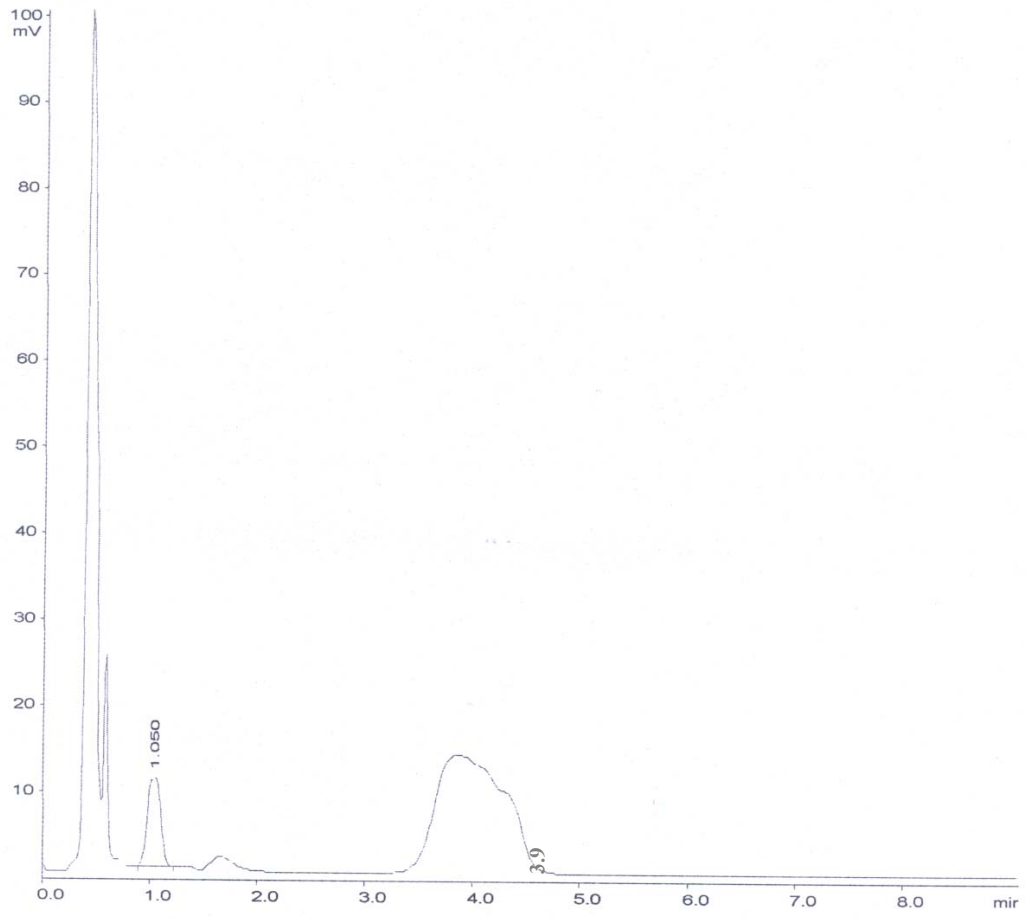

HPLC chromatogram to demonstrate the separation of the compounds during the penicillin amidase catalysed hydrolysis of benzylpenicillin.

Retention times: 0.6 min 6-aminopenicillanic acid; 1.0 min phenylacetic acid; 3.9 min benzylpenicillin.

HPLC separation conditions:

Separation column: RP 8, 5 µm, 125/4 mm (Merck)

Column temperature: 56 °C

Flow rate: 2 ml·min^{-1}

Detection: absorbance at 210 nm

Injection volume: 100 µl

Eluent: isocratic elution with methanol / 67mM KH_2PO_4 (pH 4.7) (30:60 v/v)

APPENDIX V:

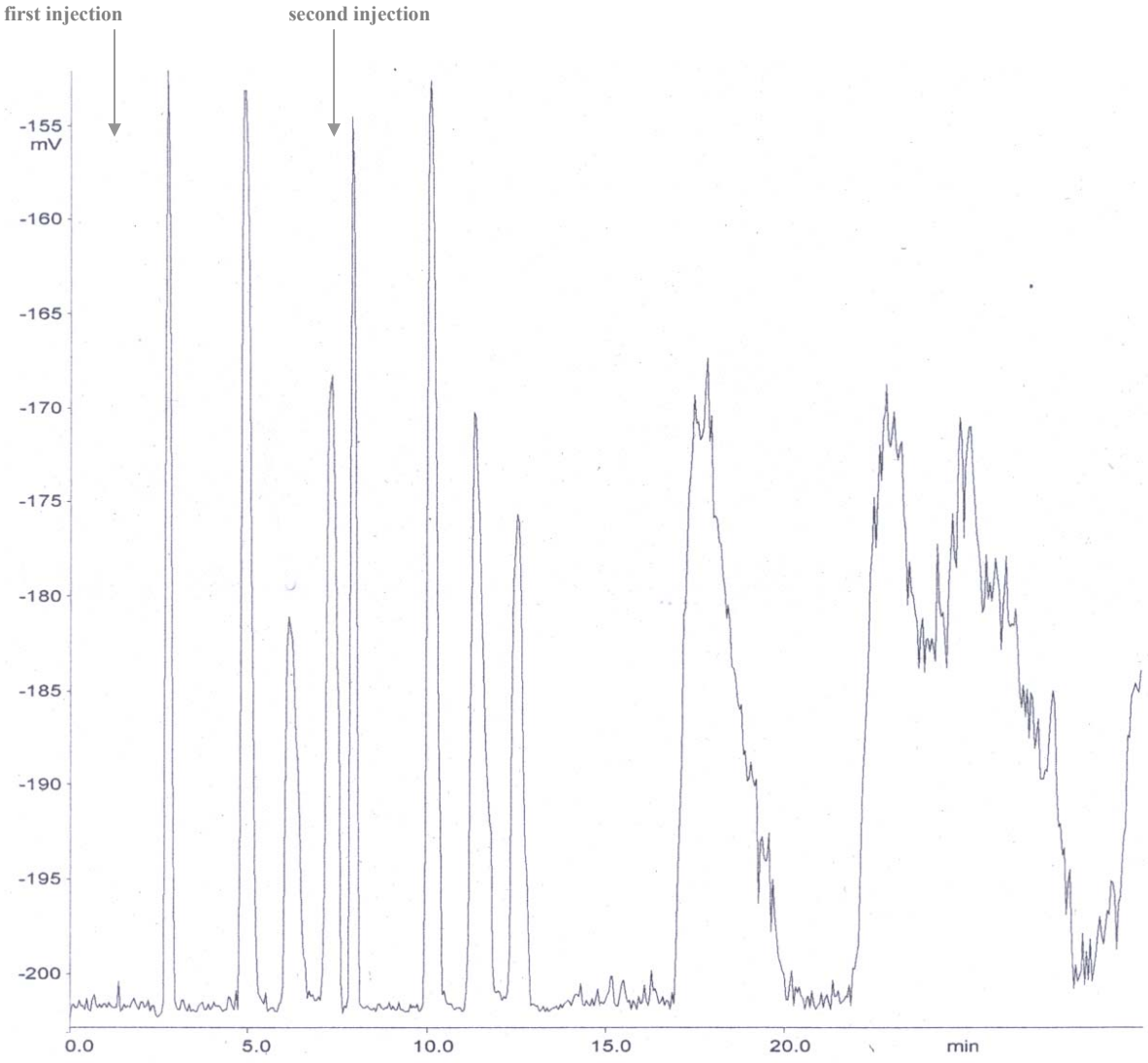

HPLC chromatogram to demonstrate the separation of the compounds during the penicillin amidase catalysed hydrolysis of racemic phenylacetyl-phenylalanine.

Retention times: 5.0 min S-phenylalanine; 6.5 min R-phenylalanine; 7.5 min phenylacetic acid; 18.0 and 25 min racemic phenylacetyl-phenylalanine.

Remark: in order to shorter the duration of the analysis two samples were injected during the same chromatographic analysis.

HPLC separation conditions:

Separation column: Chiral Column Chirobiotic TAG, 5 µm, 250/4.6 mm (Astec)

Column temperature: 30 °C

Flow rate: 1.4 $ml \cdot min^{-1}$

Detection: absorbance at 210 nm

Injection volume: 100 µl

Eluent: isocratic elution methanol / 20mM ammonium acetate (pH 4.0) (10:90 v/v)

Eidesstattliche Erklärung

Ich erkläre hiermit, dass ich die vorliegende Arbeit selbstständig und ohne unzulässige Hilfsmittel angefertigt und nur die im Literaturverzeichnis aufgeführten Quellen und Hilfsmittel verwendet habe.

Die Arbeit wurde am Institut für Technische Chemie, Bereich Wasser- und Geotechnologie, des Forschungszentrums Karlsruhe angefertigt.

Die Polyvinylalkoholpartikel (M-PVA) wurden von der chemagen Biopolymer Technologie AG, Baesweiler, zur Verfügung gestellt.